DOCTOR OF PHILOSOPHY

Exploring the Pharmacological Potential of Bioactive Peptides in Amphibians and Plants: from Identification to Rational Design

Ying, Yuan

Award date:
2019

Awarding institution:
Queen's University Belfast

QUEEN'S UNIVERSITY BELFAST

School of Pharmacy

Faculty of Medicine, Health and Life Science

Exploring the Pharmacological Potential of Bioactive Peptides in Amphibians and Plants: from Identification to Rational Design

Yuan Ying

A thesis submitted to Queen's University, Belfast, for the degree of Doctor of Philosophy

2019

Contents

Acknowledgements

It was an unforgettable and meaningful experience to study at the Natural Drug Discovery Group, School of Pharmacy, Queen's University, Belfast.

Firstly, I would like to express my sincere gratitude to my advisors Prof. Chris Shaw and Prof. Tianbao Chen for their overwhelming support of my Ph.D study and related research, for their patience, motivation, and immense knowledge. Their guidance helped me in all the time of research and writing of this thesis. I could not have imagined having better advisors and mentors for my Ph.D study.

Besides my advisors, I would like to thank the rest of my thesis committee: Dr. Mei Zhou, Dr. Lei Wang, Dr. Chengbang Ma and Dr. Xinping Xi, for their insightful comments and encouragement, but also for the hard questions which incentivised me to widen my research from various perspectives. In particular, I am grateful to Dr. Chengbang Ma and Dr. Xinping Xi for enlightening me at the first glance of research and for all the fun we have had in the last three years. Moreover, I thank my fellow labmates for the stimulating discussions and for the sleepless nights we had working together before deadlines.

Last but not the least, I would like to thank my parents for supporting me spiritually throughout writing this thesis and for my life in general.

Declaration

I declare that the research reported in this thesis is my own work except where acknowledgement has been made. All work was carried out in the Molecular Therapeutics Research Group, School of Pharmacy, Faculty of Medicine, Life and Health Sciences, Queen's University, Belfast.

I hereby declare that for 5 years following the date on which the thesis is deposited in the Library of Queen's University, Belfast, the thesis shall remain confidential with access or copying prohibited. Following expiry of the period I permit the librarian of the University to allow the thesis to be copied in whole or in part without reference to me on the understanding that such authority applies to the provision of single copies made for study purposes or for inclusion within the stock of another library. This restriction does not apply to the British Library Thesis Service. IT IS A CONDITION OF USE OF THIS THESIS THAT ANYONE WHO CONSULTS IT MUST RECOGNISE THAT THE COPYRIGHT RESTS WITH THE AUTHOR AND THAT NO QUOTATION FROM THE THESIS AND NO INFORMATION DERIVED FROM IT MAY BE PUBLISHED UNLESS THE SOURCE IS PROPERLY ACKNOWLEDGED.

Abbreviations

ACN, acetonitrile;

AMP, antimicrobial peptide;

BLAST, Basic Local Alignment Search Tool;

CD, circular dichroism;

cDNA, DNA complementary to RNA;

CF, cystic fibrosis;

CFRD, cystic fibrosis-related diabetes;

CFTR, cystic fibrosis trans-membrane conductance regulator;

CFU, colony-forming units;

CHCA, α-cyano-4-hydroxycinnamic acid;

CL, cardiolipin;

DCM, dichloromethane;

ddH_2O, distilled deionised water;

DEPC, diethyl pyrocarbonate;

DIOS, distal intestinal obstruction syndrome;

DMEM, Dulbecco's Modified Eagle's Medium;

DMF, dimethylformamide;

DM-PC, Dermaseptin-PC;

DMSO, dimethyl sulphoxide;

dNTP, deoxyribonucleotide triphosphate;

DTT, 1,4-dithiothreitol;

EDT, 1,2-ethanedithiol;

ESKAPE pathogens, [*Enterococcus faecium*, *Staphylococcus aureus*, *Klebsiella pneumoniae*, *Acinetobacter baumannii*, *Pseudomonas aeruginosa*, and *Enterobacter* species];

Et_2O, diethyl ether;

FA, formic acid.

FBS, foetal bovine serum;

Fmoc, fluorenyl methoxycarbonyl;

HBTU, 2-(1H-benzotriazol-1-yl)-1,1,3,3-tetramethyluronium hexafluorophosphate;

HiDi, highly deionised-formamide;

IAA, iodoacetamide;

IPTG, isopropyl β-D-1-thiogalactopyranoside;

LB, lysogeny broth;

LPS, lipopolysaccharides;

MALDI-TOF, matrix-assisted laser desorption/ionization time-of-flight;

MBC, minimum bactericidal concentration;

MBHA, methylbenzylhydryl amine;

MHB, Mueller-Hinton broth;

MIC, minimum inhibitory concentration;

MRSA, methicillin-resistant *Staphylococcus aureus*;

MS, mass spectrometry;

MTT, 3-(4,5-Dimethylthiazol-2-yl)-2,5-Diphenyltetrazolium Bromide;

m/z, mass-to-charge ratio;

NCBI, National Center for Biotechnology Information;

NMM, N-methylmorpholine;

NMR, nuclear magnetic resonance;

NUP, nested universal primer A;

OD, optical density;

PBS, phosphate-buffered saline;

PC, phosphatidylcholine;

PCR, polymerase chain reaction;

PE, phosphatidylethanolamine;

PG, phosphatidylglycerol;

RACE, rapid amplification of cDNA ends;

RNase, ribonuclease;

RP-HPLC, reversed-phase high performance liquid chromatography;

RPMI-1640, Roswell Park Memorial Institute-1640;

SAR, structure-activity relationship;

SDS, sodium dodecyl sulphate;

TCM, Traditional Chinese medicine;

TFA, trifluoroacetic acid;

TI, therapeutic index;

TIS, thioanisole;

Tris-HCl, Tris hydrochloride;

TSB, Tryptic Soy Broth;

X-Gal, 5-bromo-4-chloro-3-indolyl-β-D-galactopyranoside;

Abstract

Bioactive peptides, which can be seen as a part of the innate immune response in most living things, are derived from bacteria, fungi, amphibians, insects, mammals, plants and many other sources. Here, Dermaseptin-PC (DM-PC) and PLX-PC, two novel AMPs (antimicrobial peptides), were discovered from the skin secretion of a tree-dwelling, South American frog (*Phyllomedusa coelestis*), using the combination of 'shotgun' cloning and tandem mass spectrometry fragmentation sequencing. Besides, the successful molecular cloning of a novel trypsin inhibitor (as the probable alleleic variants TKTI-2 and TKTI-3) from the dried root of *Trichosanthes kirilowii* indicates that mRNA can persist in decoction pieces and so could present a viable option for the molecular cloning from other TCMs.

It is noteworthy that host-defence peptides have evolved as highly potent alternatives to antibiotics, exerting powerful physiological effects and high susceptibility of multidrug-resistant strains. However, some intrinsic weaknesses limit the direct usage of naturally occurring peptides as convenient therapeutics. Consequently, DM-PC was rational designed with the objective of a higher therapeutic index, while PLX-PC was further modified by substitution of amino acids and truncating the effective part for higher potency and broader spectrum of antimicrobial activity. With the optimisation of physicochemical characteristics of these two bioactive natural peptides, their bio-efficacy and therapeutic indices were enhanced. The study of these together with their analogues provides new insights on lead antibiotic drug discovery and design, especially against resistant strains.

Chapter 1

General Introduction

1.1 Natural Distribution of Bioactive Peptides

Bioactive peptides, short protein fragments that can influence a multitude of bodily functions, are formed by approximately 50 or fewer amino acids joined by peptide bonds. They are inactive within sequences of big protein molecules, and exhibit physiological activities after being released by hydrolysis. Consequently, bioactive peptides can be identified directly from their natural sources, but also from their parent proteins mainly by enzymatic processes. In general, bioactive peptides are universal compounds existing in all forms of life, ranging from bacteria to plants and invertebrate and vertebrate species, including mammals. Both amphibian skin secretion and dried plant material were involved in the discovery of novel bioactive peptides in this thesis.

1.1.1 Amphibians

1.1.1.1 The Evolutionary Trajectory of Amphibians

Amphibians are one of the oldest groups of tetrapod vertebrates, presenting a curiously bimodal pattern of diversity, that emerged in the Late Devonian, around 370 million years ago (Hallam, 1977). The class name '*amphibia*' is derived from the Ancient Greek words, *amphi* represents 'two' and *bios* stands for 'mode of life' because most species have a diphasic lifestyle by possessing the properties of both aquatic and terrestrial survival modes (Crump and Crump, 2011). In doing so, they have obtained incredible and fantastic morphological, physiological, behavioral, and ecological traits that mold their evolution. From these ancient lobe-finned fish to modern amphibians, the prolonged but spectacular transitional stage has been witnessed. For creeping along the ocean floor, their fins initially

evolved into multi-jointed leg-like structures with digits. Since the circumstances that primitive amphibians need to hoist themselves out of the water and even crawl on the land, their fins became increasingly strong, which eventually developed into limbs and they would become the ancestors to all tetrapods.

Apart from the evolution from the aquatic life to a more unfriendly terrestrial survival mode, amphibians have exhibited various adaptations to occupy ultimate living environment types, for instance deep freshwater lake, cloud forest canopy, arid desert and even the Arctic Circle (Duellman and Trueb, 1994). In particular, frogs and toads (*Anura*) are so cosmopolitan that they are distributed all over the world excepting Antarctic regions (Clarke, 1997). Being ectothermic animals with highly permeable skin that loses water and complex reproductive needs, whose traces have been found in nearly every habitat except for open oceans, most oceanic islands, polar regions, and some badly dry deserts, amphibians have already adapted to a remarkable diversity of environmental conditions (Wells, 2007).

The ability to overcome these restrictions imposed on them may be attributed to the evolvements in various aspects (Mahoney, 2017). For instance, amphibians living in dry areas or some places with seasonal rainfall suffer from water loss, but learning to absorb water by contacting moist soil along with shifting to the lowest metabolic rates even estivation, enables them to survive the unfavorable periods (Parker, 2013, Warburg, 1997). Moreover, due to a cold-blooded characteristic, amphibians can only absorb the energy from outside to raise their body temperatures and become inactive at low temperatures. Thus,

hibernation is their common response to the cold winter of temperate climates, but for freezing or below-freezing temperatures, antifreeze is the key factor which has enabled them to survive. Once ice crystals begin to form on the skin, the liver is signaled to turn glycogen into glucose, and then the sweet antifreeze is transferred to life-or-death tissues and organs, preventing cells from dehydrating and shrinking (Boernke, 1973).

1.1.1.2 The Population Decline and Extirpation of Amphibians

Amphibians with biphasic life cycle and permeable skin are extremely sensitive to ecosystem stress. Consequently, the population of amphibians has experienced a dramatic decline in recent years, and apparently many factors contribute to this phenomenon. The most critical one is habitat destruction, as well as the environmental contamination, followed by over-exploitation caused by human beings (Collins and Crump, 2009).

The problem of worldwide amphibian decline, as it is worth pointing out, sounds an alarm bell for ecological civilisation. It is not, however, simply a matter of biodiversity decrease or species extinction, which has already garnered global attention. The predisposing factors to the population decline of amphibians across the planet indeed are so complicated that not only biologists but also geneticists have been dedicated to this project, over a long period of time. The scientific basics of conservation policy are of great importance to preserve both ecosystems and species.

1.1.1.3 Normal Functions of Amphibian Skin

Given thoroughly modified ambient conditions, amphibians are confronted with a series of related physiological issues, including retrimming of respiration in answer to volatile oxygen saturation, regulation of water and osmolyte homeostasis (Acher et al., 1997), and acclimation to temperature fluctuations (Myhre et al., 1977). Additionally, the damp places, where are definitely swarming with microbes and pathogens, appeal to most amphibians, hence, there is no doubt that an integrated and powerful antimicrobial defence system has been developed for the prevention of infection, in which epidermis acts as the first physical barrier against potentially pathogenic bacteria and fungi. As a result, without the complete cutaneous surface, amphibians would easily succumb to infections, and concededly skin is a predominant functional organ for them in host-defence system.

Aside from respiration, water regulation, temperature control and host-defence mentioned in last paragraph, the basic function of amphibian integument also covers excretion, reproduction and camouflage. Thus, adaptive characters for amphibian skin play a vital role in acclimatising to new surroundings quickly. Another considerable factor in amphibian survival is that all these functions are able to work simultaneously (Clarke, 1997).

1.1.1.4 Amphibian Defensive Skin Secretion

Two remarkable amphibian skin glands — mucus glands and granular glands, are renowned for a large quantity and diversity of compounds in their secretion with broad spectra of pharmacological activities. Literally, the former one excretes mucus to keep the epidermis

moist and slippery enough to prevent mechanical damage like abrasion, to make it difficult for potential predators to seize, as well as to decelerate evaporative water loss. At the same time, mucus plays a part in most cutaneous functions in accordance with species. While the latter one, the way of whose distribution is probably connected with the protection, synthesises wide-ranging substances that usually play a defensive role (Delfino et al., 1999). In response to environmental stress and life threat, these extremely specialised skin structures are employed to produce a complex chemical cocktail which possesses a toxic or even lethal effect on most vertebrates who are the major consumers of amphibians (Chen et al., 2003).

An arsenal of bioactive compounds secreted by amphibian skin glands involve amines, bufodienolides (steroids), alkaloids (dietary origin), peptides and proteins (Daly et al., 1987). Being of the production of bacteria can be the reason why other certain molecules which are phylogenetically unrelated can be found in some species (Clarke, 1997). Here, most amines are vasoconstrictors with hallucinogenic and hypertensive properties (Daly, 1995). When it comes to bufodienolides, they are capable of changing the strength and rate of the heart beat to eventually accelerate cardiac function (Buckalew, 2015). The breathtaking discovery of magainins by Zasloff, a new class named AMPs, has impelled large numbers of scientists to exploit amphibian biochemicals (Zasloff, 1987). Since then, more than 3,000 AMPs have been deposited in the Antimicrobial Peptide Database (http://aps.unmc.edu/AP/main.php, acessed: 21.10.2019). It is likely that this list represents only a small fraction of gene-encoded antibiotic proteins produced in nature. Therefore, there is a high possiblity that more AMPs can be identified from amphibians.

In addition to those biologically active molecules secreted by amphibian skin, other ingenious strategies are applied to their daily defence. For example, to effectually avert predation from diurnal animals, several amphibians choose to conceal themselves during the daytime and become nocturnally active (Wilczynski et al., 2005). Furthermore, some amphibians are able to camouflage themselves through changing their skin colours to deceive predators (Rodel et al., 2013). Besides, a few risky ways of escape are adopted, like salamanders shed their tails (Gvozdik and Smolinsky, 2015).

1.1.1.5 The Significance of Research on Amphibian Skin Secretion

It is worth pointing out that the amphibian skin works day by day for survival and the exploitation of diverse habitats by a broad variety of bioactive chemical compounds secreted by its glands (Delfino et al., 1999). The damp places, where are definitely swarming with pathogens, appeal to most amphibians (Wells, 2007). As a result, an integrated and powerful antimicrobial defence system has been developed, in which epidermis acts as the first physical barrier against potentially pathogenic bacteria and fungi (Gvozdik and Smolinsky, 2015). Additionally, amphibians show a noted preference for defending themselves against predations and infections by the peptide arsenal (Rollins-Smith, 2009). Another important advance occurred when Zasloff and colleagues in 1987 isolated and characterised cationic AMPs, named ‘magainins’ from the African clawed frog *Xenopus laevis* (Zasloff, 1987).

Under the perspective of genetics, preserving as much genetic diversity as possible is the ultimate goal (Szczecinska et al., 2016). For those reasons mentioned above, amphibian skin secretion was chosen as a research object. Based on ‘shotgun’ cloning, a cDNA library was constructed, sequenced and analysed in this thesis, to identify new gene products encoding AMPs. According to the results of DNA sequence comparisons, the phylogenetic status of some groups could be found and it is these genetic and genome explorations that contribute to design a peptide or protein with improved functionality.

1.1.2 Plants

Cereal grains such as wheat, barley, rice, rye, oat, millet, sorghum, and corn, are a rich source of bioactive peptides which are released during digestion (Kitts and Weiler, 2003). Bioactive peptides from vegetal sources have been proven to be instrumental in preventing cardiovascular diseases, diabetes, and even cancer (Malaguti et al., 2014). Digestion of wheat and oats provided peptides with ACE inhibitory, dipeptidyl peptidase inhibitory, anti-thrombotic, antioxidant, hypotensive, and opioid activities (Mason et al., 2018). Besides, wheat and rice showed the presence of proteins with peptide sequences which exhibit anticancer activity. Among cereals, wheat and barley showed the highest abundance of peptides with potential biological activity.

1.2 Pharmacological Properties of Bioactive Peptides

For a peptide to be considered bioactive, it should have a physiological effect in a positive manner, which means this component must have a beneficial impact on body functions or

conditions and exclude the possibility of side effects such as toxicity, allergenicity, and mutagenicity. Currently, the SAR of bioactive peptides remain to be studied, as their activities are affected by multiple factors, such as amino acid composition, peptide chain length, charge, hydrophobicity, and so on. Some of the pharmacological properties of bioactive peptides are discussed below.

1.2.1 Antimicrobial Peptides

1.2.1.1 Characteristics of AMPs

AMPs, an omnipresent and fundamental constituent of inborn immunity, not only act rapidly in organisms, but also have a potent effect on most pathogenic microbes (Rollins-Smith, 2009). They have been demonstrated to be able to kill both Gram-positive and Gram-negative bacteria, fungi, enveloped viruses and even carcinomatous cells (Thomas et al., 2012). Peptides with bactericidal activity, which can be seen as a part of the innate immune response existed in living things, are derived from bacteria, fungi, amphibian, insects, mammals, plants and many other sources (Wang, 2015). Despite the lack of certain amino acid sequences connected with bioactivity, most AMPs do share some physicochemical properties, like peptide length, net charge, hydrophobicity and conformation. 20-50 amino acid residues long, cationic, amphipathic, α-helical AMPs are in majority, whose biological target hosts are on the cell surface or intracellular molecules.

I. Charge

The charge is a crucial property affecting the antimicrobial activity. It is generally thought that the cholesterol in target membrane not only stabilises the lipid bilayer but also reacts with the peptide, ultimately reducing the activity of AMPs (Zasloff, 2002). Similarly, the increasing ionic strength of AMPs does so partly because of weakening the electrostatic interaction between oppositely charged ions (Lee et al., 2015). Cationicity, typically ranging from +1 to +6, is responsible for the electrostatic attraction to anionic molecules of the membrane. And it is suggested that increasing the number of negatively charged amino acids, typically lysine and arginine residues, to some extent, may contribute to a stronger antimicrobial activity as well as the haemolytic activity (Zhu et al., 2015).

A sufficient positive charge is vital for the peptides to be attracted to bacterial surfaces via electrostatic bonding, and there is an optimum cationicity window, usually +4 to +6, in which the electrostatic adsorption of AMPs to the negatively charged bacterial membrane surface could be achieved. Besides, hydrogen bonding between the side chains of cationic amino acid residues and lipid phosphate-rich membrane surface of the bacteria could facilitate the initial electrostatic attraction, stabilise the peptides in a hydrophobic environment and further enhance the insertion capacity of the peptides toward the hydrophobic bacterial membrane core, and finally enhance the potency of antibacterial activity.

II. Conformation

Although the primary structure of AMPs varies significantly even among the same genus, their secondary structure appears to have a preference for α-helix rather than β-sheet (Huang et al., 2010). Here, α-helicity works as a universal conformation for transmembrane pore formation. In most cases, linear AMPs are extended or unstructured in aqueous solution. Upon being exposed to the lipid bilayer, they can adopt helicity as a conformation with distinct hydrophobic face to attack bacterial plasma membrane (Amiche and Galanth, 2011). Moreover, the amidation at C-terminus could contribute to the formation of an alpha-helical structure (Yount and Yeaman, 2013). In summary, no matter what the conformation is, α-helix, β-sheet or extended AMPs, the secondary structure is closely connected with amphipathicity and plays a key role in membrane penetration.

III. Amphipathicity

On account of amphipathicity, AMPs are water-soluble but also can penetrate the lipid bilayer of the membrane (Li et al., 2015). To be specific, amphipathic peptides, having the hydrophilic face of the molecule for dissolution, and hydrophobic face on the other side to partition into the membrane lipid bilayer, demonstrate antimicrobial traits (Lee et al., 2016). In general, amphipathicity, quantified by hydrophobic moment, is affected by the ratio and polarisation of hydrophilic and hydrophobic areas, as well as the conformation of the peptide (Edwards et al., 2016). And it is this particular physicochemical property of AMPs that works as a vital parameter in the whole process, from membrane binding to partition and penetration, and even the final lysis (Chang et al., 2015).

IV. Hydrophobicity

Hydrophobicity can be measured by the percentage of hydrophobic residues within a peptide chain (Bechinger and Gorr, 2016). Commonly, increased hydrophobicity had a positive effect on peptide access to both prokaryotic and eukaryotic membranes, and this was consistent with the predicted mode of action of linear amphipathic alpha-helical antimicrobial peptides that AMPs accumulated to a threshold concentration due to some affinities, and the hydrophobic residues could be inserted into the lipid bilayer of bacterial membrane, resulting in the formation of transient or prolonged transmembrane pores can not only lead to the final membrane disintegration but also permit extra peptides to enter the membrane to work on intracellular targets and finally causing cell death. However, a higher content of hydrophobic residues may be conducive to the attachment and interaction with the membrane but result in haemolysis and loss of cytotoxic selectivity (Chen et al., 2007). To sum up, there is an optimum hydrophobicity window (around 50%) in which selective antimicrobial activity could be obtained, and the integrity of the hydrophobic face of the amphipathic peptides plays a decisive role on the bioactivity.

V. Polar Angle

Polar angle refers to the angle subtended by the hydrophilic face within a peptide that conformed to an amphipathic helix, partly reflecting the relative distribution of hydrophilic and hydrophobic residues (Zairi et al., 2009). Independent of amphipathicity and hydrophobicity mentioned above, polar angle is estimated to be a determinant of the position of the AMP (antimicrobial peptide) within a membrane and the construction of the transmembrane channels in an amphipathic α-helix-lipid interaction. For most AMPs, a

smaller polar angle means a higher possibility of permeating the lipid bilayer membranes (Carlier et al., 2015).

1.2.1.2 Mechanism of Antimicrobial Activity

Lots of methods have been used to detect how AMPs actually lead to the death of microorganisms, or to research the mechanism of their bactericidal effect (Lohner and Blondelle, 2005). Although the visualised information about target sites can be obtained from microscopy by monitoring the effects of AMPs on microbial cells, sometimes the rapid peptide-mediated cell killing process makes it tougher to characterise the steps preceding cell death (Brogden, 2005). Therefore, detailed perceptions of the mechanism can be supplied by model membranes, with the assistance of CD, solid-state NMR spectroscopy, neutron diffraction and other valuable techniques (Oliveira et al., 2013, Wang et al., 2016).

Studies on AMPs have been carried on for decades, and there are several models to clarify the mechanisms of action which vary among microbes and different classes of AMPs. Hypotheses comprise lethal depolarization of the charged lipid membrane, the formation of physical holes in the membrane that causes a leak of nutrients, proteins and other essential components of the cytoplasm, the induction of autolysis such as the stimulation of hydrolases that destroys the cell wall, and so on (Yeaman and Yount, 2003). Generally, the primary target of AMPs is cell membrane (also known as a lipid, cytoplasmic or plasma membrane) (Yang et al., 2000). And some certain steps would occur, to be specific, they are attraction via electrostatic or receptor-mediated bonding, attachment, peptide insertion and membrane

permeability. Aside from disrupting the integrity of cell membrane, other mechanisms of AMPs refer to the situation where the targets are some vital cellular processes (Lee and Lee, 2015).

I. Attraction

There is a widespread acceptance that the positively charged AMPs are initially attracted to bacterial surfaces via electrostatic bonding (Zhao et al., 2001). This mutual and vigorous attraction occurs because of the negatively charged compositions of bacterial lipid membranes, for example, CL and PG. On the contrary, mammalian plasma membranes are usually composed predominantly of zwitterionic phospholipids like PE and PC (Lakshmaiah Narayana and Chen, 2015). Consequently, cationic AMPs tend to first be attracted to bacterial pathogens, whose cytoplasmic membranes are highly electronegative (Lee et al., 2015). However, a small and cyclic peptide named nisin, one well-characterised exception, has a specific affinity for lipid II. As lipid II is a precursor molecule in the synthesis of the bacterial cell wall, used for peptidoglycan synthesis, nisin exhibits a relatively high antimicrobial activity (nM range) against Gram-positive bacteria (Breukink and de Kruijff, 1999). Moreover, a series of studies have demonstrated non-equivalent antimicrobial activities for D- and L-isoforms, which suggests the existence of receptor-mediated membrane interactions.

II. Attachment

The events subsequent to initial membrane attraction may involve one or more steps of the threshold concentration, conformational phase transition and peptide aggregation. Theoretically, it is the accumulation of peptides on bacterial surface reaching the threshold concentration that results in the commencement of attachment. Upon getting close enough to the target surface, peptides need to traverse the phospholipid bilayer to eventually achieve or extend their antimicrobial action (Yang et al., 2000). At this moment, undergoing a magical structural transition might be crucial for peptides to interact with the lipid bilayer. Sometimes, self-association (peptide-peptide interaction) and multimerization (peptide-lipid interaction) could happen, forming complex structures, in specific modes of membrane interaction (Carlier et al., 2015).

III. Peptide Insertion and Membrane Permeability

Membrane permeabilisation may take place when the AMP accumulated to a threshold concentration due to some affinities like electrostatic, hydrophobic or receptor-mediated attractions. The formation of transient or prolonged transmembrane pores can not only lead to the final membrane disintegration but also permit extra peptides to enter the membrane to work on intracellular targets (Kim et al., 2009). Given a multitude of AMP families and the inconsistency of microbial membrane composition, the models depicted below here are summarised from the activities of representative AMPs in distinct artificial membrane environments.

In this ‘barrel-stave’ model, AMPs acted as ‘staves’, are positioned in a circle with aqueous centre, creating a ‘barrel-like’ pore (Li et al., 2015). Based on the similarity-intermiscibility theory, the hydrophobic faces turn outward, while the hydrophilic faces gather together to form the pore-lining. Briefly, these peptides initially bind to the membrane outer leaflet, turning their positively charged or hydrophilic surfaces to the phospholipid head groups. Once accumulating to a threshold concentration, AMPs start integrating themselves into the intermediate lipid level, followed by displacement of fatty acid tails and formation of transient pores. With the accretion of peptides and relaxation of the pores, nonpolar surfaces of the peptides align with the hydrophobic membrane core, while polar ones form the interior surface of the pore gradually. This type of transmembrane channel is unique and induced by alamethicin, which is a fungus-derived peptide consisting mostly of hydrophobic amino acids (Lee and Lee, 2015).

In the ‘toroidal pore’ model, the transmembrane channel, where phospholipid head groups are intercalated with peptide, is the primary difference between this model and ‘barrel-stave’ model (Yeaman and Yount, 2003). Taking magainins as an example, during the formation of toroidal pores, nonpolar faces of the peptide are always associated with the lipid head groups, even when they are vertically inserted into the lipid bilayer (Kim et al., 2009). To be specific, AMP helices firstly induce the lipid monolayer to bend continuously through the pore. The lipids in the openings then tilt from the lamellar normal and connect the two leaflets of the membrane, and the dynamic peptide-lipid supramolecular pore is formed (Brogden, 2005).

The carpet mechanism is a traditional model of nonspecific membrane permeabilisation, in which peptides act like detergents and perform antimicrobial activities through a comparatively diffuse manner (Lohner and Blondelle, 2005). To begin with, plenty of peptides accumulate on the bilayer surface, covering the membrane outer leaflet in a carpet-like way, mainly because of the electrostatic interaction between AMPs and the anionic phospholipid head groups at countless sites. When the concentration of peptides orientating parallel to the membrane reaches a critical point, they are believed to disrupt the bilayer by phospholipid displacement and finally form the micelles (Wang et al., 2016). From this perspective, the process of microorganisms killing does not involve any channel construction or peptide insertion (Li et al., 2015).

1.2.1.3 Limitations of Host-Defence Peptides

It is noteworthy that host-defence peptides have evolved as highly potent alternatives to antibiotics, exerting powerful physiological effects and high susceptibility of multidrug-resistant strains (Hancock et al., 2016). However, some intrinsic weaknesses, like poor chemical and physical stability, tendency for aggregation, short half-life and fast elimination, limit the direct usage of naturally occurring peptides as convenient therapeutics (van der Does et al., 2018). Consequently, rational peptide design focused on mitigating these drawbacks is the key contributor to the therapeutic peptides.

1.2.1.4 Peptide design

AMPs, indispensable components of innate immune system, act as a first line of defence against invading pathogens, whose characteristics and mechanism of action have been described above. Both physicochemical properties of AMPs and parameters of external environments are vital factors for the interaction between AMP molecules and the lipid bilayer of bacteria. In AMP modification, these factors affecting the activities of AMPs need to be considered together, since even a simple change could alter more than one parameter (Wang et al., 2015).

I. Terminal Capping

Although N-terminal acetylation is a major type of chemical modifications, which is able to increase peptide stability by preventing N-terminal degradation in some circumstances, this modification can rarely be found in natural AMPs. On the contrary, another N-terminal modification forming pyroglutamates has been detected in a great quantity of AMPs isolated from different organisms. The cyclisation of glutamine residue at the amino end to become pyroglutamic acid has a positive effect on structural integrity of the N-terminal helix. In addition, C-terminal amidation is critical for antimicrobial activity of some short AMPs. To be specific, the deamidation of anoplin, which is a antimicrobial decapeptide from wasp venom, causes a loss of amphipathicity as well as its biological activities (Dos Santos Cabrera et al., 2008).

II. Changes of Amino Acid Content

Tampering with the composition of primary sequence that changes hydrophobicity, amphipathicity, conformation or even the net charge, affects bioactivity of the peptide dramatically and results in a different cytotoxicity (Feder et al., 2000). Since the physicochemical characteristics play an undeniable role in the potency of antibacterial activity and in the target spectrum of AMPs, alteration of amino acid residues is one of the most studied tactics of AMP modification. In general, these studies replaced certain amino acids, especially those in hydrophobic domains, with other amino acid residues, causing a series of analogues that display changed bioactivities, which suggested that the cationicity, the amphipathic α-helicity and the hydrophobicity were fundamental factors for antimicrobial action.

As a general rule, peptides produced by ribosomal synthesis contain amino acids only in the L-isoform. However, there are some large enzymes, referred to as nonribosomal peptide synthetases (NRPS), which assemble peptidic products containing more than the 20 common amino acids (Cotter et al., 2005). D-amino acids, first found in bombinins from amphibians (Simmaco et al., 2009), are more tolerant to proteases, therefore the substitution of which is one of useful strategies to improve AMP stability.

III. Induction of AMP Expression in Host Cells

Not all AMPs possess all the required properties for direct uses as antibiotics. Alternatively, AMPs may be applied indirectly by inducing gene expression from host cells or by

engineering probiotic bacteria as an AMP delivery vehicle (Mishra et al., 2017). Most naturally occuring AMPs are directly synthesised in their bioactive form, followed by different post-translational modifications. In some cases, recombinant cell systems can be applied to produce new synthetic AMPs with post-translational modifications, which are often required for the efficacy and stability of therapeutic proteins and peptides (Bahar and Ren, 2013).

1.2.2 Immunomodulatory Peptides

Host defence peptides are also known as important components of the immune response. For example, the human cathelicidin peptide LL-37 shows an inhibitory effect on the growth of *E. coli* in the low μg/ml range. Nevertheless, there is a rising trend of its MIC values in the presence of higher concentrations of NaCl, and its antibacterial activity is virtually abolished when tested in tissue culture media (Chalamaiah et al., 2018). In contrast, LL-37 displays a broad array of immunomodulatory properties, including suppressing pro-inflammatory cytokines, preventing activation of macrophages and promoting wound healing, both *in vitro* and in animal models (Burton and Steel, 2009).

Unlike AMPs, immunomodulatory peptides affect multiple signalling pathways within a cell. In comparison with the well-researched SARs regarding the straightforward antimicrobial activity of AMPs, relatively little is known concerning the sequence and structural requirements of the immunomodulatory peptides (Hancock and Sahl, 2006). Hence, one of the greatest obstacles in the development of them as drugs is understanding their mechanisms

of immune cell stimulation. Mostly, natural host defence peptides with inherent immunomodulatory activity are ideal templates for the generation of artificial immunomodulatory peptides.

1.2.3 Cytomodulatory Peptides

A large number of peptides derived from natural sources are known to specifically target carcinogenic cells and exhibit cytotoxic effects (Bhat et al., 2015). Studies with magainin II have shown to directly target certain cell membranes, where it forms permeable ion channels, and inhibit the proliferation of various types of carcinogenic cells without any effect on normal cells (Meisel and FitzGerald, 2003). Due to the selectivity between malignant cells and normal cells, these cytotoxic peptides have a great potential to be an alternative to conventional cancer treatments.

1.2.4 Antioxidant Peptides

Free radicals refer to uncharged molecules having an unpaired valency electron. Because of the unpaired electron in their outer orbit, free radicals are unstable, highly reactive and short-lived, and are involved in many biochemical activities of cells (Chai et al., 2017). In human body, Oxygen free radicals and other reactive oxygen species are produced through numerous physiological and biochemical processes like signal transduction, gene transcription and regulation of soluble guanylate cyclase activity, primarily as a result of aerobic metabolism (Zou et al., 2016, Hamley, 2017). However, overproduction of these free

radicals are linked to a host of chronic and degenerative diseases, as they can cause oxidative damage to important biomolecules such as lipids, proteins and DNA.

Bioactive peptides, as specific protein fragments that exert great influence in the metabolic functions of living organisms, and one of the most crucial of which is the antioxidant activity. Antioxidant activity of these peptides can be attributed to their radical scavenging, metal ion chelation properties and the ability to inhibit lipid peroxidation (Admassu et al., 2018). Evidence suggests that, various antioxidant peptides are supplied to human body through diet. For instance, peptides derived from milk can prevent the peroxidation of essential fatty acids. Digestion of casein also produces phosphorylated peptides with antioxidant activity (Wu et al., 2015).

1.2.5 Opioid Peptides

The plentiful endogenous opioid peptides, including enkephalins, endorphins and dynorphins, as well as the exogenous opioids like morphine have been shown to be active both as hormones and as neuromodulators, through the interactions with four major categories of opioid receptors, mu (μ), delta (Δ), kappa (k) and epsilon(ε) (Garg et al., 2016, Labuz et al., 2016). As opioidergic neurones where opioid peptides are released and opioid receptors where opioid peptides act on are largely distributed centrally and peripherally, it is not surprising that opioid peptides are involved in the physiological control of numerous functions, ranging from pain relief, decreasing respiration, preventing diarrhea to inducing euphoria (Marco and Gentilucci, 2017, Lazaro et al., 2016).

1.2.6 Mineral-Binding Peptides

Among peptides with mineral-binding abilities that have been identified, caseins are the main mineral chelators of calcium (Brown et al., 2017). In addition, the whey proteins and lactoferrin give rise to peptides with abilities to bind specific minerals like calcium, magnesium, zinc, iron, sodium and potassium (Bhat et al., 2017). In contrast, less documented is the binding of trace elements. These mineral trappers function as carriers or chelators through specific and non-specific binding sites and thus affect *in vivo* absorption and bioavailability of minerals (Sultan et al., 2018). In view of this, fortification of foods with minerals in a low concentration through mineral-binding peptides has been used in the food industry for a long time to overcome mineral deficiency.

1.2.7 Peptides in Metabolic Syndrome

The growing prevalence of metabolic syndrome, such as centripetal obesity, type 2 diabetes, arterial hypertension, and dyslipidemia has garnered increased attention in recent years (Santhekadur et al., 2017). Several bioactive peptides are related to the metabolic regulations, and they may play an important role in the prevention and treatment of metabolic disorders, via diverse mechanisms like the regulation of insulin secretion and lipolysis in adipose tissue, the satiety response and reducing the activity of carbohydrate degrading digestive enzymes (Guo, 2014). There is increasing evidence of the involvement of natriuretic peptides (NP) in the pathophysiology of metabolic diseases. The natriuretic peptides are cardiac hormones, which are produced in the cardiac atrium, ventricles of the heart and the endothelium. These

peptides are involved in the homeostatic control of body water, sodium intake, potassium transport, lipolysis in adipocytes and regulates blood pressure. The three known natriuretic peptide hormones present in the natriuretic system are atrial natriuretic peptide (ANP), brain natriuretic peptide (BNP) and c-type natriuretic peptide (CNP). These three peptides primarily function as endogenous ligands and mainly act via their membrane receptors such as natriuretic peptide receptor A (NPR-A), natriuretic peptide receptor B (NPR-B) and natriuretic peptide receptor C (NPR-C) and regulate various physiological and metabolic functions (Santhekadur et al., 2017).

1.3 Applications of Bioactive Peptides

1.3.1 Multidrug-Resistant Bacterial Infections

As for how bacteria become resistant, the very first step is a genetic change in a bacterium since selective pressure induced by inappropriate antibiotic use. Bacteria can be resistant to certain antibiotics via spontaneous mutation in the bacterium's DNA but can also attain resistance through transfer of antibiotic-resistant genes (Viehman et al., 2014).

The intrinsic resistance of an individual bacterial species to a specific therapeutic agent is to protect itself from various antibiotics by inactivating them. For instance, Genetic change leading to an increased production of antibiotic's target enzyme or antibiotic-inactivating enzyme result in antibiotic inactivation at last. Also, target modification can prevent therapeutic agents from binding or it if does bind, prevent it from inactivating the target. As well, the bacterium may reduce permeability to antibiotics via changes in outer membrane

or inhibition of metabolic pathway (Giedraitiene et al., 2011). A transfer of existing antibiotic-resistant genes from one bacterium to another, which is called a horizontal gene transfer, is the second way for bacteria to gain resistance.

Since pathogen bacteria occupy all manner of tissues and niches where they must conquer the host defences mediated by antimicrobial peptides to survive, it is unrealistic to expect that no antimicrobial peptide resistance would arise. Nonetheless, most AMPs perform a non-receptor type interaction with most membranes, which means they could escape several certain mechanisms of resistance to AMPs and are promising compounds for developing a new therapy for multidrug-resistant bacterial infections.

For instance, cystic fibrosis is the most common life-limiting, autosomal-recessive genetic disease in Europe, North America, and Australia, with lung disease characterised by chronic infection and inflammation accounting for most morbidity and mortality (Reihill et al., 2016). It is mutations in CFTR gene that result in dysfunctional chloride channels in mucus and sweat producing cells, which further affect multiple organs with lungs, lead to life threatening complications and cause a high mortality rate. According to the universal screening of newborn babies, there is an autosomal recessive inheritance pattern in white people of north European ancestry today, affecting 1 in 2000-3000 neonates, while Asian-Americans have 1 in round 30,000 newborns (Rafeeq and Murad, 2017).

In the respiratory system, lack of the CFTR function in the bronchial epithelia results in abnormally dense mucous, increased inflammatory response and reduced bacterial killing capacity, which would end up with chronic pulmonary infection leading to pneumonia and ultimately respiratory failure (Winstanley et al., 2016). Upper airways, like nose and sinus, are also invariably affected by CF, but it has been found somehow sustaining lower infections than lower airways (Rafeeq and Murad, 2017, Castellani and Assael, 2017). For the respiratory system, the infection and chronic bacterial colonisation of the lung can be prevented and controlled by rational usage of antibiotics. MRSA, one of the prevalent infectious human pathogens, colonising the respiratory tract and responsible for severe infection in people with CF. In addition, the bacterium *Pseudomonas aeruginosa* permanently colonises cystic fibrosis lungs despite the aggressive use of antibiotics, which employs some strategies that promote chronic pulmonary colonisation instead of acute infection (Murray et al., 2007). Indicated for the chronic pulmonary infection due to *P. aeruginosa*, Cayston was designed and approved as the first CF medicine in 2009, followed by four other antibiotics (Ponzano et al., 2018). A large number of AMPs discovered from natural sources have demonstrated remarkable biological efficacy and retained potent antimicrobial activities in physiological salt and divalent cation environment, which showed great potential as alternatives to antibiotics for chronic lung infection of CF patients.

1.3.2 Immunity Modulation

Many species of life contain cationic antimicrobial peptides as components of their immune systems. The antimicrobial activity of these peptides has been studied extensively, and many peptides have a broad spectrum of activity not only against Gram-positive and Gram-

negative bacteria but also against antibiotic-resistant bacteria, fungi, viruses, and parasites. Such cationic antimicrobial peptides can also act in synergy with host molecules, such as other cationic peptides and proteins, lysozyme, and also conventional antibiotics, to kill microbes (Drago-Serrano et al., 2018). It has been found that certain peptides are produced in large quantities at sites of infection/inflammation, and their expression can be induced by bacterial products such as endotoxic lipopolysaccharide (LPS) and proinflammatory cytokines, such as tumor necrosis factor-α (TNF-α) (Radek and Gallo, 2007). These peptides often have a high affinity for bacterial products, such as LPS, allowing them to modulate the host response and reduce the inflammatory response in sepsis. More recently, they have been found to interact directly with host cells to modulate the inflammatory process and innate defenses.

1.3.3 Oncology

Excepting multidrug-resistant bacterial infections mentioned above, oncology is another disease that drive the therapeutic use of bioactive peptides (Prado Montes de Oca, 2013, Shin et al., 2016). Cancer inflicts a serious global public health problem as it represents a rising morbidity and mortality as well as the significant economic burden. Regardless of advancements in chemotherapy and cancer supportive care, the high risk of cancer recurrence has necessitated the ongoing search for novel therapies (Bosso et al., 2018). Owing to their good efficacy, safety and tolerability along with high selectivity and potency, peptide-based therapeutics have attracted great interest for development as drug candidates (Scorciapino et al., 2017). Anticaner peptides can be divided into two major groups regarding the cell targets. The former comprises peptides active against microbial and cancer cells

rather than normal mammalian cells, for example cecropins and magainins, while the latter consists of all peptides that act against all three types of cells including microbial, cancerous and normal ones (Boohaker et al., 2012). Still there are several intrinsic weaknesses like poor chemical and physical stability and being prone to hydrolysis and oxidation that make these naturally occurring anticancer peptides not directly suitable for clinical use (Mishra et al., 2017). Thus rational design can start with a known anticancer peptide, with the advance of SAR about therapeutic peptides.

1.4 Aims and Objectives of this Thesis

1) To isolate and chemically-characterise novel bioactive peptides either from lyophilised skin secretion of *Phyllomedusa coelestis* or dried root of *Trichosanthes kirilowii*.
2) To screen for pharmalogical activities using synthetic replicates of each peptide in a battery of bioassys, including antimicrobial assay, cell proliferation assay and haemolysis assay.
3) Cloning of peptide precursor-encoding cDNAs of cDNA libraries.
4) To study the mode of action of cationic AMPs by time killing assay and dynamic membrane permeability assay.
5) To rationally design peptide analogues with a higher selectivity between the target and mammalian cells.

Chapter 2

General Methods

2.1 Specimen Biodata and Secretion Harvesting

Specimens of *Phyllomedusa coelestis* (n=3) were obtained from commercial sources in the United States. They were conditioned for 4 months prior to secretion harvesting. They were housed in our purpose-designed amphibian facility at 20-25 ℃ under a 12/12 h light/dark cycle and fed with multivitamin-loaded crickets three times per week. Defensive skin secretions were acquired using gentle transdermal electrical stimulation (5V, 100Hz, 140ms pulse width). A bipolar electrode of 21G platinum was placed on the dorsal skin of the frogs every 10 s until the secretion was visible. A stream of ddH_2O was used to rinse off the resulting secretion, which was collected into a glass beaker. Lastly, it was snap-frozen with liquid nitrogen, lyophilised and preserved at -20 ℃ before analysis.

2.2 Molecular Cloning

2.2.1 mRNA Isolation

Polyadenylated mRNA was isolated from the lyophilised skin secretion by using the Dynabeads® mRNA DIRECT™ Kit (Invitrogen, Lithuania). After the preparation of lysate from *Phyllomedusa coelestis* skin secretion, the supernatant of the lysate was transferred to the tube that contained the Dynabeads Oligo$(dT)_{25}$, which allowed the Poly-A tail of mRNA to hybridise to the bead-bound oligo-dTs through A-T base pairing. Thereafter, the beads combined with mRNA were washed three times with 500 µl Washing Buffer A and then twice with 500 µl Washing Buffer B. The elution of mRNA from the beads was achieved by adding18 µl Tris-HCl to the mRNA/bead complex. The tube was incubated at 80 °C for 2

min later and placed immediately on the magnet device. Finally, the supernatant was transferred to a new RNase-free 0.2 ml PCR tube and kept on ice immediately.

2.2.2 cDNA Library Construction

The isolated polyadenylated mRNA was reverse transcribed by means of a BD SMART^{TM} RACE cDNA Amplification Kit (Clontech, UK) following the protocol for first-strand cDNA synthesis. The mixture was incubated at 70 °C for 2 min and cooled down on ice for 2 min. Then, Master Mix was added to each reaction tube which will be incubated at 42 °C for 1.5 h in a hot lid thermal cycler.

Table 2.1 Components of each tube for 3'/5'-RACE-Ready cDNA

Reagent	Volume	Final concentration
mRNA sample	4 µl	40%
3'-CDS primer (10 µM)	1 µl	1 µM
5'-CDS primer (10 µM)	1 µl	1 µM
SMART II (10 µM)	1 µl	1 µM
5×First-Strand Buffer	2 µl	1×
DTT (20 mM)	1 µl	2 mM
dNTP Mix (10 mM)	1 µl	1 mM
BD RTase (100Unit/µl)	1 µl	10 Unit/µl

After the incubation step, the reaction mixture was diluted by adding 50 µl PCR water each tube, and all the tubes were heated at 72 °C for 7 min. Synthesised cDNA was used as the template for RACE PCR and can be stored at -20 °C for up to three months.

2.2.3 RACE PCR

The library was subjected to rapid amplification of cDNA ends (RACE) procedures using a BD SMART™ RACE cDNA Amplification Kit (Clontech, UK) following manufacturer's instructions.

Table 2.2 Components in each tube of sample group in RACE PCR

Reagent	Volume	Final concentration
PCR-Grade Water	3.1 µl	
10×BD Advantage 2 PCR Buffer	1.5 µl	1.5×
dNTP Mix (10 mM)	0.2 µl	0.2 mM
NUP (20 µM)	0.5 µl	1 µM
Sense Primer (20 µM)/Anti-sense primer	0.5 µl	1 µM
50×BD Advantage™ 2 Polymerase Mix	0.2 µl	1×
cDNA library	5 µl	10-1000 ng/µl

*The 3' RACE-Ready cDNA templates were substituted with water in the negative control.

The RACE polymerase chain reaction (PCR) programme was as follows: initial denaturation at 94 °C for 60 s; followed by additional 40 cycles: denaturation at 94 °C for 20 s; primer annealing at 55 °C for 10 s; extension at 72 °C for 240 s; and ended with a final extension phase at 72 °C for 10 min.

2.2.4 Gel Analysis for RACE PCR Products

The resultant PCR products were analysed by electrophoresis on a 1.3% (w/v) alkaline agarose gel. 2.5 µl 100bp DNA Ladder (BioLabs, UK) were loaded into the first well, while 1.5 µl of each PCR product were mixed with 0.5 µl loading dye and 2 µl mixture were added to each well of the gel. The gel was run at 90 Volts for about 30 min until the dye front

migrated approximately two-thirds of the way down the gel, after which the gel was viewed by an electronic UV Transilluminator (Ultra-Lum Inc) and the image was taken and saved.

2.2.5 Purification of RACE PCR Products

The PCR products were rapidly purified using E.Z.N.A.® Cycle Pure Kit (Omega Bio-Tek, USA) as described in the instruction manual. Briefly, 5 volumes of CP Buffer and 1 volume of the sample were mixed and added to Hi-Bind® DNA Mini Column with a 2 ml collection tube outside. After the cartridge was centrifuged at 15,000 × g for 1 min, the filtrate was discarded and the collection tube was reused. After being washed by DNA Wash Buffer, the Hi-Bind® DNA Mini Column was transferred to a new RNase-free 1.5 ml tube. DNA elution was the last period and was performed by adding 30 µl PCR-Grade Water directly to the centre of column matrix and sitting at room temperature for 2 min. The cartridge was centrifuged at 18,000 × g to elute purified DNA for 2 min afterwards, and the mini column was discarded. At last, the tube was placed into concentrator to dry for up to 3 hours.

2.2.6 Ligation

A pGEM®-T and pGEM®-T Easy Vector (Promega, USA) kit was used for ligation, transformation, blue and white colony screening and isolation of recombinant DNA reactions. The vectors with a 3' single terminal thymidine (T) in the insertion site were re-cyclized with a single guanosine (A)-ending DNA sequence derived from Taq DNA Polymerase through A-T base pairing. The following prepared reagents were combined and mixed without pipetting in a DNase-free PCR tube.

Table 2.3 The components of the ligation reaction

Reagent	Volume	Final concentration
2 × Rapid Ligation Buffer	2.5 µl	1×
pGEM®-T Easy Vector (50 ng/µl)	0.5 µl	5 ng/µl
Diluted PCR products	1.5 µl	10-1000 ng/µl
T4 DNA Ligase (3 Unit/µl)	0.5 µl	0.3 Unit/µl

The reaction was incubated for 1 hour at room temperature and kept incubating overnight at 4 °C for the maximum number of transformants.

2.2.7 Transformation

Eight LB plates with ampicillin/IPTG/X-Gal were prepared before transformation: 100 µl IPTG plus 20 µl X-Gal (Promega, USA) were added to each LB plate with ampicillin and spread symmetrically with a disposable spreader. All Petri dishes were stored at 4 °C after them solid and equilibrated to room temperature before use.

Two point five microliter ligation products and 50 µl JM109 cells were added to an RNase-free 1.5 ml tube on ice. The reaction tube was flicked gently to mix and placed on ice for 20 minutes, after which the cells were heat-shocked for 47 s using a heating block at exactly 42 °C, and the tube was immediately returned to the ice for at least 2 minutes. 950 µl of S.O.C medium were added to the tube before it was put in the incubator for 1.5 hours at 37 °C with shaking (~150 rpm). After these steps, 120 µl of transformation culture in the

reaction tube were plated on each of five plates. At last, these plates were incubated upside down overnight (14~15 hours) at 37 °C.

2.2.8 White and Blue Colony Screening

The upper air of the operation table was disinfected with a moving Bunsen burner, also the table surface was cleaned by means of an alcohol bottle and tissues before inoculating. Pure white colonies were chosen for inoculating and labelled obviously. The bottoms of three LB plates with ampicillin/IPTG/X-Gal were lined and divided into eighteen plots. The inoculating loop was fired for sterilising and cooled down by shaking softly (temperature of the inoculating loop can be tested using the 18th plot), followed by dipping one white colony lightly and drawing a continuous curve in a prepared Petri dish. This step was repeated until all white colonies were inoculated. After inoculation, Petri dishes were kept in incubator upside down for 14~15 hours at 37 °C.

2.2.9 Isolation of Recombinant DNA from JM109 Cells & Cloning PCR

The white colonies were chosen and labelled obviously. The bacteria were scraped by tips and transferred to each RNase-free 1.5 ml tube containing 20 µl of PCR-Grade water. Two temperature extremes were used from heating up to 100 °C for 5 min then immediately cooling down on ice for 5 min to make the cells fragile. Then, each tube was vortexed for 30 s and centrifuged at 20,000 × g for 5 min to break the cell walls and release the vectors. Finally, the supernatant which contained recombinant DNA were ready to use.

Table 2.4 Components of each tube in cloning PCR

Reagent	Volume	Final concentration
5×Cloning Buffer	10 µl	1×
dNTP Mix (10 mM)	1 µl	0.2 mM
$M_{13}F$ (20 µM)	2.5 µl	1 µM
$M_{13}R$ (20 µM)	2.5 µl	1 µM
PCR-Grade water	31 µl	
Taq polymerase (5 Unit/µl)	0.25 µl	0.025 Unit/µl
DNA supernatant	2.5 µl	10-1000 ng/µl

The cloning PCR programme was as follows: initial denaturation at 94 °C for 60 s; followed by additional 31 cycles: denaturation at 94 °C for 30 s; annealing at 55 °C for 30 s; extension at 72 °C for 180 s; and ended with a final extension phase at 72°C for 10 min and storage at 4°C prior to use.

2.2.10 Gel Analysis and Purification of Cloned PCR Products

Gel analysis and purification of cloned PCR products were performed as described before. According to the principle that the molecular weight was around 200 bp higher than the RACE-PCR result, the DNA band of the samples was compared with the ladder to determine whether the target DNA was of expected size or not. All the possible samples were stored at -20°C in the freezer.

2.2.11 Sequencing Reaction

DNA sequencing was carried out by means of Big Dye® Terminator v3.1 Cycle Sequencing Kit (Applied Biosystems, USA).

Table 2.5 Components in each sequencing reaction tube

Reagents	Volume
PCR-Grade water	12.4 µl
Diluted $M_{13}F$ or $M_{13}R$	1.14 µl
2.5×Ready reaction mix	2.86 µl
5×BigDye Sequencing Buffer	3.57 µl
Purified cloned PCR products	2.5 µl

The sequencing reaction PCR programme was as follows: initial denaturation at 96 °C for 60 s; followed by additional 26 cycles: denaturation at 96 °C for 20 s; annealing at 55 °C for 10 s; extension at 60 °C for 240 s; and ended with preservation at 4 °C for 7 min.

2.2.12 Purification of Extension Products

Ten microliters of deionized water were added to each RNase-free 1.5 ml tube first, and 72 µl of 95% ethanol (Sigma-Aldrich, USA) were added to each sequence reaction tube, followed by being transferred together with extension products to the 1.5 ml tubes. Then the tubes were vortexed briefly and incubated at room temperature for 20 min, after which they were centrifuged at 20,000 × g for 20 min, and the supernatant was immediately discarded. Next, 260 µl of 70% ethanol were added to each tube, and the tubes were vortexed for 30 s and centrifuged at 20,000 × g for 10 min. The supernatant was discarded quickly and the redundant liquid in the tubes was evaporated in a concentrator for at least 3 h.

2.2.13 Sequencing

Ten microliters of HiDi were added to each tube containing dried DNA fragments. Then, the tubes were vortexed for 30 s, centrifuged briefly and placed in a heating block at 95 °C for 4.5 min, followed by being put on ice for 3.5 min. Prior to transferring 10 µl of each sample to a 96-well sequencing plate, the tubes were centrifuged briefly. Finally, DNA was sequenced by an ABI 3730 automated sequencer (Applied Biosystems, USA).

2.3 Isolation and Identification of the Putative cDNA-Encoded Peptides from Skin Secretion

An additional 5 mg of lyophilised skin secretion was reconstituted in 1 ml of deionised water containing 0.05% (v/v) TFA. The sample was then centrifuged at 5,000 × g for 20 min and the supernatant was injected into a RP-HPLC system, followed by elution with a gradient programme from 0.05/99.95 (v/v) TFA/ddH_2O to 0.05/19.95/80.00 (v/v/v) TFA/ddH_2O/ACN in 240 min. The column effluent was monitored by UV absorbance at 214 and 280 nm, and fractions were collected automatically at 1 min intervals. Chromatographic fractions were then analysed by MALDI-TOF MS (Perspective Biosystems, USA) in positive detection mode using CHCA as the matrix. The system was calibrated with known peptide standards to a precision of ±0.1%. Peptides in fractions having identical molecular masses to that calculated for the peptide deduced from the cloned cDNA were then subjected to primary structural analysis by MS/MS fragmentation sequencing using an LCQ-Fleet electrospray ion-trap mass spectrometer (Thermo Fisher Scientific, USA).

2.4 Solid Phase Peptide Synthesis

2.4.1 Calculations and Weighing of Amino Acids, HBTU and MBHA Resin

The desired quantity of peptide was 0.3 mmol, suitably, each amino acid and HBTU should be at least 1.2 mmol (4-fold molar excess) to synthesise the sequence. According to its loading capacity, Rink Amide MBHA resin which contained an amide group for the C-terminus was calculated and weighed in a 30 ml reaction vessel.

2.4.2 Synthesis Using the Tribute Synthesiser

The peptides in this study were synthesised automatically using a Tribute Peptide Synthesiser (Protein Technologies, USA). The reaction vessel and pipeline were washed by DMF first, and then the Fmoc protecting groups were deprotected using 20% (v/v) piperidine in DMF. Each amino acid residue was activated and coupled using 11% (v/v) NMM in 89% (v/v) DMF combined with activator HBTU. After that, the peptide was synthesised from C-terminal to N-terminal. Finally, degassed DCM was employed for washing the resin/peptide complex after the synthesis reaction. The resin/peptide was dried in a vacuum desiccator overnight.

2.4.3 Cleavage Reaction

The dried resin/peptide powder was weighed and then placed into a 50 ml round-bottomed flask. After adding the cleavage cocktail which was prepared at 25 ml/g resin according to

the recipe: 94% TFA + 2% EDT + 2% TIS + 2% H_2O, the cleavage and deprotection reaction was performed at the room temperature for 2 h with stirring. Next, a Buchner funnel was employed to filter the complex, after which, the remaining solution was transferred to a 50 ml universal tube and Et_2O (stored in a refrigerator at -20 ºC) was supplemented up to 50 ml for the peptide precipitation in the freezer overnight.

2.4.4 Peptide Washing

The above tube was centrifuged at 5000 × g for 5 min to collect the precipitated peptide, followed by discarding the supernatant carefully and adding another 45 ml Et_2O. The procedure was repeated 3 times. The peptide was then dried in a tinfoil-covered tube pierced by a needle at room temperature.

2.4.5 Peptide Dissolving and Lyophilisation

Ten millilitres of Solution A (ddH_2O) were added to the dried peptide. If it was difficult to dissolve, another 5 ml Solution B (80% ACN + 20% H_2O) were used to dissolve completely. The tube was then snap frozen in liquid nitrogen and lyophilised using the Alpha 1-2 freeze-drying system (Martinchrist, Germany) for around 60 h. The product was preserved at -20 ºC.

2.5 Identification and Purification of the Chemically Synthesised Peptides

2.5.1 Purification of Peptides using RP-HPLC

A Cecil Adept CE4200 HPLC system (Amersham Biosciences) was employed to purify the peptide, which was eluted from a 1 cm × 25 cm Jupiter semi-preparative C-18 column (Phenomenex, UK) with a linear gradient formed from 100% Buffer A : 0% Buffer B to 0% Buffer A : 100% Buffer B in 80 min at a flow rate of 1 ml/min. The column effluent was continuously monitored to detect peptide bonds at a wavelength of 214 nm.

Before separation, the column was washed with Buffer B (TFA/ddH_2O/ACN, 0.05/19.95/80.00, v/v/v) for 30 min, and then it was equilibrated with Buffer A (TFA/ddH_2O, 0.05/99.95, v/v) for another 30 min. One milligramme of synthetic peptide was dissolved in 1 ml of Buffer A and Buffer B, which was then centrifuged for 15 min at maximum speed. Subsequently, 1 ml of supernatant was subjected to RP-HPLC and Powerstream HPLC software. Finally, the fractions were collected in polypropylene tubes (Starstedt, Germany) at every peak and subjected to MALDI-TOF MS analysis (as outlined in section 2.4.2).

2.5.2 Analysis of the Novel Peptides by MALDI-TOF MS

The molecular masses of peptides in reversed-phase HPLC fractions were obtained by a MALDI-TOF mass spectrometer (Voyager DE, PerSeptive Biosystems, Framingham, MA, USA) in positive detection mode. Internal mass calibration was verified using the standard

peptides corresponding with standard molecular masses to ensure high accuracy of ±0.1%. A volume of 2 µl from each HPLC fraction was loaded and spotted onto the MALDI ground-steel target plate and left to dry. Then 1 µl of excess matrix solution (CHCA in ACN/Water/TFA, 70/29.98/0.02, v/v/v) at a concentration of 10 mg/ml was added to the spot of each sample and left to dry. Then the plate was inserted into the instrument, and subsequently, a pulsed nitrogen laser (337 nm) was used to irradiate the sample spot triggering the molecules to be ionised and protonated. Based on the time-of-flight arriving at the detector, the ion was detected by its m/z which was proportional to the TOF. Finally, the pure peptide was identified and subjected to lyophilisation and biological activity assay.

2.6 MIC and MBC Assays

Ten types of microorganisms were employed in this thesis: a panel of reference bacteria (*S. aureus* NCTC 10788, *E. coli* NCTC 10418, MRSA ATCC 12493, *E. faecalis* NCTC 12697, *K. pneumoniae* ATCC 43816, *P. aeruginosa* ATCC 27853 and *C. albicans* NCYC 1467) and clinically isolated bacteria (MRSA B038 V1S1 A, MRSA B042 V2E1 A and *P. aeruginosa* B004 V2S2 B). All tests were performed with a peptide concentration range from 512-1 µM in two-fold dilution and the assays were done by triplicate.

2.6.1 Microorganism inoculation

One bead covered with bacteria on the surface was transferred from frozen stock into a 100ml flask containing with Mueller Hinton Broth (MHB) medium, and then the labelled flask was

incubated in the orbital incubator (Stuart, UK) at a speed of 150 rpm at 37 °C overnight (16-20 h).

2.6.2 Peptide preparation

Lyophilised peptide was weighed and dissolved in dimethyl sulphoxide (DMSO) to make the stock solution at a final concentration of 5.12×10^4 μM. Then 10 μl stock solution was double-diluted in the ratio of 1:1 in DMSO to prepare a range of gradient concentrations from 512×10^2 μM to 1×10^2 μM.

2.6.3 Subculture

Five hundred microlitres of bacterial suspension were transferred and grown in a pre-warmed McCartney bottle with 20 ml MHB medium. Then, the McCartney bottle was incubated in the orbital incubator (Stuart, UK) at 37 °C for several hours until the subcultured bacteria reached their respective logarithmic growth phases. The optical density (OD) value of the subcultured bacteria was measured at 550 nm wavelength by a UV spectrophotometer. In the following table, the appropriate OD values of the three kinds of microorganism cultures and their corresponding concentrations are given. One hundred microlitres of subculture suspensions of bacteria were transferred into 19.9 ml of pre-warmed MHB medium and dispersed completely in the Petri dish. In terms of *C. albicans,* 2 ml subculture suspension were transferred into 18 ml of pre-warmed MHB medium and mixed evenly to achieve the required concentration.

Table 2.6 The appropriate OD values for the three microorganisms used

Organism	Subculture incubation time	OD	Concentration (CFU/ml)
Gram-positive bacteria	1.5 h	0.23	1×10^8
Gram-negative bacteria	1.0 h	0.41	1×10^8
C. albicans	0.5 h	0.15	$1 \times 10^{\mathbf{6}}$

2.6.4 Minimum inhibitory concentration (MIC) measurements

One microlitre of peptide dilution in 7 replicates at each concentration was arranged in the wells of a 96-well plate and 99 μl adjusted bacterial suspension were also added into the wells. One hundred microlitres of adjusted bacterial suspension in 7 replicates were added as positive controls which tested the growth of the organisms and 100 μl of pre-warmed MHB medium in 7 replicates were added as negative controls (blank control). In addition, 1 μl DMSO and 99 μl adjusted bacterial suspensions in 7 replicates were added as vehicle controls to observe the impact of 1% DMSO on the growth of bacteria in the 96-well plate. Subsequently, the 96-well plate was incubated in the orbital incubator (Stuart, UK) for 5 min and then transferred into the incubator (Genlab Limited, UK) to culture at 37 °C overnight (16-20 h). Afterwards, the absorbance in each well was measured by the Synergy HT plate reader (BioTek, USA) at 550 nm wavelength. Finally, the minimum inhibitory concentration (MIC) value was obtained as the wells in which no growth of organism was detectable. Furthermore, the antimicrobial activity in the presence of 2, 5, 10 mM of $MgCl_2$ was investigated.

2.6.5 Viable cell counts

One hundred microlitres of adjusted bacterial suspension were transferred into the microtube with 900 µl phosphate-buffered saline (PBS) and mixed completely. Then, 10-fold dilutions of this were prepared including 10^{-1} to 10^{-6}. Next, 20 µl of culture in 3 replicates at each concentration were transferred and spotted onto the dried Mueller Hinton Agar (MHA) plate and incubated in the incubator (Genlab Limited, UK) at 37 °C overnight (16-20 h). Then the numbers of the bacteria in each drop were counted. Finally, the exact concentrations of bacteria were calculated using the following formula: $C= N/3 \times 50 \times 10^{n}$, where N represented the total quantity of the bacteria at each concentration while n was the ratio of dilution.

2.6.6 Minimum bactericidal concentration (MBC) measurements

Twenty microlitres of clear solution in 7 replicates were transferred, spotted onto a new MHA plate and then incubated at 37 °C overnight (16-20 h). Finally, the MBC value was obtained as that in which no colonies grew at the lower concentration.

2.7 Time Killing Assays

The time-killing curves were constructed to investigate the antimicrobial efficiency of peptides. The instantaneous viable cell count was evaluated according to the method adopted by Khan *et al.* (Khan et al., 2017). In brief, mid-log phase bacterial culture (10^7 CFU/ml) were inoculated into culture medium MHB containing peptides at the concentration of

2×MIC and incubated at 37 ºC with shaking (200 rpm). Appropriate time points were selected, as indicated, to observe the viable counts. The experiment was repeated once.

2.8 Dynamic Membrane Permeability Assay

Dynamic membrane permeability assay was conducted using SYTOX green to detect the interactions between antimicrobial peptides and bacterial cell membranes. Bacteria were inoculated in TSB (Gram-positive bacteria) or LB (Gram-negative bacteria) at 37 °C overnight, and then subcultured until reaching the logarithmic growth phase. Then, cell culture was centrifuged at 1000× g for 10 min at 4 °C to collect bacteria at the bottom, where after, bacterial cells were washed twice with 5% TSB in 0.85% NaCl solution. The pellet was resuspended with 5% TSB in 0.85% NaCl solution to obtain a cell concentration of 1×10^8 CFU/mL by measuring OD at wavelength 590 nm (Gram-positive bacteria: 0.7, Gram-negative bacteria: 0.65 and yeast: 0.9). Peptide concentrations of MIC, 2×MIC and 4×MIC were mixed with bacteria suspension in a 96-well black plate, followed by staining with SYTOX^{TM} green nucleic acid stain (Life technologies) dissolved in 5% TSB in 0.85% NaCl to a final concentration of 5 μM. The fluorescent intensity was measured with a Synergy HT plate reader (BioTek, USA) at an excitation and emission wavelength of 485 and 528 nm, respectively. Bacteria cells treated with 70% (v/v) isopropanol for 1 h were used as positive control. The dynamic membrane permeability assay was done by triplicate.

2.9 MBIC and MBEC assays

To quantify the biofilm formation of bacteria in the absence and presence of peptides, MBIC and MBEC assays were performed using 96-well microplates, and biofilm mass was evaluated by crystal violet staining assay. Besides, the clinical isolates, MRSA (B038 V1S1 A), MRSA (B042 V2E1 A) and *P. aeruginosa* (B004 V2S2 B) from cystic fibrosis (CF) patients, were employed in this study. Gram-positive bacteria were inoculated overnight in TSB, while the Gram-negative bacteria formed in LB, and then sub-cultured until reaching the logarithmic growth phase by measuring OD of the cultures at wavelength 550 nm. For MBIC assay, a suspension of broth-diluted bacteria culture (5×10^5 CFU/ml) was incubated with the peptide solutions whose final concentration range from 1 to 256 μM in a 96 well flat-bottomed microtiter cell culture plate at 37 °C for 24 h. For MBEC assay, 100 μl inoculum culture (5×10^5 CFU/ml) was seeded to a 96-well-flat-bottom plate and incubated at 37 °C for 48 h to obtain the mature biofilm. Afterwards, the plate was washed by sterile PBS twice and treated with a series of peptide solutions at 37 °C for 24 h. Then, all the plates were washed with PBS, fixed with methanol for 10 min, stained by 125 μl 0.1% crystal violet solution for 30 min (Sigma-Aldrich, UK), and washed with PBS again until no apparent stain was observed. Evaporating crystal violet stain was further dissolved by 30% acetic acid (Sigma-Aldrich, UK). The absorbance values of each well were recorded by Synergy HT plate reader (BioTek, USA) at 595 nm. The minimum concentration that inhibits the formation of biofilm is defined when compared to the negative control group as MBIC. The minimum concentration that eradicates the biofilm is defined when compared to the negative control group as MBEC. The biofilm assays were done by triplicate.

2.10 Cell Proliferation Assays

2.10.1 Resuscitation of Frozen Cell Lines

The cell lines, PC-3 (ATCC® CRL-1435™, human prostate carcinoma), NCI-H157 (ATCC® CRL-5802™, non-small cell lung cancer), BxPC-3 (ATCC® CRL-1687™, adenocarcinoma), U251MG (ECACC 09063001, human neuronal glioblastoma) were retrieved from the -80 ºC freezer and thawed rapidly in the 37 ºC water bath with continuous stirring, after which the cells were added into the flask with specific pre-warmed growth medium, and incubated at 37 ºC with 5% CO_2.

The PC-3, NCI-H157 and BxPC-3 were cultured in RPMI-1640 medium (Invitrogen, Paisley, UK), whereas U251MG was cultured in DMEM with high glucose (25 mM) (Sigma, St. Louis, MO, USA). Importantly, both the 10% FBS (Sigma, UK) which provided nutrition for cells growing and 1% penicillin streptomycin solution (Sigma, UK) which inhibited the growth of bacteria were also added into the medium.

2.10.2 Medium Changing

All the spent medium in the flask was pipetted out, PBS was used to wash the adherent cells, which was removed later and replaced with fresh growth medium.

2.10.3 Subculture of Adherent Cell Lines

After pipetting out the spent medium and washing with PBS, adherent cells were detached in the presence of trypsin for 2-5 min. The serum (FBS) in growth medium was employed to inactivate trypsin. The trypsinised cells were then centrifuged, resuspended in fresh growth medium and counted as below.

2.10.4 MTT Cell Proliferation Assays

2.10.4.1 Cell Quantification & Inoculation

Fifty microliters of 0.4% (w/v) trypan blue (Invitrogen, UK) was mixed with the same volume of cell suspension. After being added to the pre-cleaned counting area between the haemocytometer chamber and the coverslip by capillary action, the stained cells in a specific chamber were counted with the assistance of an inverted microscope and counter. The cell density was calculated using the formula below (where N represented the total quantity of counted cells, while n was the number of counted chambers):

$$\textbf{Cell Density (cells/ml)} = N/n \times 2 \times 10^4$$

Subsequently, the cell suspension was diluted with growth medium to achieve a concentration of 5×10^4 cells/ml, followed by being plated (100 µl) into each slot of a 96-well plate and incubated for 24 h.

2.10.4.2 Starvation

The nutrient medium was removed from each well and replaced by fresh medium without FBS, after which the cells were incubated for 6-12 h to starve the cells which can eliminate the impact of FBS in the parallel assay.

2.10.4.3 Dosing

Five milligrammes of pure lyophilised peptide were weighed and dissolved in DMSO to make the stock solution with a final concentration of 10^{-2} M. Then, 70 µl of this stock solution were 10-fold diluted in 630 µl of pre-warmed FBS-free medium to achieve a range of concentrations: 10^{-3} to 10^{-9} M. All medium from the wells were discarded and 100 µl of peptide dilutions in 5 replicates at each concentration were loaded in the 96-well plate. Then, 100 µl of the pre-warmed FBS-free medium in 5 replicates were used as positive controls, and an equal volume of 1% DMSO solution were also added as vehicle controls which reflected the impact of 1% DMSO on the cell growth. Lastly, the 96-well plate was incubated at 37 ºC with 5% CO_2.

2.10.4.4 Addition of MTT & Detection

Ten microliters of MTT solution (5 mg/ml) (Sigma, UK) were added to each well in a dark environment and incubated for 4-6 h later. After removing all the solution, 100 µl of DMSO were added to each well, and then the plate was placed in a shaking incubator for 10 min before the detection of Synergy HT plate reader (BioTek, USA) at λ=540 nm.

2.11 Haemolysis Assays

The haemolysis assay was performed by mixing peptides with mammalian erythrocytes obtained from fresh defibrinated horse blood. An appropriate volume of horse blood was transferred and washed with PBS until the supernatant was clear. A series of peptide solutions were incubated with 2% suspension of red blood cells at final concentrations of 512 µM to 1 µM at 37 °C for 2 h. For positive and negative controls, the red blood cells were incubated with 1% Triton-X 100 and PBS, respectively. After incubation, 100 µl of the supernatant from each sample was transferred to a microtiter plate and the absorbance at 570 nm was measured with a Synergy HT plate reader (BioTek, USA). The percentage of haemolysis was calculated using the formula below:

$$\% \text{ Haemolysis} = (A\text{-}A_0) / (Ax\text{-}A_0) \times 100\%$$

where (A) is the OD value of the peptide containing suspensions, (A_0) is the OD value of the negative control, and (Ax) is the OD value of the positive control. The haemolysis assay was done by triplicate.

2.12 Molecular Modelling, Validation of Modelled Structure and Physicochemical Properties of the Peptides

The secondary structures and 3D models of the novel peptides were predicted through Iterative Threading ASSEmbly Refinement (I-TASSER) (http://zhanglab.ccmb.med.umich.edu/I-TASSER/). Moreover, the helical wheel plots and

physiochemical properties of the peptides were obtained from Heliquest (http://heliquest.ipmc.cnrs.fr/).

In addition, CD analyses were conducted using a JASCO J815 Spectropolarimeter (JASCO Inc., USA) and a quartz cuvette with a 1-mm path length. Each sample was analysed at 20 °C within the range of 190-260 nm. The parameters were set at 100 nm/min scanning speed, a bandwidth of 1 nm, and 0.5 nm data pitch and obtained using three passes ("accumulation"). Peptide samples were dissolved in 10 mM ammonium acetate buffer and 50% TFE in 10 mM ammonium acetate buffer at a concentration of 100 μM.

Chapter 3

Rational Design of Short Cell-Penetrating Peptides Based on A Novel Antimicrobial Peptide from the Defensive Skin Secretion of *Phyllomedusa coelestis*

Abstract

The broad-spectrum antimicrobial peptides (AMPs) have the prodigious potential to be an efficient alternative to antibiotics, for their selective disruption of bacterial membranes and low probability of drug resistance. Dermaseptin-PC (DM-PC), a novel broad-spectrum AMP, was discovered from the skin secretion of a South American tree frog (*Phyllomedusa coelestis*), using the combination of 'shotgun' cloning and tandem mass spectrometry fragmentation sequencing. DM-PC was then rationally modified with the objective of a higher therapeutic index. Here, truncated mimetics DMPC-19 and DMPC-10 were designed to improve selectivity against microorganisms. DMPC-19, causing less rupturing of erythrocytes, maintained the antimicrobial activity. However, both antimicrobial and haemolytic activities of DMPC-10 exhibited significant decreases. Furthermore, DMPC-10A, containing a substituted Cha at the C-terminus of DMPC-10, demonstrated potent yet selective bioactivity. Additionally, DM-PC, DMPC-19 and DMPC-10A not only rapidly killed the planktonic bacteria but also effectively eradicated the biofilm matrix as well as the sessile bacteria. In conclusion, with the optimisation of physicochemical characteristics of bioactive natural peptides, their bio-efficacy and therapeutic index can be enhanced. The study of DM-PC together with its analogues provides new insights on lead antibiotic drug discovery and design, especially against Gram-negative bacteria and resistant strains.

3.1 Introduction

Unlike in the so-called golden age of antibiotics, the pharmaceutical industry has been slow in the discovery and release of novel antimicrobial agents (Fair and Tor, 2014). At the same time, extensive drug-resistance in bacteria has been identified both in human and veterinary clinics (Allcock et al., 2017). A tremendous increase in population of drug-resistant bacteria has been witnessed in the past decade, arising from inappropriate use of antibiotics, for example, over-prescription of antibiotics, patients not finishing the entire antibiotic course and overuse of antibiotics in livestock and fish farming (Stanton, 2013). Consequently, the time has come for the discovery of new antibacterials to combat untreatable infections caused by multidrug-resistant bacteria.

Being part of the first line of defence, antimicrobial peptides are present in a wide variety of organisms ranging from prokaryotes to human beings (Ebenhan et al., 2014). So far, hundreds of naturally occurring AMPs have been isolated and characterized and are recognized for high efficacy, safety and tolerability (Cao et al., 2015, Fosgerau and Hoffmann, 2015). Given their propensity to interact with bacterial cytoplasmic membranes in a non-receptor way, AMPs have great potential to be broad-spectrum and suppress pathogen resistance at the same time (Yeaman and Yount, 2003, Vineeth Kumar and Sanil, 2017). Such advances about their modes of action have revealed new insights into the development of AMPs as a novel therapeutics to treat multidrug-resistant bacteria infections (Moravej et al., 2018, Zanjani et al., 2018).

A striking cocktail of peptides of amphibian skin secretion with antimicrobial, neuro, and hormonal activities have been revealed, especially those belonging to the subfamily Phyllomedusinae (Amiche et al., 2008). It is the diversity of these peptides that leads to the increasing capacity to respond to potential variance in ecological niches (Rodel et al., 2013). AMPs, the most varied class, include several distinct families (*Dermaseptin, Dermatoxin, Distinctin, Phylloseptin* and so on), working as a passive defence barrier (Amiche et al., 2000, Azevedo Calderon et al., 2011, Chen et al., 2005, Nicolas and El Amri, 2009). Most of them appear to target the cell membrane, whose elementary component is the phospholipid bilayer. Moreover, central nervous system active peptides (*Deltorphin* and *Dermorphin*) and smooth muscle active peptides (*Bradykinin*), respectively, cause the imbalance of predator homoeostasis (Zasloff, 2002). There is also a novel group of peptides termed *Hyposins*, whose bioactivity is still unknown (Azevedo Calderon et al., 2011). Regardless of the impressive variations in amphibian skin secretion, AMPs, emerging as an alternative antibiotic aimed at the infections caused by drug-resistant bacteria, have drawn a great deal of attention and interest (Caillon et al., 2013).

Dermaseptins, linear polycationic (lysine-rich) AMPs damaging plasma membranes, are found in the skin of *Phyllomedusa* frogs (Nicolas and El Amri, 2009). Generally, they are composed of 28-34 amino acids and structured in amphipathic helices in nonpolar solvents, which means these compounds undergo coil-to-helix transition upon binding to lipid bilayers (Castiglione-Morelli et al., 2005). Furthermore, they all share a signature pattern consisting of a conserved tryptophan residue at position 3 which is regularly preceded by AL- or GL-, an AG(A)K(Q)A(M)A(V)L(G)G(N/K)A(F)V(A/L) consensus motif in the mid-region or C-

terminal area, and positive charge owing to the presence of lysine residues which punctuate an alternating hydrophilic and hydrophobic sequence (Amiche et al., 1999).

In spite of sequence similarities, dermaseptins and their analogues still differ in the potency and spectrum of antimicrobial activities (van Zoggel et al., 2012). Overall, they perform an express and permanent lytic activity against various microorganisms *in vitro* and no toxic effects on mammalian cells, except dermaseptin-S4 analogues which have a powerful activity against human sperm (Amiche and Galanth, 2011). Sometimes other biological functions, having uncertain connections with the removal of pathogens, can be observed from this superfamily, for example, dermaseptin-B4 with insulin-releasing activity (Marenah et al., 2004).

In this study, a novel dermaseptin, named DM-PC, was identified from the skin secretion of *Phyllomedusa coelestis* by molecular cloning and MS/MS sequencing. DM-PC showed nonspecific bactericidal effects against ESKAPE pathogens but was observed to possess moderate haemolytic activity. Two truncated mimetics DMPC-19 and DMPC-10 were then designed for lower cytotoxicity. DMPC-19 maintained potent and broad-spectrum antimicrobial activity, while further reduction of helical domain resulted in a dramatic reduction in biological activity of DMPC-10. Besides, as peptides with substitution of Cha have more potential to fold into an amphipathic α-helical conformation when permeating lipid bilayer membranes (Rao et al., 2013), DMPC-10A was synthesised and found to be a possible drug candidate.

3.2 Materials and Methods

3.2.1 Acquisition of Skin Secretion of South American Tree-frog, *Phyllomedusa coelestis*

The skin secretion of the frogs was acquired by mild transdermal electrical stimulation through the dorsal skin, as described in Chapter 2.1.

3.2.2 Identification of Precursor-Encoding cDNA from the Skin Secretion

The prepropeptide encoding cDNA from the lyophilised skin secretion was achieved as described previously (Chapter 2.2).

3.2.3 Isolation of the Putative Mature Peptide from Skin Secretion

The isolation and identification of mature peptides in skin secretion were performed as previously described (Chapter 2.3).

3.2.4 Peptide Design

According to the structure-activity relationships of dermaseptins, shortening the chain length yielded peptide derivatives, DMPC-19 and DMPC-10, were designed for optimisation of physicochemical parameters. In addition, the incorporation of unnatural amino acid

generating DMPC-10A was expected for different physicochemical properties that are not available in peptides composed of the 20 naturally occurring RNA encoded amino acids, like high hydrophobicity and protease stability.

3.2.5 Molecular Modelling, Physicochemical Properties and Chemical Synthesis of the Peptides

The secondary structures and 3D models of the peptides were predicted through Iterative Threading ASSEmbly Refinement (I-TASSER) (http://zhanglab.ccmb.med.umich.edu/I-TASSER/). Moreover, their helical wheel plots and physiochemical properties were obtained from Heliquest (http://heliquest.ipmc.cnrs.fr/). In addition, the secondary structures of all peptides were examined by circular dichroism (CD) as described in Chapter 2.12. All peptides involved in this report were chemically synthesised by a standard solid-phase method (Chapter 2.4). The purification of DM-PC and it analogues were achieved by RP-HPLC and MALDI-TOF MS after lyophilisation.

3.2.6 Antimicrobial Assays

The antimicrobial activity of each synthetic peptide was evaluated by the standard microdilution assay described previously (Chapter 2.6). The medium for antimicrobial activity in the presence of salts was supplemented with different concentrations of Mg^{2+}.

3.2.7 Time Killing Assay

The instantaneous viable cell count was evaluated according to the method adopted by Khan *et al.* (Khan et al., 2017) as previously described (Chapter 2.7).

3.2.8 Dynamic Membrane Permeability Assay

Dynamic membrane permeability assay was conducted using SYTOX green as described in Chapter 2.8.

3.2.9 MBIC and MBEC Assays

To quantify the biofilm formation of bacteria in the absence and presence of peptides, MBIC and MBEC assays were performed using 96-well microplates, and biofilm mass was evaluated by crystal violet staining assay as described in Chapter 2.9.

3.2.10 Cell Proliferation Assay

The MTT assay was performed with a typical method described previously (Chapter 2.10).

3.2.11 Haemolysis Assay

The haemolysis assay was performed by mixing peptides with mammalian erythrocytes obtained from fresh defibrinated horse blood and carried out as previously described in Chapter 2.11.

3.3 Results

3.3.1 Identification and Characterisation of DM-PC from the Skin Secretion

A novel bioactive peptide precursor-encoding cDNA was consistently cloned from the *Phyllomedusa coelestis* skin secretion-derived cDNA library, using the 'shotgun' cloning strategy. The novel gene-encoded peptide was named DM-PC. As shown in Figure 3.1, the open reading frame of peptide precursor consists of 76 amino acid residues, which were divided into five definite domains including, a highly conserved putative signal peptide region containing 22 amino acid residues; an acidic amino acid residue-rich 'spacer' peptide region of 23 amino acid residues which contains 13 glutamic acid and aspartic acid residues; a typical –Lys-Arg- (-KR-) propeptide convertase processing site between the putative 'spacer' peptide and mature peptide; a putative mature peptide region containing 28 amino acid residues; a C-terminal glycine residue which acts as an amide donor to terminate the glutamine residue of the mature peptide and results in post-translational amide modification.

The deduced primary structure of DM-PC was subjected to bioinformatics analysis by means of NCBI Protein BLAST programme (https://blast.ncbi.nlm.nih.gov/Blast.cgi?PROGRAM=blastp&PAGE_TYPE=BlastSearch&LINK_LOC=blasthome), which found that DM-PC was a novel dermaseptin because of the obvious sequence homologies to other members of this family (Figure 3.2).

The fractionated skin secretion samples from RP-HLPC (Figure 3.3A) with identical molecular mass to that of the predicted mature peptide were further analysed by MS/MS fragmentation sequencing (Figure 3.3B,C), which validated the primary structure of DM-PC. Moreover, the y-ions of DM-PC were found to be 1 Da less than the calculated value, confirming the amidation modification at C-terminal end.

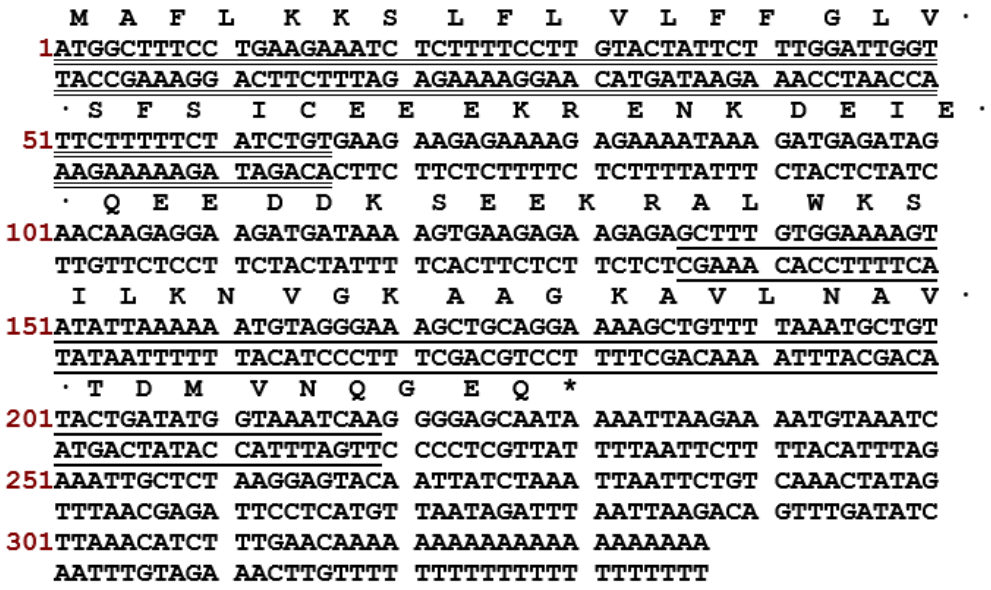

Figure 3.1 Nucleotide and translated open-reading frame amino acid sequences of a cloned cDNA encoding the biosynthetic precursor of DM-PC. The putative signal peptide sequence is double-underlined, while the putative mature peptide sequence is single-underlined, and the stop codon is indicated by an asterisk.

```
DM-PC                1-ALWKSILKNVGKAAGKAVLNAVTDMVNQ-28
Dermaseptin-2        1-ALWKDILKNVGKAAGKAVLNTVTDMVNQ-28
Dermadistinctin-L    1-ALWKTLLKNVGKAAGKAALNAVTDMVNQ-28
Dermaseptin-J9       2- LWKSLLKNVGKAAGKAALNAVTDMVNQ-73
Dermaseptin-B4      46-ALWKDILKNVGKAAGKAVLNTVTDMVNQ-73
```

Figure 3.2 Alignments of cDNA-deduced open-reading frame amino acid sequences of DM-PC and top NCBI BLAST analytes. Fully-conserved residues are shaded in black.

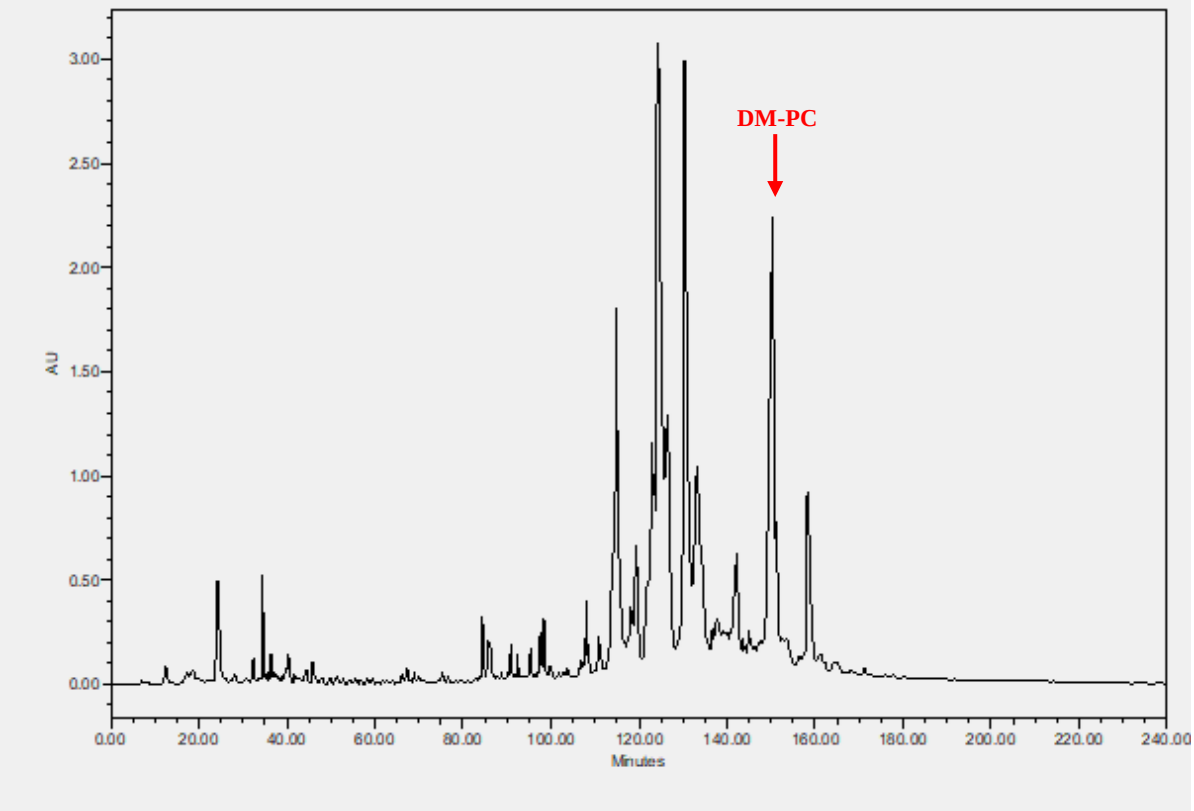

(A)

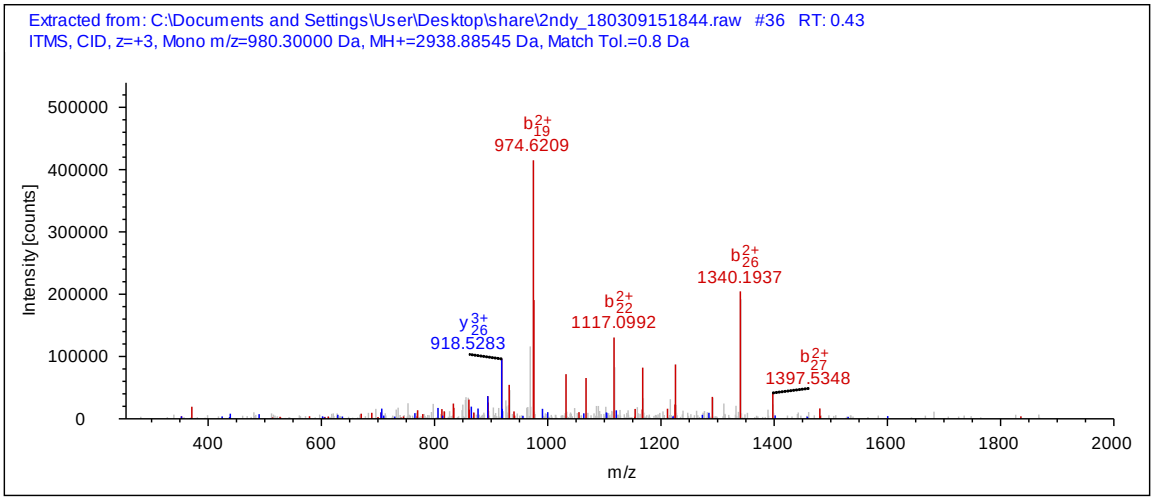

(B)

#1	b(1+)	b(2+)	b(3+)	Seq.	y(1+)	y(2+)	y(3+)	#2
1	72.044	36.526	24.686	A				28
2	185.128	93.068	62.381	L	2867.629	1434.318	956.548	27
3	371.208	186.108	124.407	W	2754.545	1377.776	918.853	26
4	499.303	250.155	167.106	K	2568.466	1284.736	856.827	25
5	586.335	293.671	196.116	S	2440.371	1220.689	814.128	24
6	699.419	350.213	233.811	I	2353.339	1177.173	785.118	23
7	812.503	406.755	271.506	L	2240.254	1120.631	747.423	22
8	940.598	470.803	314.204	K	2127.170	1064.089	709.728	21
9	1054.641	527.824	352.218	N	1999.075	1000.041	667.030	20
10	1153.709	577.358	385.241	V	1885.033	943.020	629.016	19
11	1210.731	605.869	404.248	G	1785.964	893.486	595.993	18
12	1338.826	669.916	446.947	K	1728.943	864.975	576.986	17
13	1409.863	705.435	470.626	A	1600.848	800.927	534.287	16
14	1480.900	740.954	494.305	A	1529.811	765.409	510.608	15
15	1537.921	769.464	513.312	G	1458.773	729.890	486.929	14
16	1666.016	833.512	556.010	K	1401.752	701.380	467.922	13
17	1737.053	869.030	579.689	A	1273.657	637.332	425.224	12
18	1836.122	918.565	612.712	V	1202.620	601.814	401.545	11
19	1949.206	975.107	650.407	L	1103.551	552.279	368.522	10
20	2063.249	1032.128	688.421	N	990.467	495.737	330.827	9
21	2134.286	1067.647	712.100	A	876.424	438.716	292.813	8
22	2233.354	1117.181	745.123	V	805.387	403.197	269.134	7

23	2334.402	1167.705	778.806	T	706.319	353.663	236.111	6
24	2449.429	1225.218	817.148	D	605.271	303.139	202.429	5
25	2580.470	1290.738	860.828	M	490.244	245.626	164.086	4
26	2679.538	1340.273	893.851	V	359.204	180.106	120.406	3
27	2793.581	1397.294	931.865	N	260.135	130.571	87.383	2
28				Q-Amidated	146.092	73.550	49.369	1

(C)

Figure 3.3 Identification of the specific AMP DM-PC derived from the skin secretion of *P. coelestis* (A) RP-HPLC chromatogram of skin secretion of *P. coelestis* monitored at 214 nm. The red arrow indicates the retention time of DM-PC. (B) Annotated MS/MS spectrum of DM-PC. (C) Predicted b- and y-ions arising from collision induced dissociation of the triply-charged (980.30 m/z, $[M+3H]^{3+}$) precursor ion. The observed b- and y-ions are indicated in blue and red typefaces.

3.3.2 Peptide Design

Here, DM-PC represents a fresh member of vertebrate AMPs, belonging to dermaseptins, and was utilised as a template to design a series of analogues. Two routes towards rational AMPs design were employed here. One was shortening the peptide chain length by trimming off decorative residues to make truncated mimetics antibacterial. The other was the introduction of synthetic amino acid residues to further increase the antibacterial potency of these small peptides.

It is widely accepted that strong basicity and potential amphipathicity of dermaseptins are extremely important and necessary for membrane permeabilisation to succeed (Table 3.1)

(Shai, 1999). However, the carboxyl-terminus of DM-PC, residues 19-28, is the only part that does not fit the regular pattern of amphipathicity. To be specific, although a high percentage of α-helical structure can be observed from this host defence peptide DM-PC not only through the secondary structure prediction (Table 3.1) but also through the CD spectrum (Figure 3.4B), the last ten amino acid residues disturb both the hydrophobic face and the positively charged (lysine-rich) hydrophilic face (Figure 3.4A). Besides, this undesired amino-terminal region contains an acidic aspartic acid residue which potentially reduces the interaction of DM-PC with negatively charged microbial membranes. Last but not least, 19 residues in an α-helical conformation are sufficient to span a phospholipid bilayer. As a result, one truncated analogue of DM-PC, DMPC-19, was expected to lead to a progressive recovery of the parent molecule. As shown in Table 3.1, this truncated mimetic not only carries more positive charges but also has a wider hydrophobic face than DM-PC. At the same time, DMPC-19 conserves the α-helical domain of the template peptide. Moreover, a large value of μH means that the helix is amphiphilic perpendicular to its axis. Consequently, shortening the chain length to residues 1-19 yielded peptide derivative, synthetic peptide DMPC-19, was employed for further explore this hypothesis.

On one hand, keeping critical amino acid residues for basicity and adopting helicity as an amphipathic conformation to further simplify DM-PC, like positively charged lysine, hydrophobic tryptophan, leucine and isoleucine, as well as the amidation of C-terminus (Mura et al., 2016), generated $L_2W_3K_4I_6L_7K_8K_{12}K_{16}$-$NH_2$. On the other hand, Feder et al. (Feder et al., 2000) demonstrated dermaseptin K_4-S4-(1-10)a, whose primary structure is ALWKTLLKKV-NH_2, was the shortest peptide whose charge-to-length ratio is most

favourable for potent yet selective antimicrobial activity, among a few analogues of dermaseptin S4. Two short artificial AMPs, DMPC-10 and DMPC-10A were therefore designed to enhance the membrane association, based on the vital amino acid residues of DM-PC along with the skelecton of dermaseptin K_4-S4-(1-10)a. Firstly, changing threonine into lysine increased positive net charge of dermaseptin K_4-S4-(1-10)a from +3 to +4, which could promote the initial interaction with negatively charged cell membranes. Furthermore, hydrophobicity of the nonpolar face of the amphipathic helix was rationally decreased or increased by replacing valine residue with less hydrophobic alanine residue or with more hydrophobic cyclohexylalanine (Cha) residue, respectively. Alanine, whose kdHydrophobicity is the lowest among hydrophobic amino acid residues, is known to be one of the simplest amino acids in terms of molecular structure and one of the most widely used for protein construction. The unnatural amino acid Cha, in which the benzene ring of Phe was replaced by cyclohexane, is similar to Phe in both size and shape, but with a higher hydrophobicity. Except as increased hydrophobicity, Cha can potentially confer proteolytic stability to degradation by carboxy- or amino- peptidases.

Table 3.1 Physicochemical properties of DM-PC and its analogues

	Primary Sequence	**Net charge**	**Hydrophobic moment (μH)**	**Hydrophobicity (H)**	**% Helix**
DM-PC	ALWKSILKNVGKAAGKAVLNAV TDMVNQ-NH_2	3	0.280	0.367	27.9
DMPC-19	ALWKSILKNVGKAAGKAVL-NH_2	4	0.411	0.433	9.7

DMPC-10	ALWKKLLKKA-NH_2	4	0.692	0.401	9.5
DMPC-10A	ALWKKLLKK-Cha-NH_2	4	NA	NA	29.6

Notes: Net charge, hydrophobicity and hydrophobic moment were predicted by Heliquest online tool. Because of the incorporation of the unnatural amino acid Cha, the hydrophobicity and hydrophobic moment of DMPC-10A were unpredictably online. The percentage of the α-helix structure was calculated from the CD spectra of each peptide in 50/50 (v/v) TFE/10mM NH_4Ac using BeStSel online software.

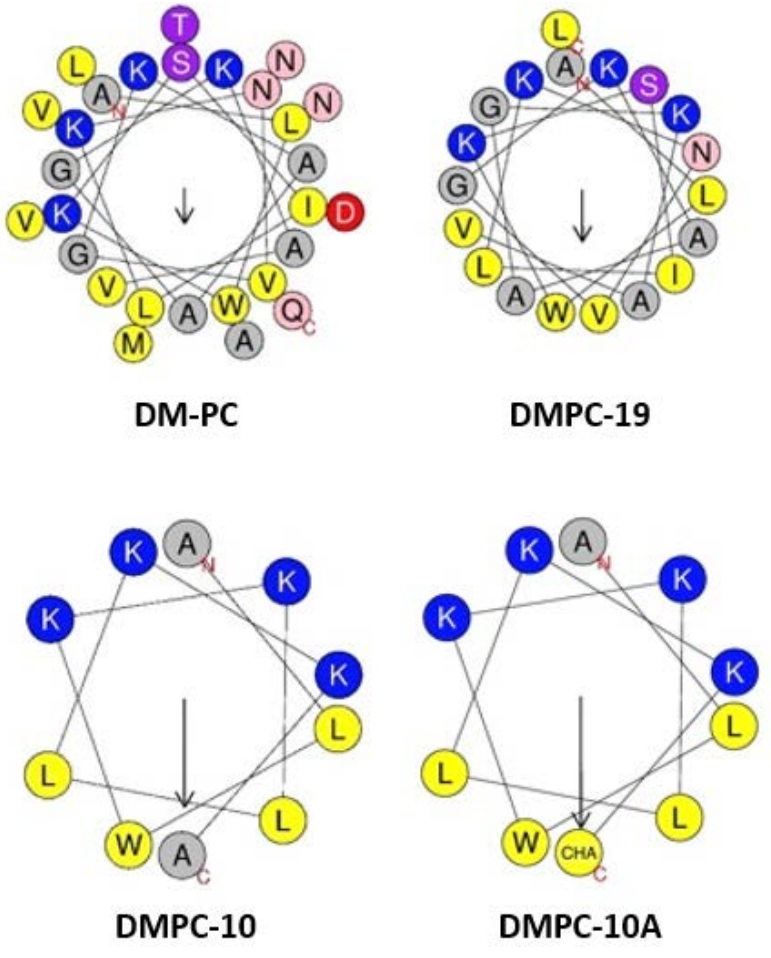

(A)

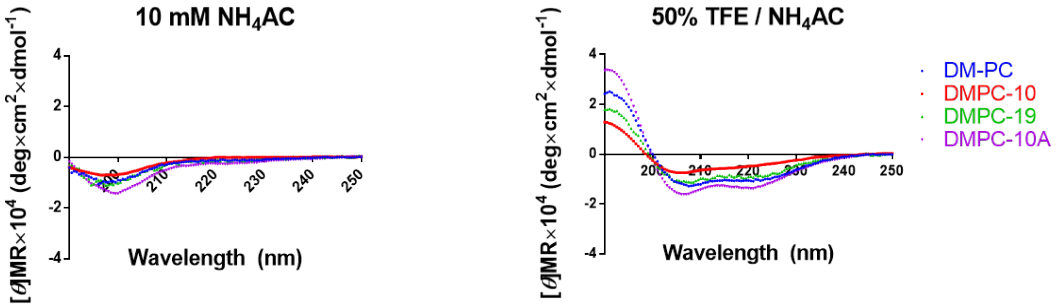

(B)

Figure 3.4 (A) Helical wheel projections of the four peptides DM-PC, DMPC-19, DMPC-10 and DMPC-10A with arrows indicating the direction of summed vectors of hydrophobicity. (B) Superimposition of CD spectra recorded for the four peptides (100 μM) in 10mM in ammonium acetate buffer and in 50% TFE ammonium acetate buffer.

3.3.3 Chemical Synthesis of Peptides

The solid phase peptide synthesis of DM-PC, DMPC-19, DMPC-10 and DMPC-10A was successful as determined by MALDI-TOF MS. As shown in Figure 3.5, the major single charged ions $[M+H]^+$ were consistent with their theoretical ones.

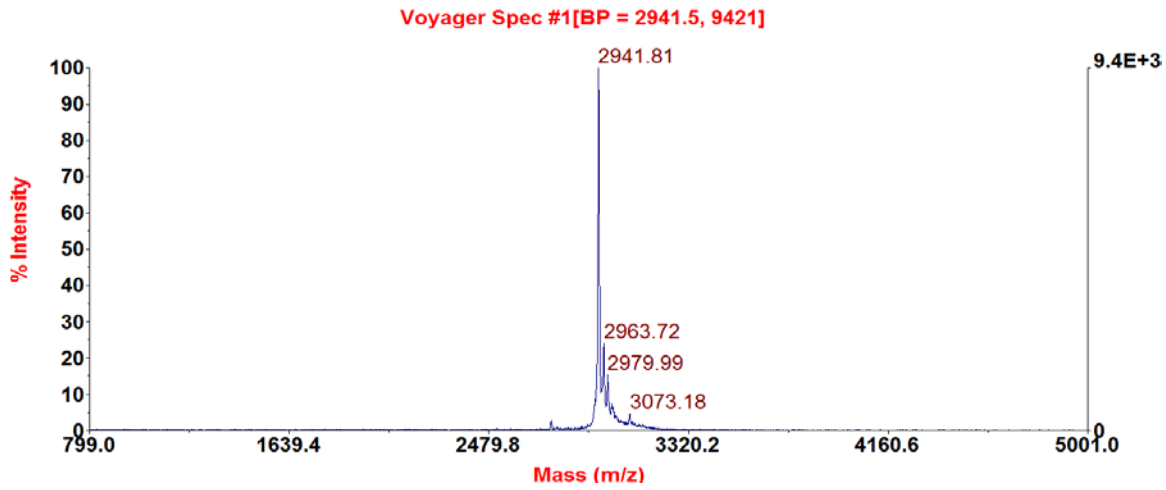
Voyager Spec #1[BP = 2941.5, 9421]
2941.81
9.4E+3
100
90
80
70
60
50
40
30
20
10
0
% Intensity
2963.72
2979.99
3073.18
799.0
1639.4
2479.8
3320.2
4160.6
5001.0
Mass (m/z)

(A)

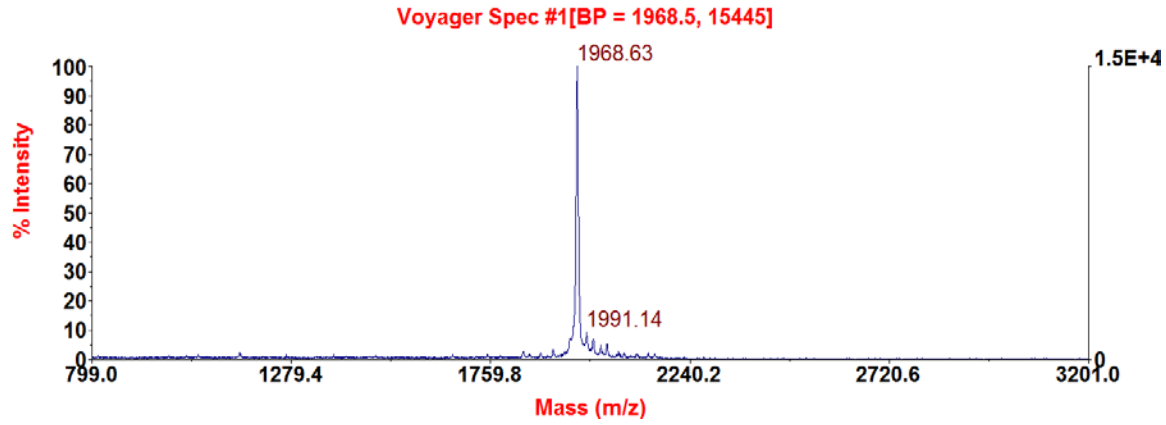
Voyager Spec #1[BP = 1968.5, 15445]
1968.63
1.5E+4
100
90
80
70
60
50
40
30
20
10
0
% Intensity
1991.14
799.0
1279.4
1759.8
2240.2
2720.6
3201.0
Mass (m/z)

(B)

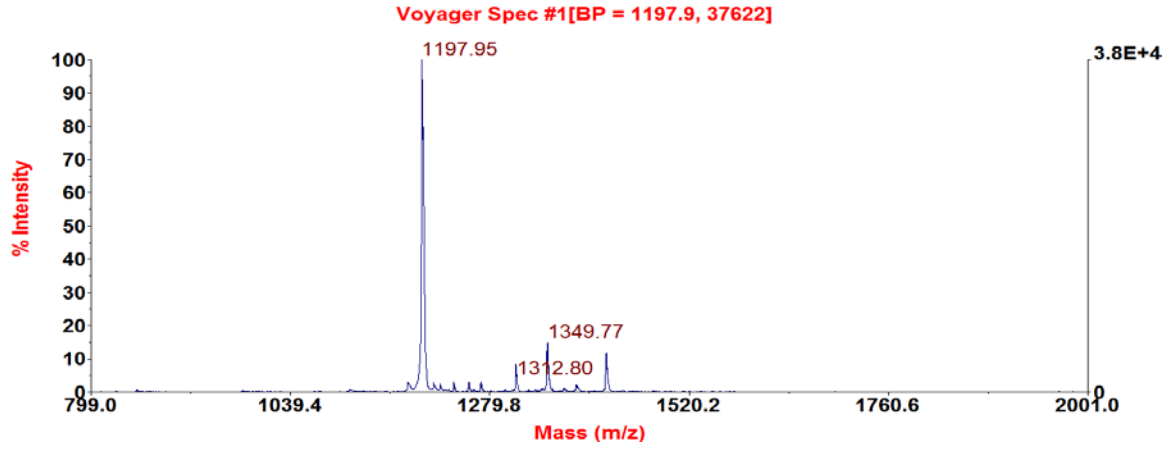
Voyager Spec #1[BP = 1197.9, 37622]
1197.95
3.8E+4
100
90
80
70
60
50
40
30
20
10
0
% Intensity
1349.77
1312.80
799.0
1039.4
1279.8
1520.2
1760.6
2001.0
Mass (m/z)

(C)

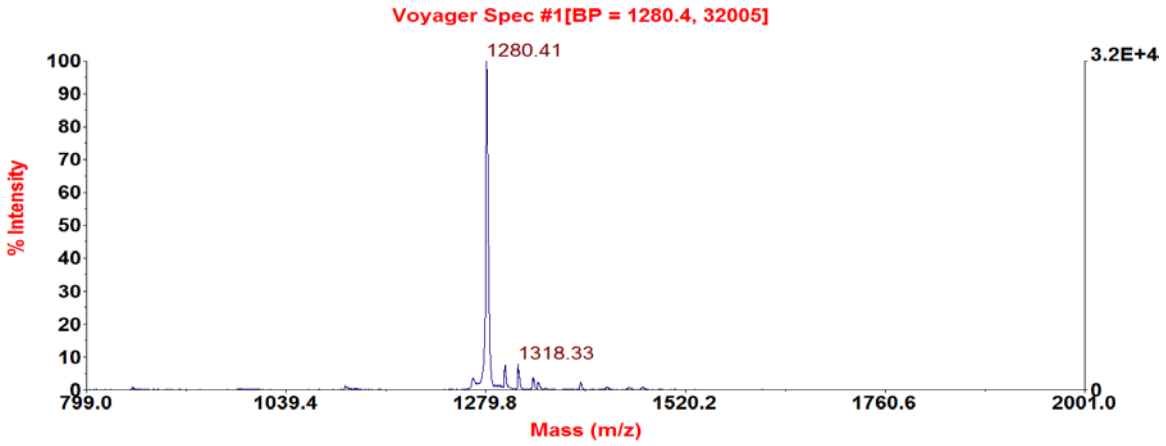

(D)

Figure 3.4 MALDI-TOF mass spectra of chemically-synthesised DM-PC (A), DMPC-19 (B), DMPC-10 (C) and DMPC-10A (D).

3.3.4 Antimicrobial Activities of DM-PC and Its Analogues

As represented in Table 3.2, both DM-PC and its truncated mimetic DMPC-19 demonstrated significant and nonspecific inhibitory effects against *S. aureus*, *E. coli* and *C. albicans*. Moreover, four drug-resistant pathogens (MRSA, *E. faecalis*, *K. pneumoniae*, *P. aeruginosa*) were not capable of resisting them. Compared with DMPC-10, DMPC-10A showed a promising antimicrobial activity against a panel of laboratory reference and clinically isolated Gram-positive and Gram-negative bacteria, some of which are multidrug resistant. In conclusion, two truncated mimetics, DMPC-19 and DMPC-10A, act as broad-spectrum AMPs without inducing a collateral damage to normal mammalian cells, which is promising for them to be considered as potential alternative antibiotics, especially given their high TI values.

One possible limitation with the clinical use of AMPs is their potential inactivation by salts present in the human body. Therefore, we tested the MICs of peptides against *P. aeruginosa* both in cation adjusted MHB and in regular MHB, for comparison (Table 3.3). In the presence of a physiological concentration of $MgCl_2$ (2 mM), a four-fold increase was observed in the MIC of DM-PC and a sixteen-fold increase in the MIC of DMPC-19. In summary, there is a rising trend of MIC values in the presence of higher concentrations of cations.

Table 3.2 MICs, MBCs and TI of ampicillin, DM-PC and its analogues against reference microorganisms

	MICs / MBCs (μM)				
	Ampicillin	**DM-PC**	**DMPC-19**	**DMPC-10**	**DM-PC10A**
S. aureus	0.1 / 0.1	2 / 4	2 / 8	64 / 128	4 / 8
E. coli	12.8 / 12.8	4 / 16	2 / 16	8 / 32	8 / 8
C. albicans	>512 / >512	2 / 8	2 / 16	64 / 128	4 / 8
MRSA	>512 / >512	2 / 4	8 / 64	512 / >512	8 / 16
E. faecalis	12.8 / 12.8	32 / 32	256 / >512	>512 / >512	64 / 64
K. pneumoniae	>512 / >512	8 / 64	32 / 128	>512 / >512	4 / 64
P. aeruginosa	>512 / >512	4 / 8	4 / 16	32 / 128	4 / 4
HC_{50}	>512	125.2	>512	>512	322.9
TI (overall)	13.08	28.35	128	8	44.56

Notes: The therapeutic index (TI) is a parameter indicating the relative safety of a drug. TI here refers to the ratio of the dose of drug that causes 50% haemolysis (HC_{50}) to the dose that leads to no apparent growth of the microorganism (geometric mean of MICs against

relevant bacteria). In addition, if HC_{50} or MIC were greater than the highest test concentration, twice the highest test concentration was used in the calculation (Irazazabal et al., 2016).

Table 3.3 Effect of $MgCl_2$ on MICs of cationic antimicrobial peptides for *P. aeruginosa*

Additive	Concentration (mM)	MICs (μM)	
		DM-PC	DMPC-19
None	0	4	4
Magnesium Chloride	2	16	64
	5	64	256
	10	> 256	> 256

3.3.5 Bacterial Killing Kinetics

In a time killing assay, DM-PC and DMPC-10A revealed a potent bactericidal effect on *P. aeruginosa* at 8 μM. As depicted in Figure 3.5, there was a noteworthy and irreversible decrease of colony forming units after five minutes exposure to DM-PC. DMPC-10A drastically reduced the colony forming units to half in 45 min, followed by complete killing after 60 min. However, although DMPC-19 inhibited the growth of bacteria at 8 μM, it failed to eradicate them.

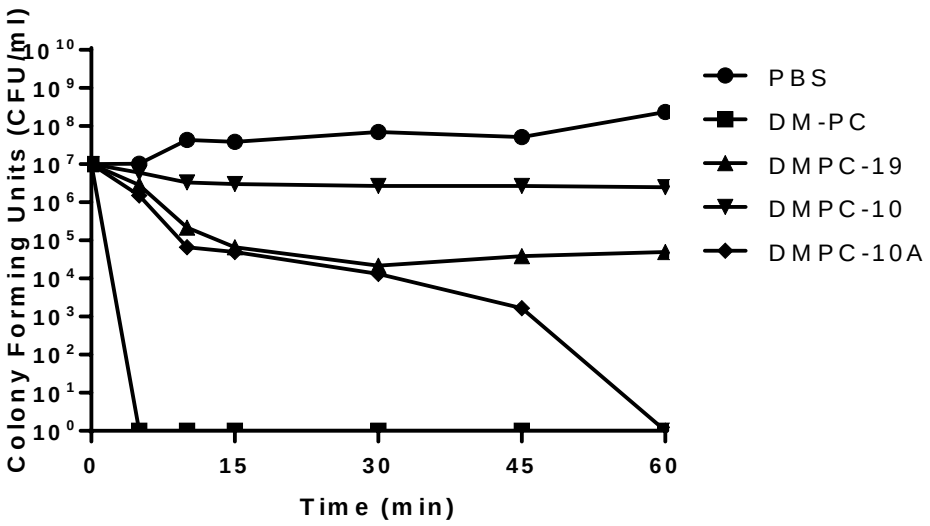

Figure 3.5 Killing effect of DM-PC and the derivatives at 8 µM against *P. aeruginosa* at various time intervals (n=1).

3.3.6 Dynamic Membrane Permeability Assay

The outer membrane of *P. aeruginosa*, whose permeability is 12-100 times less than that of *E. coli*, is a selective barrier to prevent the uptake of antibiotics (Shang et al., 2017). Therefore, investigations on the cell membrane permeabilisation of these peptides against *P. aeruginosa* was examined. DM-PC and DMPC-10A showed a significant membrane permeabilization effect against *P. aeruginosa*, however, the other two derivatives exhibited much weaker activity.

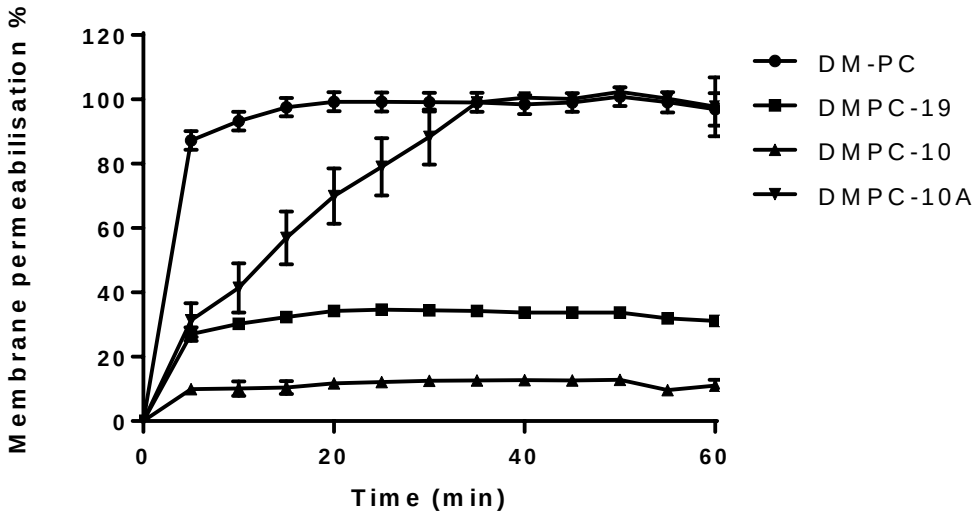

Figure 3.6 The membrane permeability of DM-PC and the derivatives at 8 μM. The percentage of membrane permeability was measured after induction by monitoring the fluorescence of SYTOX green. The error bar represents the standard error of three repeats.

3.3.7 MBIC and MBEC Assays

Herein, we employed MRSA and *P. aeruginosa* isolated from CF patients as models for studying the anti-biofilm activity of DM-PC and its derivatives. The natural peptide DM-PC, along with its truncated mimetics DMPC-19 and DMPC-10A, effectively inhibited the formation of biofilms, as well as eradicated mature biofilms. Their bioactivities were slightly reduced compared to those against planktonic bacteria (Table 3.4). However, DMPC-10 exhibited negligible effects on biofilms of MRSA and *P. aeruginosa.*

Table 3.4 The inhibition and eradication activity of DM-PC and its analogues against reference planktonic bacteria and their biofilms

MIC/MBC/ MBIC/MBEC	DM-PC	DMPC-19	DMPC-10	DMPC-10A
MRSA B038 V1S1 A	4/4/8/64	16/16/16/256	>512/>512/>512/>512	8/32/16/256
S. aureus B042 V2E1 A	4/4/4/32	8/16/16/256	256/>512/512/>512	4/16/4/128
***P. aeruginosa* B004 V2S2 B**	4/16/16/64	4/16/64/128	32/>512/512/>512	4/8/8/256
***P. aeruginosa* ATCC 27853**	4/8/16/32	4/16/64/128	32/128/512/>512	4/4/8/256

3.3.8 Anticancer Activities of DM-PC and Its Analogues

The natural peptide, DM-PC, exhibited potent inhibitory activity against the growth of BxPC-3 derived from adenocarcinoma. Besides, one of its truncated mimetics, DMPC-10A, demonstrated a weaker inhibitory effect on the proliferation of BxPC-3 at the same concentration.

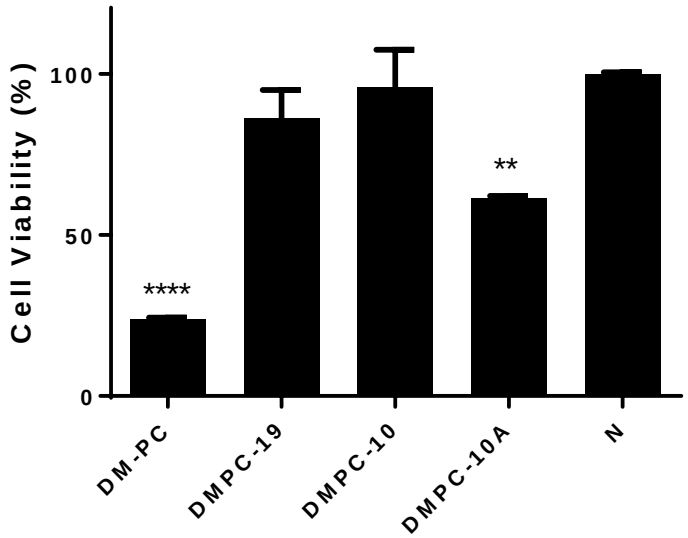

Figure 3.7 The proliferation of BxPC-3 after the treatment with DM-PC and its analogues at the concentration of 10 μM. The error bar represents the standard error of three repeats. **$p < 0.01$, ****$p < 0.0001$ significant difference between the test peptide and the negative control (PBS-treated).

3.3.9 Haemolytic Activities

DM-PC, that participates in the innate immunity of *Phyllomedusa coelestis*, has promising potential as a member of last generation antibiotics, as a result of its broad-spectrum antimicrobial activity. However, it is still cytotoxic for eukaryotic cells of horse (Figure 3.8), being a limitation for its use as medicines. Fortunately, its truncated mimetic DMPC-19 performed a better selectivity between microbial and host cells. DMPC-19 exhibited no significant haemolytic activity until 512 μM and roughly remained the antimicrobial activity of natural peptide DM-PC. On the other hand, DMPC-10 showed an extremely low haemolytic activity, since no appreciable cytotoxicity against horse erythrocytes was observed even up to the highest tested concentration of 512 μM. However, with the substitution of only one amino acid residue in C-terminus, DMPC-10A exhibited a significant increase in haemolytic activity because of the rising hydrophobicity.

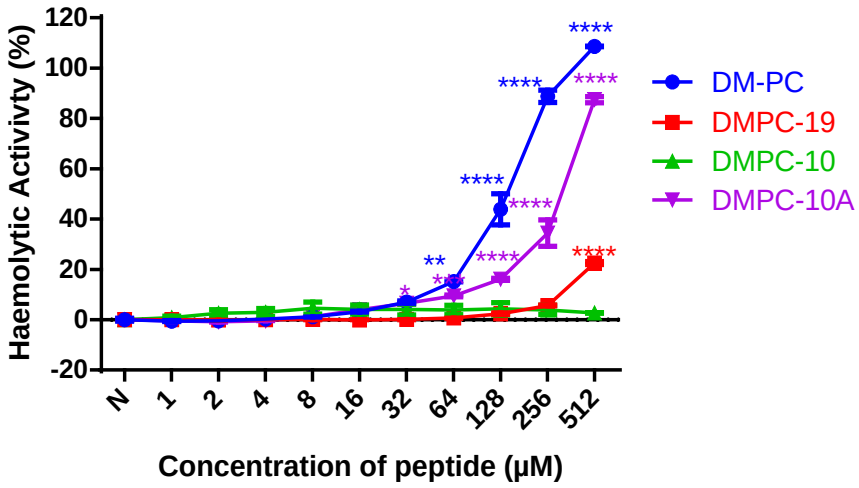

Figure 3.8 The haemolytic activities of DM-PC and its three analogues at concentrations ranging from 1 μM to 512 μM. The error bar represents the standard error of three repeats. *p < 0.05, **p < 0.01, ***p < 0.001, ****p < 0.0001 significant difference between the test peptide concentration and the negative control (PBS-treated).

3.4 Discussion

In this study, a novel AMP named DM-PC was isolated from the skin secretion of the leaf frog *Phyllomedusa coelestis*, and its full-length biosynthetic precursor-encoding cDNA was identified through 'shotgun' cloning. The putative mature peptide, DM-PC, which was then identified in the skin secretion by LCQ. DM-PC is a typical member of dermaseptins, as it possesses a conserved W residue at position 3, preceded by AL- and followed by an AGKAVLNAV consensus motif in the mid region. Similar with other dermaseptins, DM-PC demonstrated nonspecific inhibitory effects against wild-type bacteria strains as well as drug-resistant pathogens. Nevertheless, it is its cytotoxicity in mammalian erythrocytes that

becomes a major obstacle for DM-PC being a safe and effective therapeutic agent. Therefore, this 28-residue amphipathic α-helical antimicrobial peptide DM-PC was utilised as the template to design peptide analogues with a higher selectivity between the target and mammalian cells.

It was well confirmed that higher cationicity in a reasonable range is correlated with stronger cytolytic activity. A sufficient positive charge is vital for the peptides to be attracted to bacterial surfaces via electrostatic bonding, and there is an optimum cationicity window, usually +4 to +6, in which the electrostatic adsorption of AMPs to the negatively charged bacterial membrane surface could be achieved. Besides, hydrogen bonding between the side chains of cationic amino acid residues and lipid phosphate-rich membrane surface of the bacteria could facilitate the initial electrostatic attraction, stabilise the peptides in a hydrophobic environment and further enhance the insertion capacity of the peptides toward the hydrophobic bacterial membrane core, and finally enhance the potency of antibacterial activity. In this study, as a K-rich AMP, the amino groups of DM-PC are responsible for its strong basicity and the initial interaction with bacterial cytoplasmic membranes. Therefore, all lysine residues of the template peptide DM-PC were kept during rational peptide design. In expectation, the truncated mimetic DMPC-19, generated by the deletion of C-terminal end containing an acidic amino acid residue (aspartic acid) which resulted in an increase of the positive charge of peptide, demonstrated an overall rise in selectivity between microbial and red blood cells. Moreover, increasing with the metal ions around DM-PC and DMPC-19, the affinity between cationic AMPs like DM-PC and bacterial cell membranes would be weakened because of competitive inhibition, which finally affected their antibacterial

potency and indirectly proved that a higher charge can lead to more active peptides. Here, another practical modification to enhance the antimicrobial activity, in terms of charge, is replacing Lys with Arg, as the guanidinium groups of Arg residues could form stronger H-bonds than the amino groups of Lys residues.

Instead of producing a lowering in the antimicrobial potency of the peptide, the truncated mimetic DMPC-19 exhibited a close microbial inhibitory activity in comparison with the parent peptide DM-PC. So, it seems that the prerequisite for the antimicrobial activity of dermaseptins is the N-terminal helical domain rather than the C-terminal tail. Thus, we kept trimming off decorative residues from C-terminal end, and two artificial decapeptides were designed to find potent yet selective short AMPs. To be specific, hydrophobicity was rationally altered by replacing valine residue with less hydrophobic alanine residue (DMPC-10) or with more hydrophobic Cha residue (DMPC-10A) on the nonpolar face of the helix, respectively. The decreased antimicrobial activity of DMPC-10 can be explained by the interruption of the original nonpolar face by alanine, which is vital for bacterial cell membrane permeability. In contrast, with the substitution of Cha for the last amino acid residue Ala, a dramatic increase in antimicrobial activity as well as haemolysis rate could be observed. So, increased hydrophobicity had a positive effect on peptide access to both prokaryotic and eukaryotic membranes, and this was consistent with the predicted mode of action of linear amphipathic alpha-helical antimicrobial peptides that AMPs accumulated to a threshold concentration due to some affinities, and the hydrophobic residues could be inserted into the lipid bilayer of bacterial membrane, resulting in the formation of transient or prolonged transmembrane pores can not only lead to the final membrane disintegration

but also permit extra peptides to enter the membrane to work on intracellular targets and finally causing cell death. In conclusion, the integrity of the hydrophobic face of the amphipathic peptides played a decisive role on the bioactivity, and there was an optimum hydrophobicity window in which selective antimicrobial activity could be obtained. In addition, the results highlighted a significant role for the unnatural amino acid Cha at the ends of a peptide in increasing hydrophobicity, the percentage of α-helical content, and proteolytic stability to degradation by carboxy- or amino- peptidases.

Before interacting with the cytoplasmic lipid membrane, AMPs need to traverse a thick peptidoglycan layer as well as the lipoteichoic acids consisting of teichoic acids and lipoids in Gram-positive bacteria or pass through the LPS in Gram-negative bacteria (Malanovic and Lohner, 2016). Despite their thicker peptidoglycan layer, Gram-positive bacteria are more receptive to antibiotics than Gram-negatives, due to the absence of the outer membrane. However, DM-PC and its truncated mimetics showed nonspecific and rapid antimicrobial activity against these two diverse kinds of bacteria and even the yeast. Besides, the dynamic membrane permeability assay showed that DM-PC and its analogues permeabilised the bacterial cell membrane straightforward. Consequently, the N-terminal helical domain of dermaseptins is more likely to act as detergents, permeabilising membrane in a diffuse way. In other words, they perform a non-receptor type interaction with most membranes. Furthermore, we assume that their bacterial inhibitory activities are not mediated by interaction with specific receptors, which means DM-PC and its truncated mimetics could escape several certain mechanisms of resistance to AMPs.

Additionally, biofilm, a microbial community coated by an external polysaccharide matrix, could also lead up to poor drug penetration and finally antibiotic resistance. Hence DM-PC and its analogues were further investigated for their potential to suppress biofilm formation and disrupt pre-formed biofilm of drug-resistant pathogens. DMPC-19 and DMPC-10A demonstrated activity against biofilm formation but could not disrupt mature biofilms. This could indicate these peptides are binding to the surface of the bacteria to prevent their attachment to biotic or abiotic surfaces. The much more potent impact of DM-PC on biofilms, including mature biofilms, may be caused by the demonstrated cytolytic activity that could disrupt both biofilms and bacterial cells. To be specific, MRSA, one of the prevalent infectious human pathogens, colonising the respiratory tract and responsible for severe infection in people with CF. In addition, the bacterium *Pseudomonas aeruginosa* permanently colonises cystic fibrosis lungs despite the aggressive use of antibiotics, which employs some strategies that promote chronic pulmonary colonisation instead of acute infection (Murray et al., 2007). The outer membrane of *P. aeruginosa*, whose permeability is 12-100 times less than that of *E. coli*, is a selective barrier to prevent the uptake of antibiotics (Shang et al., 2017). Elimination of the biofilm formed by these CF clinical isolated strains means DM-PC and its active analogues could serve as effective alternatives to antibiotics against multiple-drug-resistant bacterial strains facing the chronic infections like CF. Furthermore, DM-PC and DMPC-10A showed an inhibitory effect on the proliferation of BxPC-3 derived from adenocarcinoma, in anticancer activity screening. Despite BxPC-3 do not express the CFTR, one point should be affirmed that there is a potential for DM-PC to be developed into a medicine for adenocarcinoma, which is a severe

CF complication. In that case, a CFTR positive pancreatic line, Capan-1, remains to be tested in the future.

Furthermore, NMR analysis showed that the helical structures were formed from the entire 16-mer and 13-mer dermaseptin S4 derivatives, but the 10-mer peptide was unable to fold in the 20% TFE environment (Kustanovich et al., 2002). Our data illustrated that DMPC-10 is able to form a helical structure in the 50% TFE environment. This might be explained by the difference of TFE % applied in the CD analysis. On the other hand, DMPC-10A possessed well-defined helical conformation in this study due to the presence of Cha, which has been reported to promote helices formation (Schnarr and Kennan, 2001).

Collectively, the results from our studies illustrate that two DM-PC-derived short cationic amphipathic α-helical peptides had great potential to replace the conventional antibiotics in the prevention and treatment of both chronic and acute infections of CF patients. One was DMPC-19 generated by trimming off decorative residues. The other was the artificial decapeptide DMPC-10A, containing an unnatural amino acid residue Cha which made it antibacterial. They have been shown to display comparable activity, superior selectivity between microbes and mammalian cells, unique membrane-disruption mechanism, suggesting that they represent a promising class of compounds for the eradication of multiple-drug-resistant bacterial strains. The balance of activity and cytotoxicity could be manipulated by the length, net charge, and the hydrophobicity at the C-terminus. This study

illustrates the possibility to design shorter derivatives from dermaseptin like peptides, which might benefit the discovery and development of new drug candidates.

Chapter 4

Role of Peptide Hydrophobicity in the Optimisation of the Antimicrobial Potency of α-Helical Antimicrobial Peptides

Abstract

It is noteworthy that host-defence peptides have evolved as highly potent alternatives to antibiotics, exerting powerful physiological effects and high susceptibility of multidrug-resistant strains. In this study, a novel phylloxin, named PLX-PC, derived from the subfamily Phyllomedusinae, was identified by molecular cloning. PLX-PC, like other peptides in this family, is a narrow-spectrum antimicrobial peptide, exhibited negligible activity against two Gram-positive bacteria *S. aureus* and MRSA. It was further modified by substitution of amino acids and truncating the effective part for higher potency and broader spectrum of antimicrobial activity. Three peptide derivatives, PLXPC-W13, PLXPC-14 and PLXPC-10, were designed for optimisation of physicochemical parameters, especially for an ideal hydrophobicity of the nonpolar face of the amphipathic α-helical peptides. After the modification, peptide analogues showed an overall rise in antimicrobial activity. Among the three analogues, PLXPC-14 displayed the most potent antimicrobial activity, with an overall TI of 9.52,which is a 25-fold improvement compared to that of the parent peptide. Moreover, the SAR study demonstrated that there is an optimum hydrophobicity window in which potent yet selective antimicrobial activity could be achieved. In summary, the study of PLX-PC together with its analogues provides new insights on lead antibiotic drug discovery and design, especially against Gram-positive bacteria and resistant strains.

4.1 Introduction

Antimicrobial peptides (AMPs) form part of the innate immune response, of many organisms, including bacteria, fungi, amphibians, insects, mammals, plants and many others (Ebenhan et al., 2014). So far, hundreds of naturally occurring AMPs have been isolated and characterised as highly efficacious, safe, and tolerable antimicrobials (Cao et al., 2015, Fosgerau and Hoffmann, 2015). Also, given their ability to interact with bacterial cytoplasmic membranes in a manner not dependent upon specific receptors, AMPs also have potential as broad-spectrum antimicrobials (Yeaman and Yount, 2003, Vineeth Kumar and Sanil, 2017) and advances in our understanding of their modes of action, have given us new insights into their potential for development as novel therapies to treat multidrug-resistant bacterial infections (Moravej et al., 2018, Zanjani et al., 2018). For instance, AMPs are promising to overcome the drug-resistant strains isolated from cystic fibrosis (CF) patients (Forde et al., 2016, Yuan et al., 2019).

Cystic fibrosis is the most common life-limiting, autosomal-recessive genetic disease in Europe, North America, and Australia, with lung disease characterised by chronic infection and inflammation accounting for most morbidity and mortality (Reihill et al., 2016). MRSA, one of the prevalent infectious human pathogens, can colonise the respiratory tract and is responsible for severe infections in people with CF. All MRSA strains possess a genetic determinant – *mecA* or *mecC* - encoding a peptidoglycan transpeptidase called penicillin binding protein 2a, which has a low affinity for β-lactams. Thus, its catalysis of peptidoglycan transpeptidation is available even in the presence of high concentrations of beta-lactam antibiotics, which leads to a high rate of antimicrobial treatment failure. In

addition, the bacterium *Pseudomonas aeruginosa* permanently colonises cystic fibrosis lungs despite the aggressive use of antibiotics, and this organism employs some strategies that promote chronic pulmonary colonisation instead of acute infection (Murray et al., 2007).

For the respiratory system, the infection and chronic bacterial colonisation of the lung could be prevented and controlled by rational usage of antibiotics. However, emergence of antibiotic resistance reduced activity of major commerial antibiotics that ultimately result in facilitating untreatable and life-threatening lung infections and respiratory failure (Fields et al., 2018, Kim et al., 2018, Xu et al., 2018). Emerging research has demonstrated that both antibiotic pressure and metabolic adaptations in CF patients may contribute to establish long-term persistence and resistance, and favour the colonisation of multidrug-resistant bacteria like MRSA and *P. aeruginosa*. Additionally, small-colony-variant adaptation, biofilm formation, and growth under anaerobic conditions were reported to be capable of reducing antibiotic activities either in CF lungs or other chronic infections. In this context, treatment options against multidrug-resistant strains are urgently needed for eradicating bacteria like MRSA from patients.

It is noteworthy that host-defence peptides have evolved as highly potent alternatives to antibiotics, exerting powerful physiological effects with high potencies against multidrug-resistant strains (van der Does et al., 2018, Chen et al., 2018). In order to discover novel bioactive peptides, *P. coelestis* was employed here instead of those widely studied species. In this study, a novel phylloxin, named PLX-PC, was identified by molecular cloning. PLX-

PC, like other peptides in this family, exhibited a narrow-spectrum of antimicrobial activity against Gram-positive bacteria. It was further modified by substitution of amino acids and truncating the effective part for higher potency and broader spectrum of antimicrobial activity. Three peptide derivatives, PLXPC-W13, PLXPC-14 and PLXPC-10, were designed for optimisation of physicochemical parameters, especially for an ideal hydrophobicity of the nonpolar face of the amphipathic α-helical peptides. After the modification, peptide analogues showed an overall rise in antimicrobial activity.

4.2 Materials and Methods

4.2.1 Acquisition of Skin Secretion of South American Tree-Dwelling frog, *Phyllomedusa coelestis*

The skin secretion of the frogs was acquired by mild transdermal electrical stimulation through the dorsal skin, as described in Chapter 2.1.

4.2.2 Identification of Precursor-Encoding cDNA from the Skin Secretion

The prepropeptide encoding cDNA from the lyophilised skin secretion was cloned as described previously (Chapter 2.2). The degenerate sense primer was 5′-TCTGAATTRYAAGMSCARACATG-3′ (R=A/G; Y=C/T; M=A/C; S=C/G), designed from a highly-conserved domain within the 5'-untranslated regions of previously characterised homologous peptide cDNAs from *Phyllomedusa bicolor*.

4.2.3 Peptide Design

Two mainstream strategies to modify a peptide, substitution of amino acids and truncating the effective part of a peptide, were employed here. Three peptide derivatives, PLXPC-W13, PLXPC-14 and PLXPC-10, were designed for optimisation of physicochemical parameters, especially for an ideal hydrophobicity of the nonpolar face of the amphipathic α-helical peptides.

4.2.4 Molecular Modelling, Physicochemical Properties and Chemical Synthesis of the Peptides

The secondary structures and 3D models of the peptides were predicted through Iterative Threading ASSEmbly Refinement (I-TASSER) (http://zhanglab.ccmb.med.umich.edu/I-TASSER/). Moreover, their helical wheel plots and physiochemical properties were obtained from Heliquest (http://heliquest.ipmc.cnrs.fr/). All peptides in this report were chemically synthesised by a standard solid-phase method (Chapter 2.4). The purification of DM-PC and its analogues was achieved by RP-HPLC and MALDI-TOF MS after lyophilisation.

4.2.5 Antimicrobial Assays

The antimicrobial activity of each synthetic peptide was evaluated by the standard microdilution assay described previously (Chapter 2.6). Six types of model microorganisms were employed here, which are the Gram-positive bacteria, *Staphylococcus aureus* (NCTC

10788) and Methicillin-resistant *Staphylococcus aureus* (MRSA) (ATCC 12493); the Gram-negative bacteria, *Escherichia coli* (NCTC 10418), *Pseudomonas aeruginosa* (ATCC 27853) and *Klebsiella pneumoniae* (ATCC 43816), and the yeast *Candida albicans* (NCYC 1467).

4.2.6 Haemolysis Assay

The haemolysis assay was performed by mixing peptides with mammalian erythrocytes obtained from fresh defibrinated horse blood and carried out as previously described in Chapter 2.11.

4.3 Results

4.3.1 Identification and Characterisation of PLX-PC from the skin secretion

A prepropeptide encoding cDNA was consistently cloned from the *Phyllomedusa coelestis* skin secretion-derived cDNA library by 'shotgun' cloning. The novel gene-encoded peptide was named PLX-PC. As shown in Figure 4.1, the open reading frame of the peptide precursor cDNA consisted of 64 amino acid residues. At the very beginning of the sequence was a highly conserved putative signal peptide region containing 22 amino acid residues, followed by a 'spacer' peptide region formed by 24 amino acid residues, where is rich in acidic amino acid residues. Then, there is a typical –Lys-Arg- (-KR-) propeptide convertase processing site, indicating the start of putative mature peptide region which contains 20 amino acid

residues. Lastly, a C-terminal glycine residue which acts as an amide donor to terminate the glutamine residue of the mature peptide and results in post-translational amide modification.

According to Protein BLAST programme in the NCBI, PLX-PC was found to be a phylloxin because of the obvious sequence homologies to other members of this family. Particularly, there is a phylloxin, whose primary sequence is GWMSKIASGIGTFLSGMQQ-NH_2, revealing striking similarity with PLX-PC, since there is only one amino acid substitution. Pierre reported that phylloxin, a 19-residue cationic and amphipathic peptide derived from *P. bicolor*, exhibited a narrow-spectrum antimicrobial activity (Pierre et al., 2000).

Figure 4.1 Nucleotide and translated open-reading frame amino acid sequences of a cloned cDNA encoding the biosynthetic precursor of PLX-PC. The putative signal peptide sequence is double-underlined, while the putative mature peptide sequence is single-underlined, and the stop codon is indicated by an asterisk.

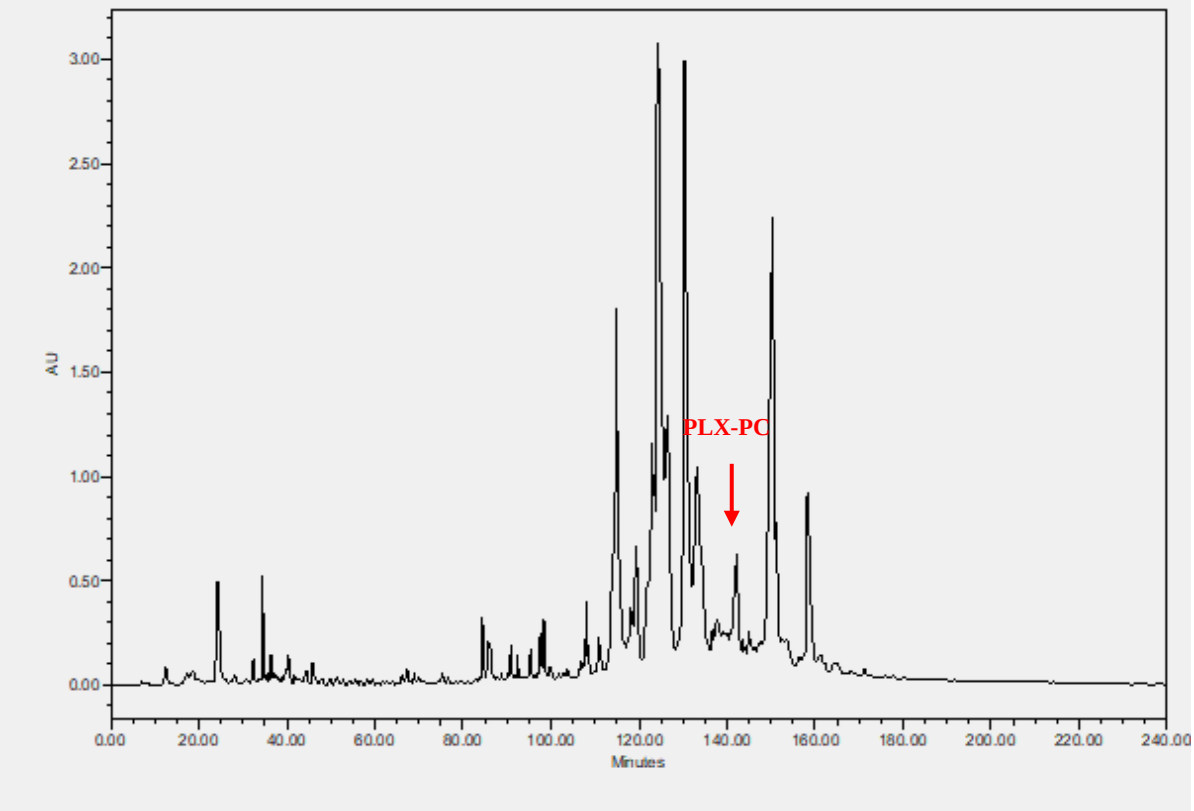
PLX-PC
AU
Minutes
3.00
2.50
2.00
1.50
1.00
0.50
0.00
0.00
20.00
40.00
60.00
80.00
100.00
120.00
140.00
160.00
180.00
200.00
220.00
240.00

(A)

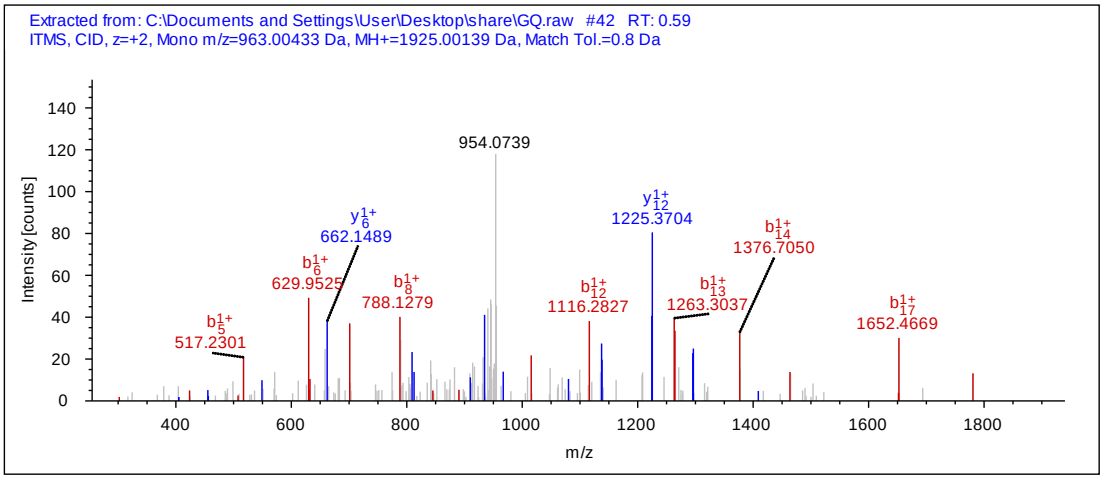
Extracted from: C:\Documents and Settings\User\Desktop\share\GQ.raw #42 RT: 0.59
ITMS, CID, z=+2, Mono m/z=963.00433 Da, MH+=1925.00139 Da, Match Tol.=0.8 Da
Intensity [counts]
m/z
954.0739
y1+ 6 662.1489
b1+ 6 629.9525
b1+ 8 788.1279
b1+ 5 517.2301
y1+ 12 1225.3704
b1+ 12 1116.2827
b1+ 13 1263.3037
b1+ 14 1376.7050
b1+ 17 1652.4669

(B)

#1	b(1+)	b(2+)	Seq.	y(1+)	y(2+)	#2
1	58.029	29.518	G			19
2	171.113	86.060	L	1867.977	934.492	18
3	302.153	151.580	M	1754.893	877.950	17
4	389.185	195.096	S	1623.852	812.430	16
5	517.280	259.144	K	1536.820	768.914	15
6	630.364	315.686	I	1408.725	704.866	14
7	701.402	351.204	A	1295.641	648.324	13
8	788.434	394.720	S	1224.604	612.806	12
9	845.455	423.231	G	1137.572	569.290	11
10	958.539	479.773	I	1080.551	540.779	10
11	1015.561	508.284	G	967.467	484.237	9
12	1116.608	558.808	T	910.445	455.726	8
13	1263.677	632.342	F	809.397	405.202	7
14	1376.761	688.884	L	662.329	331.668	6
15	1463.793	732.400	S	549.245	275.126	5
16	1520.814	760.911	G	462.213	231.610	4
17	1651.855	826.431	M	405.191	203.099	3
18	1779.913	890.460	Q	274.151	137.579	2
19			Q-Amidated	146.092	73.550	1

(C)

Figure 4.2 Identification of the specific AMP PLX-PC derived from the skin secretion of *P. coelestis* (A) RP-HPLC chromatogram of skin secretion of *P. coelestis* monitored at 214 nm. The red arrow indicates the retention time of PLX-PC. (B) Annotated MS/MS spectrum of PLX-PC. (C) Predicted b- and y-ions arising from collision induced dissociation of the doubly-charged (963.00 m/z, $[M+2H]^{2+}$) precursor ion. The observed b- and y-ions are indicated in blue and red typefaces.

4.3.2 Peptide Design

PLX-PC represents a fresh member of a vertebrate AMP family - the phylloxins - whose predicted secondary structure, 3D model, and helical wheel plot are illustrated in Figure 4.3. This peptide was utilised as a template to design a series of analogues. As shown in Table

4.1, the nautral peptide PLX-PC has relatively weak basicity and hydrophoicity, as well as potential amphipathicity. When it comes to α-helical peptides, cationicity, hydrophobicity and amphipathicity are extremely important and necessary factors for membrane permeabilisation to succeed. According to a previous study of SAR, the net positive charge is generally correlated with the initial interaction with outer and/or inner membranes of bacteria, whereas amphipathicity provides AMPs with a nonpolar face important for membrane–peptide interactions. Also there is an optimum hydrophobicity window in which potent yet selective antimicrobial activity could be achieved. Lower hydrophobicity could diminish antimicrobial activity, while increased hydrophobicity beyond this window would result in stronger haemolytic activity. Hence, to investigate the role of hydrophobicity in the selectively of cationic α-helical AMPs, we used PLX-PC as a framework to systematically alter peptide hydrophobicity on the nonpolar face of the helix. Replacing 13th Phe with the less hydrophobic Trp residue to reduce hydrophobicity generated PLXPC-W13. Afterwards, the 3rd Met was substituted with the more hydrophobic Trp residue, followed by the deletion of C-terminal tail yielded PLXPC-14. Lastly, triple Trp-substituted truncated mimetic PLXPC-10 was produced to increase peptide hydrophobicity further.

Table 4.1 Physicochemical properties of PLX-PC and its analogues

	Primary Sequence	**Net charge**	**Hydrophobic moment (μH)**	**Hydrophobicity (H)**
PLX-PC	GLMSKIASGIGTFLSGMQQ-NH_2	1	0.492	0.541
PLXPC-W13	GLMSKIASGIGTWLSGMQQ-NH_2	1	0.510	0.565
PLXPC-14	GLWSKIASGIGTWL-NH_2	1	0.643	0.786
PLXPC-10	GLWSKWAKGW-NH_2	2	0.845	0.674

Sequence	GLMSKIASGIGTFLSGMQQ
Prediction	CHHHHHHHHHHHHHHCCC
Conf.Score	9188998869998875019
	H:Helix; S:Strand; C:Coil

(A)

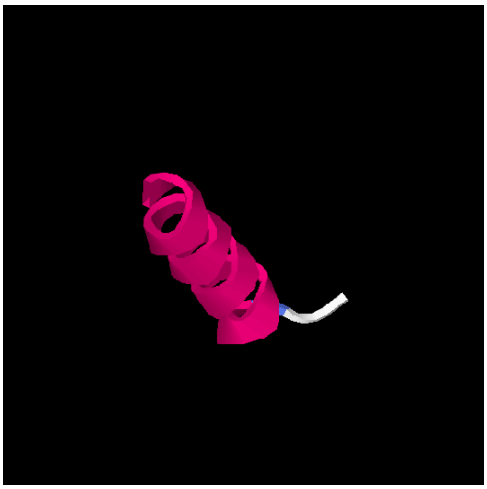

(B)

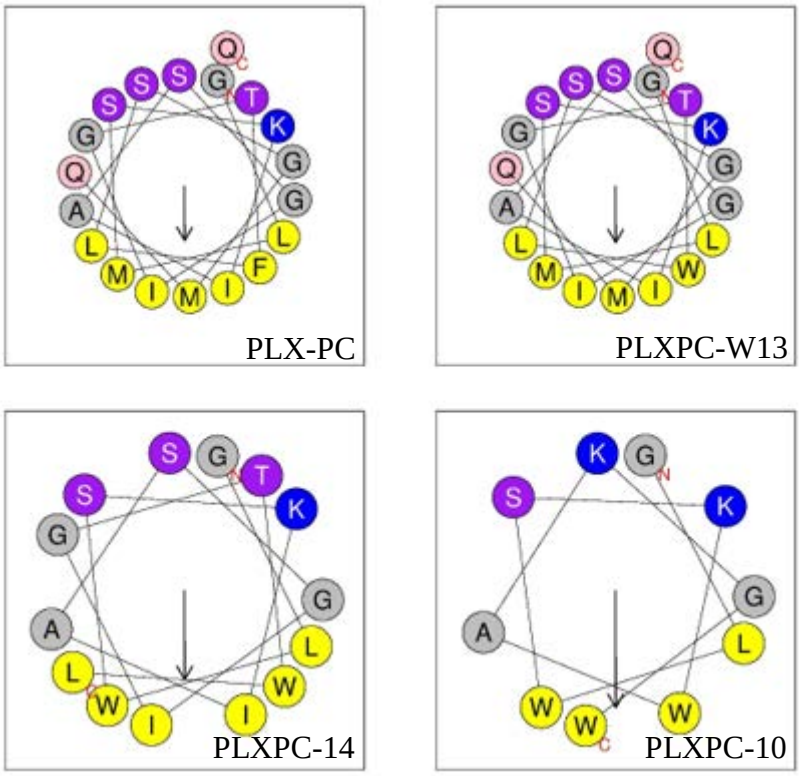

(C)

Figure 4.3 (A) Secondary structure predictions of DM-PC. (B) Expected 3D model of PLX-PC. (C) Helical wheel projections of the four peptides, PLX-PC, PLXPC-W13, PLXPC-14 and PLXPC-10 respectively.

4.3.3 Antimicrobial Activities of PLX-PC and its analogues

The natural peptide, PLX-PC, exhibited negligible activity against two Gram-positive bacteria *S. aureus* and MRSA. After the modification by Trp substitution as well as truncating the effective part, peptide analogues showed an overall rise in antimicrobial activity. Among the three analogues, PLXPC-14 displayed the most potent antimicrobial activity, with an overall TI of 9.52,which is a 25-fold improvement compared to that of the parent peptide. TI, a parameter indicating safety/efficacy usage, was calculated as the peptide concentration causing 50% haemolysis of the red bloods cells (HC_{50}) divided by the geometric mean of the peptide MICs against all tested bacterial strains, and the HC_{50} or MIC that was over 512 μM was replaced by the 2-fold maximum tested value 1024 μM for TI calculation.

Table 4.2 MICs, MBCs and TI of ampicillin, PLX-PC and its analogues.

	MICs / MBCs (μM)				
	Ampicillin	**PLX-PC**	**PLXPC-W13**	**PLXPC-14**	**PLXPC-10**
S. aureus	0.1 / 0.1	64 / 256	32 / 64	4 / 32	64 / 256
E. coli	12.8 / 12.8	>512 / >512	256 / 512	16 / 128	64 / 128
C. albicans	>512 / >512	>512 / >512	128 / >512	16 / 128	64 / 128
MRSA	>512 / >512	128 / 128	64 / 64	8 / 64	64 / 64
K. pneumoniae	>512 / >512	>512 / >512	>512 / >512	32 / 128	512 / >512
P. aeruginosa	>512 / >512	>512 / >512	>512 / >512	128 / 256	256 / 256
HC_{50}	>512	173.2	187.8	170.9	173.4
TI (overall)	13.08	0.38	0.92	9.52	1.52

4.3.4 Haemolytic Activities

The haemolytic activities of the peptides against horse erythrocytes were determined as a measure of peptide toxicity toward lower eukaryotic cells. The parent peptide, PLX-PC, exhibited no haemolysis against the red blood cells at a concentration of 64 µM. With a decrease or increase in peptide hydrophobicity, the haemolytic activity of peptide analogues was not either weakened nor strengthened. In conclusion, PLX-PC and its analogues showed a moderate haemolytic activity, which proved the existence of optimum hydrophobicity window.

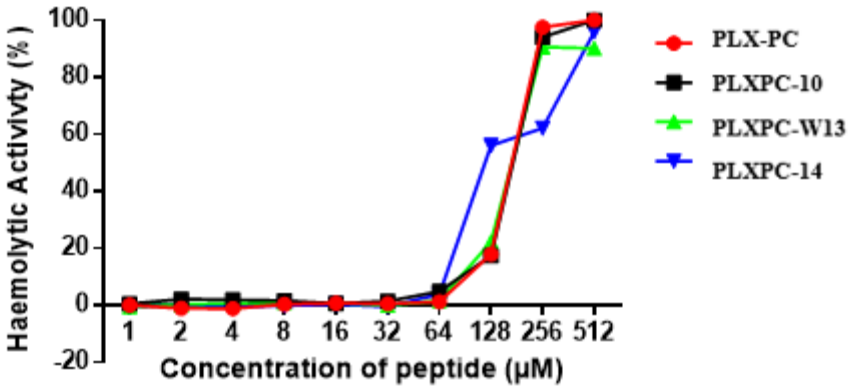

Figure 4.4 The haemolytic activities of PLX-PC and its three analogues at concentrations ranging from 1 µM to 512 µM. The error bar represents the standard error of three repeats.

4.4 Discussion

AMPs have demonstrated remarkable antimicrobial effects and appeared as potential antibiotic agents for treating emerging antibiotic resistance because most of them exert the function through membrane permeabilisation. To be specific, there is a general agreement that AMPs are among the most potent candidates for the development of new antibiotics for three reasons, rapid action on the microbial membranes, non-specific activity against numerous pathogens even resistant strains and low possibility of evoking drug-resistance due to their complex mechanism of action. Therefore, it was unexpected that PLX-PC demonstrated a considerable difference between its bactericidal activity against Gram-positive bacteria and the others. From the perspective of the mode of action of AMPs, the antimicrobial effects could be simply reversed by the differences of cell wall structures of microorganisms. In general, the cell wall of bacteria is mostly composed of peptidoglycan, while the main component of the cell wall of fungi is chitin, which is tougher than peptidoglycan to be destroyed by antimicrobial peptides. Besides, in spite of a thinner and less compact peptidoglycan layer than that of Gram-positive bacteria, the cell wall of Gram-negative bacteria remains strong, tough, and elastic to maintain their shape and protect them against damage from outside factors, because of their extra outer membrane containing lipopolysaccharides, proteins, and phospholipids. In summary, both the chitin of fungi and the outer membrane of Gram-negative bacteria provide cells protection against extreme environmental conditions, such as the invasion of PLX-PC.

The natural AMP, PLX-PC, exhibited a narrow-spectrum and negligible antimicrobial activity. However, its potential amphipathicity made PLX-PC possible to work as a

framework for peptide design. The mechanism of action of AMPs can be of great importance to the peptide design. “Barrel-stave” and “carpet-like”, are much more popular models to explain how α-helical peptides interact with the microbial membrane and finally cause cell death. In the former one, the amphipathic α-helical peptides bind with the membrane mainly due to the hydrophobic effect. But in “carpet-like” model, the electrostatic interaction between positively charged peptides and negatively charged bacterial membranes is the determinant of α-helical peptides binding to bacterial membranes. To summarise, in both “barrel-stave” and “carpet-like” models, cationicity, hydrophobicity, amphipathicity and conformation play a vital role in enabling peptides to possess bactericidal activity.

Two mainstream strategies to modify a peptide, substitution of amino acids and truncating the effective part of a peptide, were employed here. Three peptide derivatives, PLXPC-W13, PLXPC-14 and PLXPC-10, were designed for optimisation of physicochemical parameters, especially for an ideal hydrophobicity of the nonpolar face of the amphipathic α-helical peptides. Reasons for choosing Trp as the substituted amino acid residue are as follows. Firstly, Trp has a distinct preference for the interfacial region of lipid bilayers because of its capablity of participating in cation–π interactions, thereby facilitating enhanced peptide–membrane interactions. In addition, Trp sidechains are also implicated in peptide and protein folding in aqueous solution, where they contribute by maintaining native and nonnative hydrophobic contacts. These unique properties make the Trp-rich antimicrobial peptides highly active even at very short peptide lengths.

After the modification by Trp substitution as well as truncating the effective part, peptide analogues showed an overall rise in antimicrobial activity. With a decrease or increase in peptide hydrophobicity, the haemolytic activity of peptide analogues was not either weakened nor strengthened. To sum up, the optimum hydrophobicity window on the nonpolar face of the peptides allows insertion into the membrane through hydrophobic interactions, causing increased permeability and loss of barrier function of target cells.

Chapter 5

Cloning of a Novel Trypsin Inhibitor from the Traditional Chinese Medicine Decoction Pieces, Radix Trichosanthis

Published in *Anal Biochem*

PMID: 30831099

DOI: 10.1016/j.ab.2019.02.028

Abstract

Most herbs of TCM are used as air-dried decoction pieces that are manufactured and kept at ambient temperature for long periods. Given the ability of some desiccation-tolerant plants to conserve RNA, it could be worthwhile to isolate mRNA from TCM decoction pieces as part of a transcriptomic strategy to identify new substances with potential pharmaceutical application. Here, we report the molecular cloning of a novel trypsin inhibitor (as the

probable alleleic variants TKTI-2 and TKTI-3) from the decoction piece of Radix Trichosanthis, representing the dried root of *Trichosanthes kirilowii*. From this material, the total RNA was extracted and a cDNA library was constructed from the isolated mRNA from which the cDNAs of two precursors were successfully cloned and sequenced. TKTI-3 showed an amino-acid substitution in the otherwise highly-conserved P1-P1' reaction site of the mature peptide, which we confirmed to not be an artefact by extracting and trypsinising the total proteins from Radix Trichosanthis. Subsequent analysis using LC-MS/MS detected the presence of specific tryptic peptides expected from TKTI-3, confirming the presence and expression of this locus in Radix Trichosanthis. More generally, this study indicates that mRNA can persist in decoction pieces and so could present a viable option for the molecular cloning from other TCMs.

5.1 Introduction

TCM has a long history in maintaining the health of the Chinese population. In addition to continuing to fulfil that role today, TCM also represents a promising source for lead drug discovery as exemplified by the discovery of the anti-malarial drug artemisinin (Wang et al., 2018). In this new context, contemporary research has focused on the extraction, isolation and identification of bioactive compounds from TCM followed by an evaluation of their biological activities (Ahmad et al., 2018). Proteins and peptides from the herbs of TCM have

attracted the attention of the research community because of their bioactivities, especially in the areas of antimicrobial and anticancer research (Guzmán-Rodríguez et al., 2015, Dang and Van Damme, 2015), as well as their potential economic benefits (Wong et al., 2014).

To date, the discovery of proteins and peptides from TCM derives mainly via chemical extraction using organic solvents (Qi et al., 2016), although a few studies have demonstrated the discovery of novel proteins and peptides via transcriptomic studies from fresh (Yu et al., 2016) or snap-frozen fresh plant tissues (Kumar et al., 2011, Qi et al., 2010). However, most herbs of TCM are present in the form of sliced or cropped decoction pieces because they are harvested in their habitats and then air-dried. Although this situation would normally present a hindrance for transcriptomic studies, pioneering work has shown that some desiccation tolerant plants are able to conserve RNA during either rapid or slow dehydration (Dhindsa and Bewley, 1978, Oliver and Bewley, 1984) such that transcriptomic studies have been accomplished on desiccation-tolerant plant species using their dehydrated tissues (Rodriguez et al., 2010, Bartels et al., 1990). Altogether, these results suggest that it might be feasible to study the transcriptome using the RNA from dried Chinese medicinal herbs (i.e., from the decoction pieces) purchased from a pharmacy rather than the more labour-intensive option of sampling from the local habitats.

Herein we examined a typical TCM, the root of Chinese Snake Gourd (*Trichosanthes kirilowii*), known as Radix Trichosanthis, to test for potential for the conservation of RNA in dried plant material. This specimen has demonstrated extensive medicinal value in TCM

(Huang, 1998), with the dry roots, ripe fruits, ripe seeds and pericarp having been officially recorded for the treatment for different symptoms in the Chinese Pharmacopoeia. For instance, the root is used as an antiphlogistic and an abortifacient, whereas the dry, ripe fruits are used as an antipyretic and in the treatment of constipation (Tang and Eisenbrand, 1992). In addition, Radix Trichosanthis is known to contain bioactive proteins and peptides, including the ribosome-inactivating protein trichosanthin (Tsao et al., 1986) and squash trypsin inhibitors (Qian et al., 1990). Under this framework, we attempted to extract the total RNA from the decoction pieces of Radix Trichosanthis using the subsequent molecular cloning of the squash trypsin inhibitor peptide-encoded mRNA as a proof of concept. In this, our experiments were successful insofar as we can report the discovery of two variants of a novel squash trypsin inhibitor peptide.

5.2 Materials and Methods

5.2.1 Specimen biodata

Specimens of *T. kirilowii* in the form of Radix Trichosanthis, which are the dried root pieces of *T. kirilowii*, were obtained from a commercial source (lot number 20086M302P2SW1000; Hebei Anguo Medical Materials Corporation; Anguo, China) and deposited in Nanjing University of Chinese Medicine. The corresponding authors verified the samples as Radix Trichosanthis according to Pharmacopoeia of the People's Republic of China (Committee, 2010). Before being used, all samples were pulverized before being filtered through a standard sieve of mesh size 250 μm ± 9.9 μm.

5.2.2 RNA extraction

Total RNA was extracted from the powdered Radix Trichosanthis using TRIzol RNA extraction method (Invitrogen; Vilnius, Lithuania) with modifications according to Wang et al. (Wang et al., 2012). In detail, 200 mg of Radix Trichosanthis was mixed with 400 µl of lysis buffer (1% SDS and 2% β-mercaptoethanol in 100 mM Tris-HCl (pH 9.0)) and incubated at room temperature for 15 min. After centrifugation at 12,000× g for 10 min at 4 ºC, the supernatant was transferred into 800 µl of TRIzol and incubated at room temperature for 10 min. Thereafter, the total RNA from the aqueous phase was collected after adding 240 µl of chloroform and centrifugation at 12,000× g for 10 min at 4 ºC. Subsequently, the total RNA was precipitated by mixing it with an equal volume of isopropanol and incubating at -20 ºC for 20 min. The RNA pellet was collected by centrifugation for 10 min and resuspended in 400 µl of DEPC-treated water. Additional DNA residue was extracted further using an equal volume of citrate buffer saturated phenol (pH 4.3) : chloroform (1:1, v/v) after which the aqueous phase was washed using an equal volume of chloroform. The RNA was precipitated again by adding 1/10 volume of 3 M sodium chloride and two volumes of ice-cooled ethanol at -80°C for 30 min. Afterwards, the RNA pellet was washed using 70% ethanol and finally redissolved in DEPC-treated water. The concentration of extracted RNA was measured by using a NanoDrop™ One^{C}.

5.2.3 Molecular cloning

Polyadenylated mRNA was isolated from the extracted, total RNA using a Dynabeads® mRNA DIRECT™ Kit (Invitrogen; Vilnius, Lithuania). In detail, the total RNA was resuspended in 500 µl of lysis/binding Buffer (provided in the kit) and hybridized with the

magnetic Dynabeads at room temperature. The mRNA/beads complex was further washed using Washing Buffers A and B (provided in the kit) three times and finally eluted in 20 µl of DEPC-treated water. The mRNA so obtained was then reverse-transcribed into a cDNA library using SMART RACE cDNA Kit (Clontech; Palo Alto, USA) and then subjected to a nested PCR, employing forward (5'-CTTGGTGATGGCAGCTTTTGTAGAGTCT-3') and reverse primers (5'-CAGAAGATCCGACACGGCGGAGT-3') that were designed from the signal peptide and 3'-untranslated regions, respectively, of a trypsin inhibitor encoded cDNA from *T. kirilowii* (GenBank accession number X82230). The 3'-RACE PCR also served to verify the presence of the polyA tail of the peptide encoding mRNA. The PCR products were purified by an E.Z.N.A.® Tissue DNA Kit (Omega Bio-Tek; Norcross, GA, USA), cloned into a pGEM-T vector (Promega Corporation; Southampton, UK), and sequenced using an ABI3100 automated capillary sequencer (Applied Biosystems; FosterCity, CA, USA). In total, each of the 32 monoclonal DNA samples were sequenced twice.

5.2.4 Extraction of total protein

Five grams of filtered, powdered Radix Trichosanthis were mixed with 50 ml of 50% ethyl alcohol for 10 h. After removing the ethyl alcohol using an evaporator, the remaining solution was centrifuged at 13,000× g and the supernatant was snap-frozen in liquid nitrogen and lyophilised. One hundred milligrams of this lyophilised extraction was prepared for total protein isolation using the Invitrogen TRIzol Reagent Kit (Invitrogen; Vilnius, Lithuania) according to the manufacturer's recommendations.

5.2.5 Digestion, alkylation and trypsin digestion

One hundred micrograms of the extracted proteins were denatured in 8 M urea and 25 mM Tris-HCl. The cysteines were then alkylated using 40 mM IAA over a 30-min incubation period at room temperature and in the dark before being reduced using 20 mM DTT at 60 ºC for 1 h. The alkylation reaction was then quenched by adding an additional 10 mM DTT. Finally, the proteins were trypsinized using 1 µg MS-grade trypsin (Promega Corporation; Southampton, UK) for 16 hours at 37 ºC after which the protein solution was 10-fold diluted by adding 100 mM ammonia bicarbonate. The digestion was stopped by adding TFA to yield a final 1% (v/v) solution. The tryptic peptides were desalted using Ziptip (Merck; Darmstadt, Germany) and stored at -20 ºC until MS analysis.

5.2.6 Identification and structural analysis of the predicted mature peptide

MS and MS/MS characterization and detection of the tryptic peptides derived from Radix Trichosanthis was performed using an LCQ ion-trap mass spectrometer (Thermo Inc., San Jose, California, USA) by means of electrospray ionization. A gradient elution of solvents A (water containing 0.1% FA) and B (acetonitrile with 2% water and 0.1% FA) was applied with a flow rate of 200 µl/min as follows: 0-5 min, 0% solvent B; 5-80 min, 0%-50% solvent B; 80-105 min, 50%-100% solvent B; and 105-120 min, 100% B. The nitrogen sheath and auxiliary gas flow were maintained at 20 and 5 arbitrary units, respectively. The heated capillary temperature was 300 ºC and the spray voltage was set to 5 kV in positive ion mode. The three ions with the highest intensity were subjected to MS/MS fragmentation under a

normalized collision energy of 30 and the resulting fragment ion profiles were then trawled using the Protein Discoverer 1.0 (Thermo Finnigan; San Jose, California, USA) against a customized FASTA database. Only peptides with sufficient confidence (i.e., probability > 40) were retained.

5.3 Results

The total RNA was successfully extracted from Radix Trichosanthis at a concentration of 15.4 ± 4.4 μg/g dried sample weight (n = 5). The A260/A280 and A260/A230 ratios were 1.96 ± 0.06 and 1.00 ± 0.17, respectively. The subsequent isolation of the mRNA and the amplification of the squash trypsin inhibitor-encoded cDNA were confirmed via observation of the appropriate DNA band on the agarose gel (Figure 5.1). Finally, two novel trypsin inhibitors precursor-encoded cDNAs were cloned from the constructed cDNA library (Figure 5.2), with the presence of polyadenylated tails for both cDNAs being verified by 3'-RACE (Figure 5.3). The open-reading frames of both precursors consisted of 65 amino-acid residues and showed a high degree of identity with the trypsin inhibitor known from same species (GenBank accession number X82230; here named TKTI-1). A comparison of the nucleotide sequences of the cloned cDNAs (TKTI-2 and TKTI-3, respectively) with that of TKTI-1 reveals one and three differences, respectively (Figure 5.4A), resulting in amino-acid changes at positions 38 (A/G) and, for TKTI-3 only, 42 (I/V) (Figure 5.4B); only the latter change is within the putative mature peptide (Figure 5.2). A further, broader comparison with other known squash trypsin inhibitors in the Uniprot protein database from Sicyoeae, a tribe in the subfamily Cucurbitaceae to which *T. kirilowii* belongs, shows the high degree of conservation among all mature peptides as well as the same disulphide bridge

motif (Figure 5.5). The I/V mutation at the N-terminal domain of TKTI-3 is unique, however. Both cDNA encoding precursors have been deposited into GenBank with the accession numbers MF770981 and MF770982, respectively.

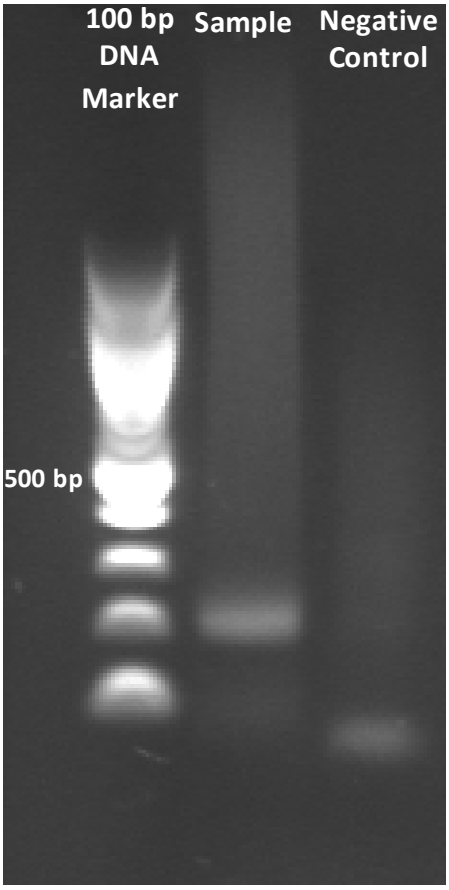

Figure 5.1 The PCR gel electropherogram of trypsin inhibitor precursor-encoded cDNAs from the cDNA library of the decoction pieces of Radix Trichosanthi. In the negative control, the PCR was performed without the cDNA template.

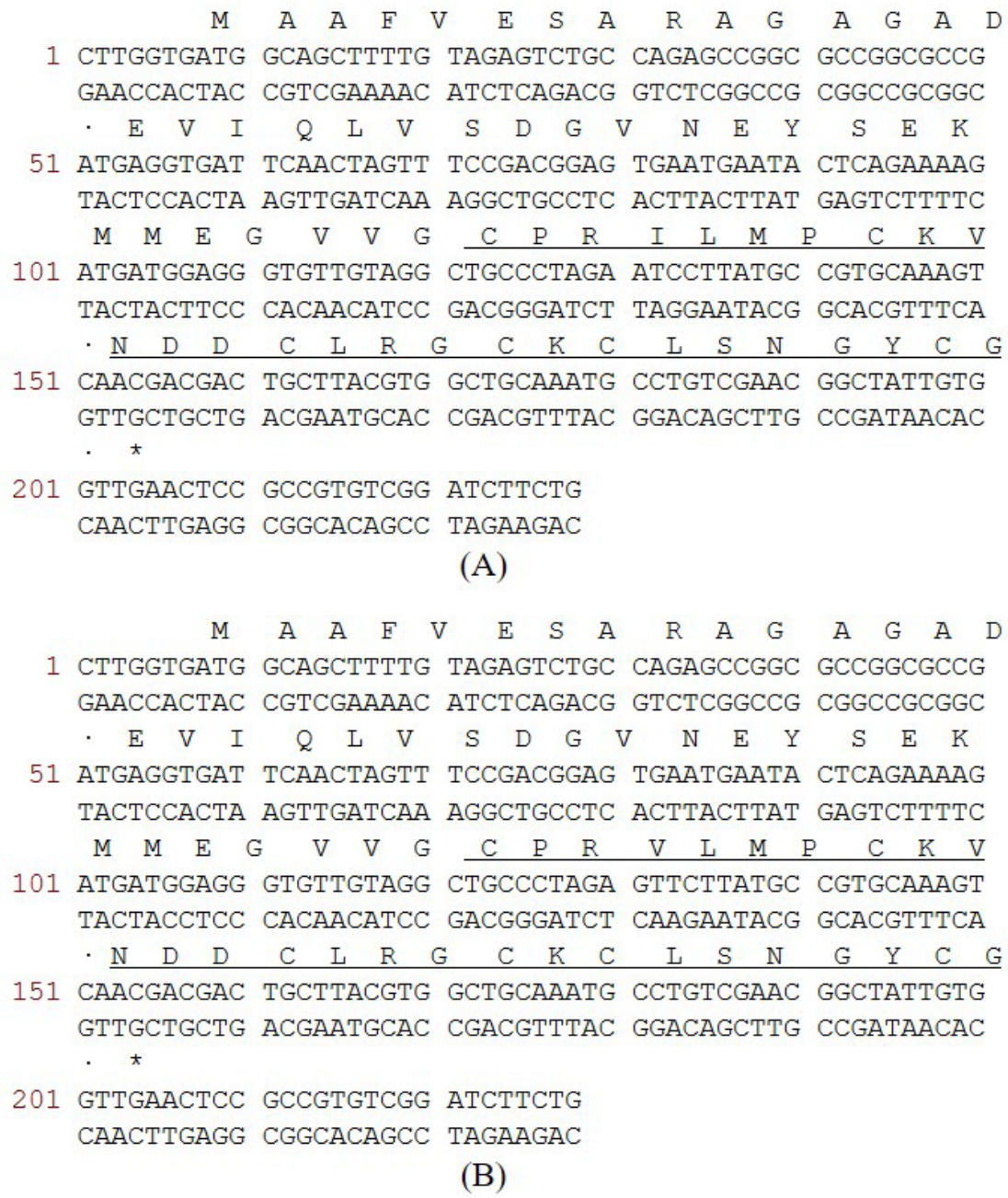

Figure 5.2 Nucleotide sequences and translated open reading frames of cloned cDNAs encoding the biosynthetic precursors of (A) TKTI-2 and (B) TKTI-3 from *T. kirilowii*. The putative mature peptide sequences as determined from (Ling et al., 1996) are underlined.

a

```
          M   A   A   F   V   E   S   A   R   A   G   A   G   A   D
  1 CTTGGTGATG GCAGCTTTTG TAGAGTCTGC CAGAGCCGGC GCCGGCGCCG
      E   V   I   Q   L   V   S   D   G   V   N   E   Y   S   E   K
 51 ATGAGGTGAT TCAACTAGTT TCCGACGGAG TGAATGAATA CTCAGAAAAG
    M   M   E   G   V   V   G   C   P   R   I   L   M   P   C   K   V
101 ATGATGGAGG GTGTTGTAGG CTGCCCTAGA ATCCTTATGC CGTGCAAAGT
     N   D   D   C   L   R   G   C   K   C   L   S   N   G   Y   C   G
151 CAACGACGAC TGCTTACGTG GCTGCAAATG CCTGTCGAAC GGCTATTGTG
       *
201 GTTGAACTCC GCCGTGTCGG ATCTTCTGTG AATGCTGTGT CTTGTCCGTG
251 TTTCTATGTC TATGTGTGTG TATTTTCTAT TTCTATGAAA ATAAAGTGTC
301 TCTTTGATCA CTCTCCTCTG TGAGTGTACG TGATCAATTT CTGTGATACC
351 CGTCTATAAT TTTAATGTAA TCTTCTCTAT GTTTTCCTAA AAAAAAAAAA
401 AAAAAAAAAA A
```

b

```
          M   A   A   F   V   E   S   A   R   A   G   A   G   A   D
  1 CTTGGTGATG GCAGCTTTTG TAGAGTCTGC CAGAGCCGGC GCCGGCGCCG
      E   V   I   Q   L   V   S   D   G   V   N   E   Y   S   E   K
 51 ATGAGGTGAT TCAACTAGTT TCCGACGGAG TGAATGAATA CTCAGAAAAG
    M   M   E   G   V   V   G   C   P   R   V   L   M   P   C   K   V
101 ATGATGGAGG GTGTTGTAGG CTGCCCTAGA GTTCTTATGC CGTGCAAAGT
     N   D   D   C   L   R   G   C   K   C   L   S   N   G   Y   C   G
151 CAACGACGAC TGCTTACGTG GCTGCAAATG CCTGTCGAAC GGCTATTGTG
       *
201 GTTGAACTCC GCCGTGTCGG ATCTTCTGTG AATGCTGTGT CTTGTCCGTG
251 TTTCTATGTC TATGTGTGTG TATTTTCTAT TTCTATGAAA ATAAAGTGTC
301 TCTTTGATCA CTCTCCTCTG TGAGTGTACG TGATCAATTT CTGTGATACC
351 CGTCTATAAT TTTAATGTAA TCTTCTCTAT GTTTTCACAA AAAAAAAAAA
401 AAAAAAAAAA A
```

Figure 5.3 Nucleotide sequences and the translated open reading frame amino acid sequences of cloned cDNAs encoding the biosynthetic precursors from Radix Trichosanthis were obtained through 3'RACE technique.

```
            67                                                  116
TKTI-1  (67) CTTGGTGATGGCAGCTTTTGTAGAGTCTGCCAGAGCCGGCGCCGGCGCCG
TKTI-2   (1) CTTGGTGATGGCAGCTTTTGTAGAGTCTGCCAGAGCCGGCGCCGGCGCCG
TKTI-3   (1) CTTGGTGATGGCAGCTTTTGTAGAGTCTGCCAGAGCCGGCGCCGGCGCCG
            117                                                 166
TKTI-1 (117) ATGAGGTGATTCAACTAGTTTCCGACGGAGTGAATGAATACTCAGAAAAG
TKTI-2  (51) ATGAGGTGATTCAACTAGTTTCCGACGGAGTGAATGAATACTCAGAAAAG
TKTI-3  (51) ATGAGGTGATTCAACTAGTTTCCGACGGAGTGAATGAATACTCAGAAAAG
            167                                                 216
TKTI-1 (167) ATGATGGAGGGTGTTGTAGCCTGCCCTAGAATCCTTATGCCGTGCAAAGT
TKTI-2 (101) ATGATGGAGGGTGTTGTAGGCTGCCCTAGAATCCTTATGCCGTGCAAAGT
TKTI-3 (101) ATGATGGAGGGTGTTGTAGGCTGCCCTAGAGTTCTTATGCCGTGCAAAGT
            217                                                 266
TKTI-1 (217) CAACGACGACTGCTTACGTGGCTGCAAATGCCTGTCGAACGGCTATTGTG
TKTI-2 (151) CAACGACGACTGCTTACGTGGCTGCAAATGCCTGTCGAACGGCTATTGTG
TKTI-3 (151) CAACGACGACTGCTTACGTGGCTGCAAATGCCTGTCGAACGGCTATTGTG
            267                     294
TKTI-1 (267) GTTGAACTCCGCCGTGTCGGATCTTCTG
TKTI-2 (201) GTTGAACTCCGCCGTGTCGGATCTTCTG
TKTI-3 (201) GTTGAACTCCGCCGTGTCGGATCTTCTG
```

(A)

```
            1                                                    50
TKTI-1   (1) MAAFVESARAGAGADEVIQLVSDGVNEYSEKMMEGVVACPRILMPCKVND
TKTI-2   (1) MAAFVESARAGAGADEVIQLVSDGVNEYSEKMMEGVVGCPRILMPCKVND
TKTI-3   (1) MAAFVESARAGAGADEVIQLVSDGVNEYSEKMMEGVVGCPRVLMPCKVND
            51          65
TKTI-1  (51) DCLRGCKCLSNGYCG
TKTI-2  (51) DCLRGCKCLSNGYCG
TKTI-3  (51) DCLRGCKCLSNGYCG
```

(B)

Figure 5.4 Alignments of nucleotide sequences (A) and translated open reading frames (B) of cloned cDNAs encoding the biosynthetic precursors of TKTI-2 and TKTI-3 and the previously identified trypsin inhibitor (TKTI-1) from *T. kirilowii* (accession number X82230). Identical nucleotides are colored in red.

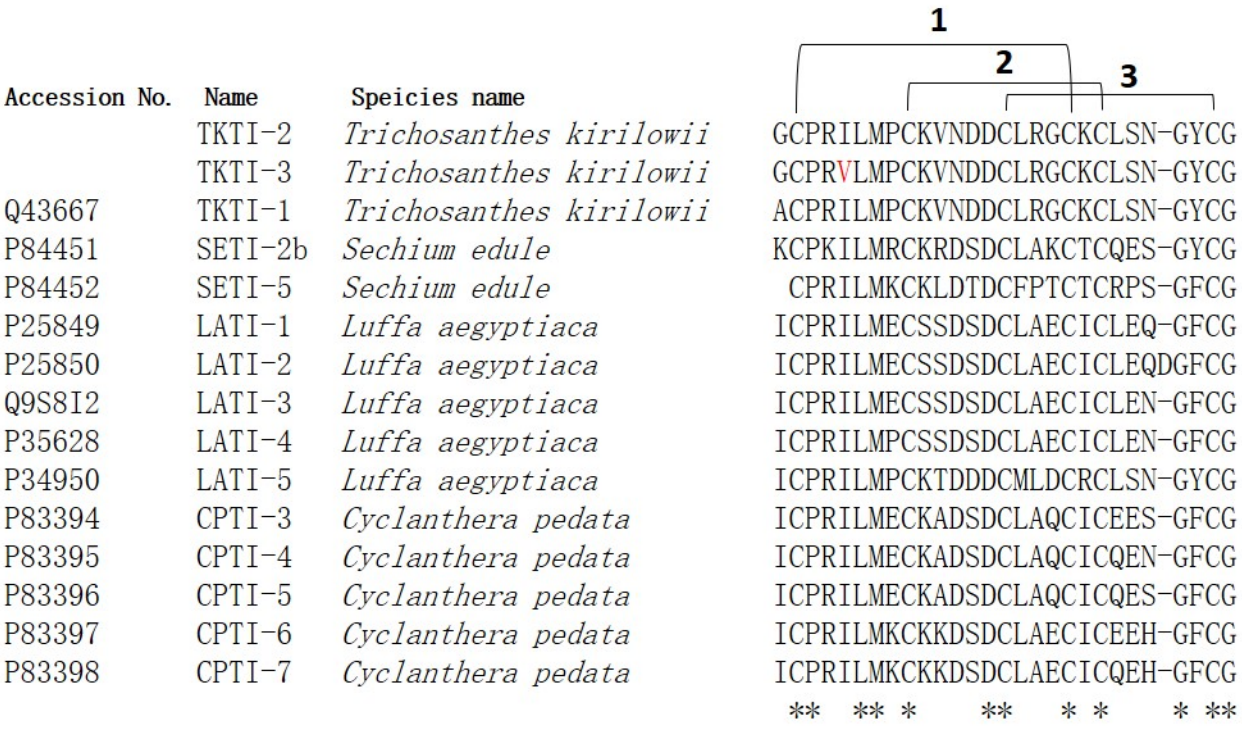

Figure 5.5 Alignment of the sequences of trypsin inhibitor peptides known from the tribe Sicyoeae and present in the UniProt database against the two novel peptides discovered in this study. The pattern of disulphate bridges are indicated by the lines 1, 2 and 3. Sites of amino acid identity are indicated by asterisks.

LC-MS/MS analysis of the tryptic peptides from the extracted total proteins of Radix Trichosanthis (Figure 5.6) identified the specific tryptic peptides from TKTI-1 and the protein trichosanthin (Table 5.1) as well as VLMPCKVNDDCLR from TKTI-3. The latter was also confirmed through the corresponding MS/MS spectrum (Figure 5.7) to support the expression of two TKTI variants in Radix Trichosanthis.

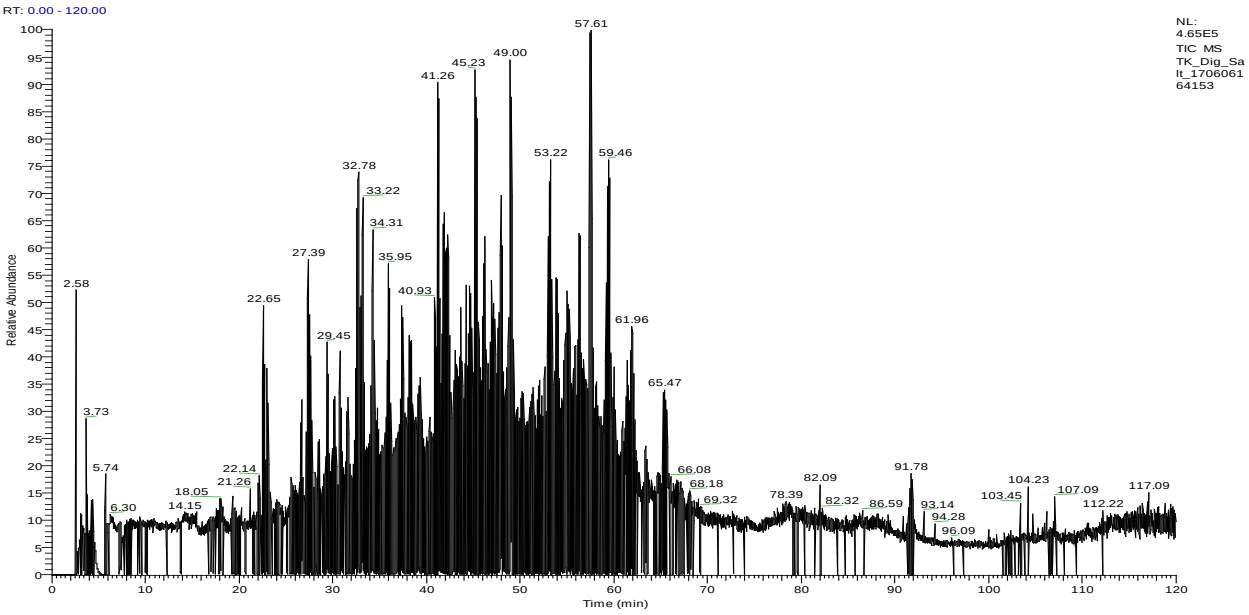

Figure 5.6 Total ion currency of mass spectrometry analysis of digestive peptides mixture of the proteins extracted from Radix Trichosanthis.

Table 5.1 Identified peptide fragments from the trypsin digestion of the alkylated proteins extracted from Radix Trichosanthis.

Sequence	Modifications	Probability	XCorr	Annotation (Accession No.)
AGDTSYFFNEASATEAAK		122.50	5.07	Trichosanthin (P09989)
AGDTSYFFNEASATEAAKYVFK		41.58	1.51	
FIEQQIGKR		50.97	2.57	
KVTLPYSGNYER		71.04	3.20	
LSGATSSSYGVFISNLR		89.31	3.21	
LYDIPLLR		45.10	2.32	

QIQIASTNNGQFESPVVLINAQNQR		114.18	4.03	
TFLPSLAIISLENSWSALSK		127.09	4.96	
VTLPYSGNYER		54.98	1.63	
YKFIEQQIGK		60.66	3.04	
YKFIEQQIGKR		45.70	1.81	
QIQIASTNNGQFESPVVLINAENQR		67.24	4.10	Trichosanthin (Q41611)
AGNNAYFLNDASAEANNVLFK		85.37	4.52	rRNA N-glycosidase (B1B626)
GINHVRLPYGGNYDGLETAAGR		91.21	4.15	
TVSNTPTFVTNVNSPVVK		107.93	3.19	
VLLAAAPQcPIPDAHLDAAIK	C9(Carbamidomethyl)	50.10	2.36	Chitinase 3-like protein
ILmPcKVNDDcLR	M3(Oxidation) C5(Carbamidomethyl) C11(Carbamidomethyl)	49.56	1.92	Trypsin inhibitor 1 (Q43667)
VLMPcKVNDDcLR	C5(Carbamidomethyl) C11(Carbamidomethyl)	68.55	2.73	

#1	b(1+)	b(2+)	Seq.	y(1+)	y(2+)	#2
1	100.076	50.541	V			13
2	213.160	107.084	L	1520.702	760.855	12
3	344.200	172.604	M	1407.618	704.313	11
4	441.253	221.130	P	1276.577	638.792	10
5	601.284	301.145	C-Carbamidomethyl	1179.525	590.266	9
6	729.379	365.193	K	1019.494	510.251	8
7	828.447	414.727	V	891.399	446.203	7
8	942.490	471.749	N	792.331	396.669	6
9	1057.517	529.262	D	678.288	339.647	5
10	1172.544	586.776	D	563.261	282.134	4
11	1332.575	666.791	C-Carbamidomethyl	448.234	224.620	3
12	1445.659	723.333	L	288.203	144.605	2
13			R	175.119	88.063	1

(A)

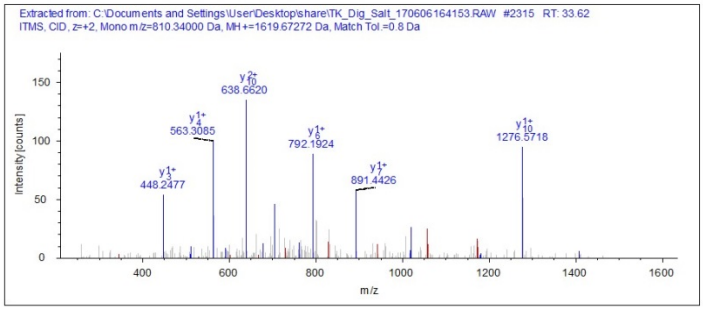

(B)

Figure 5.7 Identification of the specific tryptic peptide VLMPCKVNDDCLR derived from TKTI-3. (A) The singly- and doubly-charged b-ions (red) and y-ions (blue) that arise from MS/MS fragmentation of the peptide. (B) The annotated MS/MS spectrum of the tryptic peptide, VLMPCKVNDDCLR.

5.4 Discussion

For research involving the molecular cloning of proteins and peptides from TCMs, the availability of good-quality RNA is arguably most significant factor influencing the success of the research. However obtaining fresh specimens is often challenging and time-consuming because the herbs used for TCM are widely-distributed within China, growing in both urban areas as well as in remote localities. In addition, the harvesting period for different plants, and even different parts from the same specimen, can vary. A viable alternative, therefore, might be to perform the transcriptomic studies using the dried plant material given the finding that useful RNA can still be extracted from the dehydrated plant tissue of a desiccation-tolerant moss (Dhindsa and Bewley, 1978). Moreover, some plants exhibit vegetative desiccation tolerance when their tissues undergo a rapid or slow dehydration (Oliver et al., 1998) such that their intracellular RNA is protected from degradation and can

be used for protein synthesis during rehydration (Bewley, 1972). However, to our knowledge, the potential of performing transcriptomic studies using RNA derived from the dried herbs of TCMs has not been well investigated. Instead, the more common method remains the use of fresh material (e.g., the discovery of the ribosome inactivating protein as well as TKTI-1 from the mRNA in the fresh root tube of *T. kirilowii* (Shaw et al., 1991)), usually by flash-freezing the tissues using liquid nitrogen and the extracting the mRNA from the ground or lyophilised samples (MacRae, 2007).

To facilitate our proof of concept that mRNA could be extracted from the dried, decoction pieces of Radix Trichosanthis, we used 3'-RACE to demonstrate the presence of polyadenylated mRNA tails in our extracts. Moreover, our use of two specific primers targeted to a trypsin inhibitor sequence (TKTI-1) known for this species revealed that the mRNA is also intact. Interestingly, however, instead of recovering the TKTI-1 sequence, the two slightly modified and novel trypsin inhibitor peptides TKTI-2 and TKTI-3 were found, thereby also demonstrating the potential of investigating such material for new sequences. As demonstrated by a previous study (Ling et al., 1993), variants of squash trypsin inhibitors have been isolated from the same specimen with different mRNA expression levels in the same plant tissue, suggesting that the TKTI variants probably represent different alleles of the same gene. Reinforcing this hypothesis is the fact that the 3'-UTR regions are also identical between TKTI-2 and TKTI-3.

Together with TKTI-1, these new trypsin inhibitor peptide variants all possess the highly-conserved structural motif of the squash inhibitor family, and especially from those in the tribe Sicyoeae, which consists of 27-33 amino-acid residues containing six cysteine residues that form three cross-linked disulphate bridges (Otlewski and Krowarsch, 1996). Unlike TKTI-1, both prepropeptides of TKTI-2 and TKTI-3 contain a glycine instead of an alanine immediately before the mature peptide domain. However, this could not be confirmed via MS/MS because the glycine is not within the mature peptide domain. TKTI-3 also presents a second mutation unique within the squash inhibitor family in which a valine is present at the conservative P1' position of these Bowman-Birk-type inhibitors instead of isoleucine (Figure 5.4) (Otlewski and Krowarsch, 1996), a finding that we independently confirmed by an MS/MS analysis of the total proteins to exclude the possibility of an artefact (Figure 5.5). Although this change does take place at a conservative active site, we assume that the trypsin inhibitory activity could still remained largely unchanged because the P1' position is not essential for activity, although small effects on affinity cannot be ruled out (Brauer and Leatherbarrow, 2003).

In summary, our results document the success of molecular cloning of mRNA from the commonly-used TCM decoction pieces of Radix Trichosanthis by the identification of the corresponding cDNA and encoded peptides from a known member of the squash trypsin inhibitor family. Thus, although RNA can be extracted from such dried plant material, we also observed that less total RNA was extracted compared to values from the literature (Wang et al., 2012). We therefore speculate that the extraction method might need further modifications specific for the decoction pieces of Radix Trichosanthis or other TCMs.

However, it can not be ruled out that RNA could be partially degraded in such plant material given that the manufacturing process for TCMs is probably not performed in an “RNA friendly” manner. Nevertheless, if our result does indeed hold more generally, our study presents a cost-effective and labour-saving option to extract the mRNA from the herbs used in TCM via their decoction pieces.

Chapter 6

General Discussion

AMPs have demonstrated remarkable antimicrobial effects and appeared as potential antibiotic agents for treating emerging antibiotic resistance because most of them exert the function through membrane permeabilisation. To be specific, there is a general agreement that AMPs are among the most potential candidates for the development of new antibiotics for three reasons, rapid action on the microbial membranes, non-specific activity against numerous pathogens even resistant strains and low possibility of evoking drug-resistance due to their complex mechanism of action. Therefore, it was unsurprising that two novel peptides discovered from amphibian skin secretion exhibited antimicrobial activities in this thesis.

As described in chapter 3, DM-PC, a typical member of Dermaseptins S peptide family, was isolated from the skin secretion of a tree-dwelling, South American frog (*Phyllomedusa coelestis*). Like other peptides in this family, it is a linear polycationic peptide, with a conserved Trp residue at position 3 and an AG(A)KAV(A)L(V/G)N(G/K)AV(A) consensus motif in the mid region. Due to the presence of Lys residues, the alternatively-arranged hydrophobic and hydrophilic amino acid residues of DM-PC are punctuated, which contributes to the formation of amphipathic-helices in membrane-mimetic solvents. as might be expected, DM-PC demonstrated a potent, rapid and irreversible inhibitory effect on a broad spectrum of host-free microbes, including a series of multidrug-resistant clinical isolates. At the meantime, no significant toxic influence upon mammalian cells (in its MIC) was observed during the haemolysis assay. In fact, antimicrobial-resistant infection is an increasingly serious threat to global public health that requires action across all government

sectors and society, and this novel AMP as a substitute for traditional antimicrobials has a great potential to address antimicrobial resistance.

A previous study which investigated truncated dermaseptin S4 16-mer, 13-mer and 10-mer derivatives (Navon-Venezia et al., 2002, Krugliak et al., 2000), indicated that dermaseptin exhibited a well-defined helical structure at the N-terminus, but rather loose structures at its C-terminus, and the truncated derivatives were still active against microorganisms, even though the charge and hydrophobicity were decreased (Feder et al., 2000, Krugliak et al., 2000, Efron et al., 2002, Kustanovich et al., 2002). Therefore, when designing the truncated derivatives from DM-PC, the net positive charge was optimised first. DM-PC contained an acidic amino acid residue at its C-terminus, and DMPC-19 possessed +5 net charge after removing the C-terminal segment. The dermaseptin S4 derivatives had already shown that a +5 net charge is essential for exerting broad-spectrum antimicrobial activity (Feder et al., 2000). Indeed, the antimicrobial activity of DMPC-19 was only slightly altered, except against *E. faecalis*, where its activity was much less potent. The 10-mer dermaseptin S4 derivative had been ineffective, therefore we optimised the net charge to +5 and improved the hydrophobicity at the C-terminus. However, the antimicrobial activity of DMPC-10 was still very low, although when Cha, in which the benzene ring of Phe was replaced by cyclohexane, was employed at the C-terminus, the antimicrobial activity was restored. This indicates that the positive charge is not enough for shorter derivatives, such as K_4S4(1-10)a from dermaseptin S4 (Kustanovich et al., 2002). But higher hydrophobicity, especially at the C-terminus, can improve the bioactivity. As Kustanovich suggested, the interaction with cell membrane of N-terminal domain mainly depends on the net charge state while the C-

terminal domain also contributes to the binding affinity (Kustanovich et al., 2002). That the antimicrobial potency of DMPC-19 was retained after removal of C-terminus may be the compensation of increasing the net charges. However, when removing more residues from C-terminus, the bioactivity decreased even the net charge was unchanged, because of the reduction in the insertion affinity of peptides to lipid bilayer that contributed by the C-terminal hydrophobic domain (Gaidukov et al., 2003). It also correlates with the membrane permeability effect and haemolysis for the peptides in this study. DM-PC possesses the intact sequence that increases the binding affinity and insertion affinity towards lipid bilayers. DMPC-10A also exhibits disruption of the cell membranes of both red blood cells and *P. aeruginosa* but is less effective than DM-PC. This would indicate that optimisation of peptide length and the hydrophobicity of the C-terminus could be key to improving the therapeutic window for dermaseptin derivatives.

However little work has so far been done to evaluate dermaseptins' effects on bacterial biofilm, even with their promising features and characteristics. Biofilm, a microbial community coated by an external polysaccharide matrix, could also lead up to poor drug penetration and finally antibiotic resistance. Therefore, assessment of the effects of DM-PC against a series of Gram-positive and Gram-negative clinical isolates was performed both in planktonic and biofilm cells. Our findings revealed that DM-PC suppressed biofilm formation and disrupted pre-formed biofilm of different strains of drug-resistant pathogens in CF lungs. When it comes to the biofim, bacteria within which are slowly growing and dormant pose a serious clinical challenge for therapy. Due to the tolerance to the conventional antibiotics established by biofilms, these sessile bacteria, such as

Staphylococcus aureus and *Pseudomonas aeruginosa* triggered various chronic infections, including chronic wounds, CF, osteomyelitis, rhinosinusitis, and many types of infections associated with tissue fillers. Accordingly, the discovery of DM-PC that is active against both planktonic bacteria and their biofilms is of great public health significance.

Furthermore, a prototypical member of phylloxin, named PLX-PC, was identified from *Phyllomedusa coelestis*, which is not structurally homologous to the dermaseptins but does display some sequence identities with *Xenopus* antimicrobial peptides. The discovery of phylloxin with a rapidly evolving C-terminal ends, extended the list of bioactive peptide families. Here, PLX-PC has a distinct activity spectrum, especially against Gram-positive bacteria, and a moderate cytotoxicity towards mammalian cells. Thus, this novel AMP need to be further modified as new candidates.

The mechanism of action of PLX-PC can be of great importance to explain its narrow-spectrum and negligible antimicrobial activity. “Barrel-stave”, “toroidal pore” and “carpet-like”, are much more used models to explain how α-helical peptides interact with the microbial membrane and finally cause cell death. No matter what mechanisms are adopted, cationicity, hydrophobicity, amphipathicity and conformation play a vital role in enabling peptides to possess bactericidal activity. Though differing widely in these physicochemical characteristics, both DM-PC and PLX-PC are cationic, amphipathic, and form a well-behaved α-helix in an anisotropic environment, like bacterial cell membrane with sharply demarcated polar and non-polar surfaces. It is noteworthy that the antimicrobial potencies of

these membranotropic peptides are mostly dependent of the structure of cell envelope, as the results of dynamic membrane permeability assay suggest that these peptides take effect via permeating the target cells.

The “barrel-stave” mechanism for membrane disruption was found to be used by by the peptides that are non-specifically active on bacteria, which involves membrane-binding and insertion, followed by aggregation of peptide monomers (“staves”) to form an aqueous pore. The more “staves” are engaged, the larger pore size will be. The “toroidal pore” mechanism refers to the organisation of aqueous pores through which ions can flow, comprising the perpendicular disposition to the bilayer as well as the rearrangement of the lipid packing. Typically, magainin, from *Xenopus laevis*, is able to form toroidal pores. But in “carpet-like” model, peptides permeate the membrane by disrupting the bilayer curvature instead of inserting into the hydrophobic core of the membrane. So, the electrostatic interaction between cationic peptides and negatively charged bacterial membrane, rather than the hydrophobicity, is the determinant of AMPs covering target membrane in a carpet-like manner. To summarise, there is a high possibility that PLX-PC acts as magainins forming toroidal pores, owing to either its structural homology to the AMPs isolated from *Xenopus laevi* or the poor cationicity. Whereas, DM-PC is more likely to act as most dermaseptins, permeabilising membrane in a diffuse way.

As discussed in the above paragraph, the antimicrobial effects could be simply reversed by the differences of cell wall structures of microorganisms. In general, the cell wall of bacteria

is mostly composed of peptidoglycan, while the main component of the cell wall of fungi is chitin, which is tougher than peptidoglycan to be destroyed by antimicrobial peptides. Besides, in spite of a thinner and less compact peptidoglycan layer than that of Gram-positive bacteria, the cell wall of Gram-negative bacteria remains strong, tough, and elastic to maintain their shape and protect them against damage from outside factors, because of their extra outer membrane containing lipopolysaccharides, proteins, and phospholipids. Altogether, both the chitin of fungi and the outer membrane of Gram-negative bacteria provide cells protection against extreme environmental conditions, such as the invasion of PLX-PC.

On one hand, a large number of α-helical peptides have been proved to have potent antimicrobial activity. On the other hand, naturally occurred AMPs have been successfully proved to be good templates of being engineered to analogues with higher potencies and broader antimicrobial activity spectra. Several modification strategies which have been successfully utilised in previous studies are now available for use. Therefore, it seemed quite reasonable to carry out rational modification to obtain an activity-enhanced analogue, using the putative novel peptide as a prototype. The basic idea of conventional drug design is attempting to optimise the fit between a “lock” and its “key”, which frequently relies on computer modeling techniques and three-dimensional information about biomolecules. However, the rational design of AMPs suffers from a major stumbling block since their nonspecific mechanism of action.

There are three conventional strategies to modify a peptide: substitution of amino acids, truncating the effective part of a peptide, construct a peptide hybrid by binding truncations of two bioactive peptides. The first strategy, substitution of amino acids, have been proved to be the simplest and the most effective strategy by other researchers. Since the physicochemical characteristics play an undeniable role in the potency of antibacterial activity and in the target spectrum of AMPs, alteration of amino acid residues is one of the most studied tactics of AMP modification. In general, these studies replaced certain amino acids, especially those in hydrophobic domains, with other amino acid residues, causing a series of analogues that display changed bioactivities, which suggested that the cationicity, the amphipathic α-helicity and the hydrophobicity were fundamental factors for antimicrobial action. Secondly, keeping critical amino acid residues for basicity and adopting helicity as an amphipathic conformation to further simplify AMPs would result in analogs that display potent antibiotic activity and low cytotoxicity. Lastly, not all AMPs possess all the required properties for direct uses as antibiotics. Alternatively, they could be combined used, as one for membrane permeabilisation and the other for bacterial killing.

In this study, the novel dermaseptin and phylloxin were optimised by modification in light of the physicochemical properties. According to the structure-activity relationships of dermaseptins, shortening the chain length yielded peptide derivatives, DMPC-19 and DMPC-10, were designed for optimisation of physicochemical parameters. In expectation, the truncated mimetic DMPC-19, generated by the deletion of C-terminal end containing an acidic amino acid residue (aspartic acid) which resulted in an increase of the positive charge of peptide, demonstrated an overall rise in selectivity between microbial and red blood cells.

Moreover, increasing with the mental ions around DM-PC and DMPC-19, the affinity between cationic AMPs like DM-PC and bacterial cell membranes would be weakened because of competitive inhibition, which finally affected their antibacterial potency and indirectly proved that a higher charge can lead to more active peptides. Afterwards, we kept trimming off decorative residues from C-terminal end, and the artificial decapeptide DMPC-10 was designed and its antimicrobial activity dramatically decreased. In contrast, with the substitution of an unnatural amino acid residue Cha for the last amino acid residue Ala, a significant increase in antimicrobial activity as well as haemolysis rate could be observed. So, increased hydrophobicity had a positive effect on peptide access to both prokaryotic and eukaryotic membranes, and this was consistent with the predicted mode of action of linear amphipathic alpha-helical antimicrobial peptides that AMPs accumulated to a threshold concentration due to some affinities, and the hydrophobic residues could be inserted into the lipid bilayer of bacterial membrane, resulting in the formation of transient or prolonged transmembrane pores can not only lead to the final membrane disintegration but also permit extra peptides to enter the membrane to work on intracellular targets and finally causing cell death. In conclusion, both the cationicity and the integrity of the hydrophobic face of the amphipathic peptides played a decisive role on the bioactivity, and there were optimum charge-to-length ratio and hydrophobicity window in which selective antimicrobial activity could be obtained. In addition, the results highlighted a significant role for the unnatural amino acid Cha at the ends of a peptide in increasing hydrophobicity, the percentage of α-helical content, and proteolytic stability to degradation by carboxy- or amino- peptidases.

Similarly, two mainstream strategies, substitution of amino acids and truncating the effective part of a peptide, were employed to modify PLX-PC. Three peptide derivatives, PLXPC-W13, PLXPC-14 and PLXPC-10, were designed for optimisation of physicochemical parameters, especially for an ideal hydrophobicity of the nonpolar face of the amphipathic α-helical peptides. With the Trp substitution, all three analogues demonstrated an enhanced and extended spectrum of antimicrobial activities, showing an overall rise in antimicrobial activity. Besides, the haemolytic activity of peptide analogues was not either weakened nor strengthened as a result of a decrease or increase in peptide hydrophobicity. To sum up, the optimum hydrophobicity window on the nonpolar face of the peptides allows insertion into the membrane through hydrophobic interactions, causing increased permeability and loss of barrier function of target cells.

The MBIC and MBEC assay of DM-PC derivatives showed that some of them, such as DMPC-19 and DMPC-10A penetrated well into the biofilm structure and inhibited biofilm formation. The key question that remains is how these dermaseptins can cross a thick layer established by exopolysaccharides, DNA, and proteins to be able to reach their target cells. One possibility is that dermaseptins could directly work on biofilms, otherwise the matrix could fail to prevent them (which are positively charged) from penetrating within the biofilm because of the electrostatic interactions with negatively charged bacterial membranes. Once in contact with these cells, dermaseptins establish electrostatic interactions with the bacterial membranes, leading to the formation of ionic channels in the lipid bilayers and inducing cell death.

The molecular basis for the selective cytotoxicity of AMPs are poorly understood. The observation that there is a correlation between peptide hydrophobicity and haemolytic activity can be explained by the membrane discrimination mechanism. Peptides with higher hydrophobicities will penetrate deeper into the hydrophobic core of the red blood cell membrane, causing stronger haemolysis by forming pores or channels.

In addition, with the success of molecular cloning of mRNA from the commonly-used TCM decoction pieces of Radix Trichosanthis, a novel trypsin inhibitor (as the probable alleleic variants TKTI-2 and TKTI-3) was identified. The success of 3 prime rapid amplification of cDNA ends with two specific primers targeted to TKTI-1 verified the mRNA we got here is intact and with a polyA tail. Although RNA can be extracted from such dried plant material, we also observed that less total RNA was extracted compared to values from the literature (Wang et al., 2012). Nevertheless, our study presents a cost-effective and labour-saving option to extract the mRNA from the herbs used in TCM via their decoction pieces.

References

ACHER, R., CHAUVET, J. & ROUILLE, Y. 1997. Adaptive evolution of water homeostasis regulation in amphibians: vasotocin and hydrins. *Biol Cell,* 89**,** 283-91.

ADMASSU, H., GASMALLA, M. A. A., YANG, R. & ZHAO, W. 2018. Bioactive Peptides Derived from Seaweed Protein and Their Health Benefits: Antihypertensive, Antioxidant, and Antidiabetic Properties. *J Food Sci,* 83**,** 6-16.

AHMAD, M., MALIK, K., TARIQ, A., ZHANG, G., YASEEN, G., RASHID, N., SULTANA, S., ZAFAR, M., ULLAH, K. & KHAN, M. P. Z. 2018. Botany, ethnomedicines, phytochemistry and pharmacology of Himalayan paeony (Paeonia emodi Royle.). *J Ethnopharmacol,* 220**,** 197-219.

ALLCOCK, S., YOUNG, E. H., HOLMES, M., GURDASANI, D., DOUGAN, G., SANDHU, M. S., SOLOMON, L. & TOROK, M. E. 2017. Antimicrobial resistance in human populations: challenges and opportunities. *Glob Health Epidemiol Genom,* 2**,** e4.

AMICHE, M. & GALANTH, C. 2011. Dermaseptins as models for the elucidation of membrane-acting helical amphipathic antimicrobial peptides. *Curr Pharm Biotechnol,* 12**,** 1184-93.

AMICHE, M., LADRAM, A. & NICOLAS, P. 2008. A consistent nomenclature of antimicrobial peptides isolated from frogs of the subfamily Phyllomedusinae. *Peptides,* 29**,** 2074-82.

AMICHE, M., SEON, A. A., PIERRE, T. N. & NICOLAS, P. 1999. The dermaseptin precursors: a protein family with a common preproregion and a variable C-terminal antimicrobial domain. *FEBS Lett,* 456**,** 352-6.

AMICHE, M., SEON, A. A., WROBLEWSKI, H. & NICOLAS, P. 2000. Isolation of dermatoxin from frog skin, an antibacterial peptide encoded by a novel member of the dermaseptin genes family. *Eur J Biochem,* 267**,** 4583-92.

AZEVEDO CALDERON, L., SILVA ADE, A., CIANCAGLINI, P. & STABELI, R. G. 2011. Antimicrobial peptides from Phyllomedusa frogs: from biomolecular diversity to potential nanotechnologic medical applications. *Amino Acids,* 40**,** 29-49.

BAHAR, A. A. & REN, D. 2013. Antimicrobial peptides. *Pharmaceuticals (Basel),* 6**,** 1543-75.

BARTELS, D., SCHNEIDER, K., TERSTAPPEN, G., PIATKOWSKI, D. & SALAMINI, F. 1990. Molecular cloning of abscisic acid-modulated genes which are induced during desiccation of the resurrection plant Craterostigma plantagineum. *Planta,* 181**,** 27-34.

BECHINGER, B. & GORR, S. U. 2016. Antimicrobial Peptides: Mechanisms of Action and Resistance. *J Dent Res*.

BEWLEY, J. D. 1972. The Conservation of Polyribosomes in the Moss Tortula ruralis during Total Desiccation. *Journal of Experimental Botany,* 23**,** 692-698.

BHAT, Z. F., KUMAR, S. & BHAT, H. F. 2015. Bioactive peptides of animal origin: a review. *J Food Sci Technol,* 52**,** 5377-92.

BHAT, Z. F., KUMAR, S. & BHAT, H. F. 2017. Antihypertensive peptides of animal origin: A review. *Crit Rev Food Sci Nutr,* 57**,** 566-578.

BOERNKE, W. E. 1973. Adaptations of amphibian arginase. II. Response to temperature. *Comp Biochem Physiol B,* 44**,** 1035-42.

BOOHAKER, R. J., LEE, M. W., VISHNUBHOTLA, P., PEREZ, J. M. & KHALED, A. R. 2012. The use of therapeutic peptides to target and to kill cancer cells. *Curr Med Chem,* 19**,** 3794-804.

BOSSO, M., STANDKER, L., KIRCHHOFF, F. & MUNCH, J. 2018. Exploiting the human peptidome for novel antimicrobial and anticancer agents. *Bioorg Med Chem,* 26**,** 2719-2726.

BRAUER, A. B. & LEATHERBARROW, R. J. 2003. The conserved P1′ Ser of Bowman–Birk-type proteinase inhibitors is not essential for the integrity of the reactive site loop. *Biochemical and biophysical research communications,* 308**,** 300-305.

BREUKINK, E. & DE KRUIJFF, B. 1999. The lantibiotic nisin, a special case or not? *Biochim Biophys Acta,* 1462**,** 223-34.

BROGDEN, K. A. 2005. Antimicrobial peptides: pore formers or metabolic inhibitors in bacteria? *Nat Rev Microbiol,* 3**,** 238-50.

BROWN, L., PINGITORE, E. V., MOZZI, F., SAAVEDRA, L., VILLEGAS, J. M. & HEBERT, E. M. 2017. Lactic Acid Bacteria as Cell Factories for the Generation of Bioactive Peptides. *Protein Pept Lett,* 24**,** 146-155.

BUCKALEW, V. M. 2015. Endogenous digitalis-like factors: an overview of the history. *Front Endocrinol (Lausanne),* 6**,** 49.

BURTON, M. F. & STEEL, P. G. 2009. The chemistry and biology of LL-37. *Nat Prod Rep,* 26**,** 1572-84.

CAILLON, L., KILLIAN, J. A., LEQUIN, O. & KHEMTEMOURIAN, L. 2013. Biophysical investigation of the membrane-disrupting mechanism of the antimicrobial and amyloid-like peptide dermaseptin S9. *PLoS One,* 8**,** e75528.

CAO, H., KE, T., LIU, R., YU, J., DONG, C., CHENG, M., HUANG, J. & LIU, S. 2015. Identification of a Novel Proline-Rich Antimicrobial Peptide from Brassica napus. *PLoS One,* 10**,** e0137414.

CARLIER, L., JOANNE, P., KHEMTEMOURIAN, L., LACOMBE, C., NICOLAS, P., EL AMRI, C. & LEQUIN, O. 2015. Investigating the role of GXXXG motifs in helical folding and self-association of plasticins, Gly/Leu-rich antimicrobial peptides. *Biophys Chem,* 196**,** 40-52.

CASTELLANI, C. & ASSAEL, B. M. 2017. Cystic fibrosis: a clinical view. *Cell Mol Life Sci,* 74**,** 129-140.

CASTIGLIONE-MORELLI, M. A., CRISTINZIANO, P., PEPE, A. & TEMUSSI, P. A. 2005. Conformation-activity relationship of a novel peptide antibiotic: structural characterization of dermaseptin DS 01 in media that mimic the membrane environment. *Biopolymers,* 80**,** 688-96.

CHAI, T. T., LAW, Y. C., WONG, F. C. & KIM, S. K. 2017. Enzyme-Assisted Discovery of Antioxidant Peptides from Edible Marine Invertebrates: A Review. *Mar Drugs,* 15.

CHALAMAIAH, M., YU, W. & WU, J. 2018. Immunomodulatory and anticancer protein hydrolysates (peptides) from food proteins: A review. *Food Chem,* 245**,** 205-222.

CHANG, K. Y., LIN, T. P., SHIH, L. Y. & WANG, C. K. 2015. Analysis and prediction of the critical regions of antimicrobial peptides based on conditional random fields. *PLoS One,* 10**,** e0119490.

CHEN, H., WUBBOLTS, R. W., HAAGSMAN, H. P. & VELDHUIZEN, E. J. A. 2018. Inhibition and Eradication of Pseudomonas aeruginosa Biofilms by Host Defence Peptides. *Sci Rep,* 8**,** 10446.

CHEN, T., FARRAGHER, S., BJOURSON, A. J., ORR, D. F., RAO, P. & SHAW, C. 2003. Granular gland transcriptomes in stimulated amphibian skin secretions. *Biochem J,* 371**,** 125-30.

CHEN, T., WALKER, B., ZHOU, M. & SHAW, C. 2005. Dermatoxin and phylloxin from the waxy monkey frog, Phyllomedusa sauvagei: cloning of precursor cDNAs and structural characterization from lyophilized skin secretion. *Regul Pept,* 129**,** 103-8.

CHEN, Y., GUARNIERI, M. T., VASIL, A. I., VASIL, M. L., MANT, C. T. & HODGES, R. S. 2007. Role of peptide hydrophobicity in the mechanism of action of alpha-helical antimicrobial peptides. *Antimicrob Agents Chemother,* 51**,** 1398-406.

CLARKE, B. T. 1997. The natural history of amphibian skin secretions, their normal functioning and potential medical applications. *Biological Reviews,* 72**,** 365-379.

COLLINS, J. P. & CRUMP, M. L. 2009. *Extinction in our times : global amphibian decline*, Oxford ; New York, Oxford University Press.

COMMITTEE, N. P. 2010. Pharmacopoeia of the People's Republic of China. *Part,* 1**,** 392-393.

COTTER, P. D., O'CONNOR, P. M., DRAPER, L. A., LAWTON, E. M., DEEGAN, L. H., HILL, C. & ROSS, R. P. 2005. Posttranslational conversion of L-serines to D-alanines is vital for optimal production and activity of the lantibiotic lacticin 3147. *Proc Natl Acad Sci U S A,* 102**,** 18584-9.

CRUMP, M. L. & CRUMP, M. L. 2011. *Amphibians and reptiles : an introduction to their natural history and conservation*, Granville, Ohio, McDonald & Woodward.

DALY, J. W. 1995. The chemistry of poisons in amphibian skin. *Proc Natl Acad Sci U S A,* 92**,** 9-13.

DALY, J. W., MYERS, C. W. & WHITTAKER, N. 1987. Further classification of skin alkaloids from neotropical poison frogs (Dendrobatidae), with a general survey of toxic/noxious substances in the amphibia. *Toxicon,* 25**,** 1023-95.

DANG, L. & VAN DAMME, E. J. 2015. Toxic proteins in plants. *Phytochemistry,* 117**,** 51-64.

DELFINO, G., BRIZZI, R., ALVAREZ, B. B. & GENTILI, M. 1999. Granular cutaneous glands in the frog Physalaemus biligonigerus (Anura, Leptodactylidae): comparison between ordinary serous and 'inguinal' glands. *Tissue Cell,* 31**,** 576-86.

DHINDSA, R. S. & BEWLEY, J. D. 1978. Messenger RNA is conserved during drying of the drought-tolerant moss Tortula ruralis. *Proceedings of the National Academy of Sciences of the United States of America,* 75**,** 842-846.

DOS SANTOS CABRERA, M. P., ARCISIO-MIRANDA, M., BROGGIO COSTA, S. T., KONNO, K., RUGGIERO, J. R., PROCOPIO, J. & RUGGIERO NETO, J. 2008. Study of the mechanism of action of anoplin, a helical antimicrobial decapeptide with ion channel-like activity, and the role of the amidated C-terminus. *J Pept Sci,* 14**,** 661-9.

DRAGO-SERRANO, M. E., CAMPOS-RODRIGUEZ, R., CARRERO, J. C. & DE LA GARZA, M. 2018. Lactoferrin and Peptide-derivatives: Antimicrobial Agents with Potential Use in Nonspecific Immunity Modulation. *Curr Pharm Des,* 24**,** 1067-1078.

DUELLMAN, W. E. & TRUEB, L. 1994. *Biology of amphibians,* Baltimore, Johns Hopkins University Press.

EBENHAN, T., GHEYSENS, O., KRUGER, H. G., ZEEVAART, J. R. & SATHEKGE, M. M. 2014. Antimicrobial peptides: their role as infection-selective tracers for molecular imaging. *Biomed Res Int,* 2014**,** 867381.

EDWARDS, I. A., ELLIOTT, A. G., KAVANAGH, A. M., ZUEGG, J., BLASKOVICH, M. A. & COOPER, M. A. 2016. Contribution of Amphipathicity and Hydrophobicity to the Antimicrobial Activity and Cytotoxicity of beta-Hairpin Peptides. *ACS Infect Dis,* 2**,** 442-450.

EFRON, L., DAGAN, A., GAIDUKOV, L., GINSBURG, H. & MOR, A. 2002. Direct interaction of dermaseptin S4 aminoheptanoyl derivative with intraerythrocytic malaria parasite leading to increased specific antiparasitic activity in culture. *J Biol Chem,* 277**,** 24067-72.

FAIR, R. J. & TOR, Y. 2014. Antibiotics and bacterial resistance in the 21st century. *Perspect Medicin Chem,* 6**,** 25-64.

FEDER, R., DAGAN, A. & MOR, A. 2000. Structure-activity relationship study of antimicrobial dermaseptin S4 showing the consequences of peptide oligomerization on selective cytotoxicity. *J Biol Chem,* 275**,** 4230-8.

FIELDS, F. R., CAROTHERS, K. E., BALSARA, R. D., PLOPLIS, V. A., CASTELLINO, F. J. & LEE, S. W. 2018. Rational design of syn-safencin, a novel linear antimicrobial peptide derived from the circular bacteriocin safencin AS-48. *J Antibiot (Tokyo),* 71**,** 592-600.

FORDE, E., SCHUTTE, A., REEVES, E., GREENE, C., HUMPHREYS, H., MALL, M., FITZGERALD-HUGHES, D. & DEVOCELLE, M. 2016. Differential In Vitro and In Vivo Toxicities of Antimicrobial Peptide Prodrugs for Potential Use in Cystic Fibrosis. *Antimicrob Agents Chemother,* 60**,** 2813-21.

FOSGERAU, K. & HOFFMANN, T. 2015. Peptide therapeutics: current status and future directions. *Drug Discov Today,* 20**,** 122-8.

GAIDUKOV, L., FISH, A. & MOR, A. 2003. Analysis of membrane-binding properties of dermaseptin analogues: relationships between binding and cytotoxicity. *Biochemistry,* 42**,** 12866-74.

GARG, S., NURGALI, K. & MISHRA, V. K. 2016. Food Proteins as Source of Opioid Peptides-A Review. *Curr Med Chem,* 23**,** 893-910.

GIEDRAITIENE, A., VITKAUSKIENE, A., NAGINIENE, R. & PAVILONIS, A. 2011. Antibiotic resistance mechanisms of clinically important bacteria. *Medicina (Kaunas),* 47**,** 137-46.

GUO, S. 2014. Insulin signaling, resistance, and the metabolic syndrome: insights from mouse models into disease mechanisms. *J Endocrinol,* 220**,** T1-T23.

GUZMÁN-RODRÍGUEZ, J. J., OCHOA-ZARZOSA, A., LÓPEZ-GÓMEZ, R. & LÓPEZ-MEZA, J. E. 2015. Plant antimicrobial peptides as potential anticancer agents. *BioMed research international,* 2015.

GVOZDIK, L. & SMOLINSKY, R. 2015. Body size, swimming speed, or thermal sensitivity? Predator-imposed selection on amphibian larvae. *BMC Evol Biol,* 15**,** 238.

HALLAM, A. 1977. *Patterns of evolution as illustrated by the fossil record,* Amsterdam ; New York, Elsevier Scientific Pub. Co. : distributors for the U.S. and Canada, Elsevier North-Holland.

HAMLEY, I. W. 2017. Small Bioactive Peptides for Biomaterials Design and Therapeutics. *Chem Rev,* 117**,** 14015-14041.

HANCOCK, R. E., HANEY, E. F. & GILL, E. E. 2016. The immunology of host defence peptides: beyond antimicrobial activity. *Nat Rev Immunol,* 16**,** 321-34.

HANCOCK, R. E. & SAHL, H. G. 2006. Antimicrobial and host-defense peptides as new anti-infective therapeutic strategies. *Nat Biotechnol,* 24**,** 1551-7.

HUANG, K. C. 1998. *The pharmacology of Chinese herbs*, CRC press.

HUANG, Y., HUANG, J. & CHEN, Y. 2010. Alpha-helical cationic antimicrobial peptides: relationships of structure and function. *Protein Cell,* 1**,** 143-52.

IRAZAZABAL, L. N., PORTO, W. F., RIBEIRO, S. M., CASALE, S., HUMBLOT, V., LADRAM, A. & FRANCO, O. L. 2016. Selective amino acid substitution reduces cytotoxicity of the antimicrobial peptide mastoparan. *Biochim Biophys Acta,* 1858**,** 2699-2708.

KHAN, I., BAHUGUNA, A., KUMAR, P., BAJPAI, V. K. & KANG, S. C. 2017. Antimicrobial Potential of Carvacrol against Uropathogenic Escherichia coli via Membrane Disruption, Depolarization, and Reactive Oxygen Species Generation. *Front Microbiol,* 8**,** 2421.

KIM, C., SPANO, J., PARK, E. K. & WI, S. 2009. Evidence of pores and thinned lipid bilayers induced in oriented lipid membranes interacting with the antimicrobial peptides, magainin-2 and aurein-3.3. *Biochim Biophys Acta,* 1788**,** 1482-96.

KIM, J. S., JEONG, J. H. & KIM, Y. 2018. Design and Engineering of Antimicrobial Peptides Based on LPcin-YK3, an Antimicrobial Peptide Derivative from Bovine Milk. *J Microbiol Biotechnol,* 28**,** 381-390.

KITTS, D. D. & WEILER, K. 2003. Bioactive proteins and peptides from food sources. Applications of bioprocesses used in isolation and recovery. *Curr Pharm Des,* 9**,** 1309-23.

KRUGLIAK, M., FEDER, R., ZOLOTAREV, V. Y., GAIDUKOV, L., DAGAN, A., GINSBURG, H. & MOR, A. 2000. Antimalarial activities of dermaseptin S4 derivatives. *Antimicrob Agents Chemother,* 44**,** 2442-51.

KUMAR, G. R., ESWARAN, N. & JOHNSON, T. S. 2011. Isolation of high-quality RNA from various tissues of Jatropha curcas for downstream applications. *Anal Biochem,* 413**,** 63-5.

KUSTANOVICH, I., SHALEV, D. E., MIKHLIN, M., GAIDUKOV, L. & MOR, A. 2002. Structural requirements for potent versus selective cytotoxicity for antimicrobial dermaseptin S4 derivatives. *J Biol Chem,* 277**,** 16941-51.

LABUZ, D., CELIK, M. O., ZIMMER, A. & MACHELSKA, H. 2016. Distinct roles of exogenous opioid agonists and endogenous opioid peptides in the peripheral control of neuropathy-triggered heat pain. *Sci Rep,* 6**,** 32799.

LAKSHMAIAH NARAYANA, J. & CHEN, J. Y. 2015. Antimicrobial peptides: Possible anti-infective agents. *Peptides,* 72**,** 88-94.

LAZARO, C. P., PONDE, M. P. & RODRIGUES, L. E. 2016. Opioid peptides and gastrointestinal symptoms in autism spectrum disorders. *Braz J Psychiatry,* 38**,** 243-6.

LEE, H., HWANG, J. S., LEE, J., KIM, J. I. & LEE, D. G. 2015. Scolopendin 2, a cationic antimicrobial peptide from centipede, and its membrane-active mechanism. *Biochim Biophys Acta,* 1848**,** 634-42.

LEE, J. & LEE, D. G. 2015. Antimicrobial Peptides (AMPs) with Dual Mechanisms: Membrane Disruption and Apoptosis. *J Microbiol Biotechnol,* 25**,** 759-64.

LEE, T. H., HALL, K. N. & AGUILAR, M. I. 2016. Antimicrobial Peptide Structure and Mechanism of Action: A Focus on the Role of Membrane Structure. *Curr Top Med Chem,* 16**,** 25-39.

LI, Y., WANG, J. & SUN, H. 2015. [Research Progress in Preparation of Antimicrobial Peptides and Their Mechanisms of Action]. *Sheng Wu Yi Xue Gong Cheng Xue Za Zhi,* 32**,** 465-9.

LING, M. H., CHI, C. W. & SHAO, P. Z. 1996. Cloning and Sequence Analyzing the Gene of Trichosanthes Trypsin Inhibitor. *Sheng Wu Hua Xue Yu Sheng Wu Wu Li Xue Bao (Shanghai),* 28**,** 233-239.

LING, M. H., QI, H. Y. & CHI, C. W. 1993. Protein, cDNA, and genomic DNA sequences of the towel gourd trypsin inhibitor. A squash family inhibitor. *Journal of Biological Chemistry,* 268**,** 810.

LOHNER, K. & BLONDELLE, S. E. 2005. Molecular mechanisms of membrane perturbation by antimicrobial peptides and the use of biophysical studies in the design of novel peptide antibiotics. *Comb Chem High Throughput Screen,* 8**,** 241-56.

MACRAE, E. 2007. Extraction of plant RNA. *Methods Mol Biol,* 353**,** 15-24.

MAHONEY, E. J. 2017. *20 fun facts about amphibian adaptations,* New York, Gareth Stevens Publishing.

MALAGUTI, M., DINELLI, G., LEONCINI, E., BREGOLA, V., BOSI, S., CICERO, A. F. & HRELIA, S. 2014. Bioactive peptides in cereals and legumes: agronomical, biochemical and clinical aspects. *Int J Mol Sci,* 15**,** 21120-35.

MALANOVIC, N. & LOHNER, K. 2016. Antimicrobial Peptides Targeting Gram-Positive Bacteria. *Pharmaceuticals (Basel),* 9.

MARCO, R. & GENTILUCCI, L. 2017. Tryptophan-Containing Non-Cationizable Opioid Peptides - a new chemotype with unusual structure and in vivo activity. *Future Med Chem,* 9**,** 2099-2115.

MARENAH, L., MCCLEAN, S., FLATT, P. R., ORR, D. F., SHAW, C. & ABDEL-WAHAB, Y. H. 2004. Novel insulin-releasing peptides in the skin of Phyllomedusa trinitatis frog include 28 amino acid peptide from dermaseptin BIV precursor. *Pancreas,* 29**,** 110-5.

MASON, E., L'HOCINE, L., ACHOURI, A. & KARBOUNE, S. 2018. Hairless Canaryseed: A Novel Cereal with Health Promoting Potential. *Nutrients,* 10.

MEISEL, H. & FITZGERALD, R. J. 2003. Biofunctional peptides from milk proteins: mineral binding and cytomodulatory effects. *Curr Pharm Des,* 9**,** 1289-95.

MISHRA, B., REILING, S., ZARENA, D. & WANG, G. 2017. Host defense antimicrobial peptides as antibiotics: design and application strategies. *Curr Opin Chem Biol,* 38**,** 87-96.

MORAVEJ, H., MORAVEJ, Z., YAZDANPARAST, M., HEIAT, M., MIRHOSSEINI, A., MOOSAZADEH MOGHADDAM, M. & MIRNEJAD, R. 2018. Antimicrobial Peptides: Features, Action, and Their Resistance Mechanisms in Bacteria. *Microb Drug Resist,* 24**,** 747-767.

MURA, M., WANG, J., ZHOU, Y., PINNA, M., ZVELINDOVSKY, A. V., DENNISON, S. R. & PHOENIX, D. A. 2016. The effect of amidation on the behaviour of antimicrobial peptides. *Eur Biophys J,* 45**,** 195-207.

MURRAY, T. S., EGAN, M. & KAZMIERCZAK, B. I. 2007. Pseudomonas aeruginosa chronic colonization in cystic fibrosis patients. *Curr Opin Pediatr,* 19**,** 83-8.

MYHRE, K., CABANAC, M. & MYHRE, G. 1977. Fever and behavioural temperature regulation in the frog Rana esculenta. *Acta Physiol Scand,* 101**,** 219-29.

NAVON-VENEZIA, S., FEDER, R., GAIDUKOV, L., CARMELI, Y. & MOR, A. 2002. Antibacterial properties of dermaseptin S4 derivatives with in vivo activity. *Antimicrob Agents Chemother,* 46**,** 689-94.

NICOLAS, P. & EL AMRI, C. 2009. The dermaseptin superfamily: a gene-based combinatorial library of antimicrobial peptides. *Biochim Biophys Acta,* 1788**,** 1537-50.

OLIVEIRA, M. D., FRANCO, O. L., NASCIMENTO, J. M., DE MELO, C. P. & ANDRADE, C. A. 2013. Mechanistic aspects of peptide-membrane interactions determined by optical, dielectric and piezoelectric techniques: an overview. *Curr Protein Pept Sci,* 14**,** 543-55.

OLIVER, M. J. & BEWLEY, J. D. 1984. Plant Desiccation and Protein Synthesis: V. Stability of Poly (A)− and Poly (A)+ RNA during Desiccation and Their Synthesis upon Rehydration in the Desiccation-Tolerant Moss Tortula ruralis and the Intolerant Moss Cratoneuron filicinum. *Plant Physiology,* 74**,** 917-922.

OLIVER, M. J., O'MAHONY, P. & WOOD, A. J. 1998. "To dryness and beyond" – Preparation for the dried state and rehydration in vegetative desiccation-tolerant plants. *Plant Growth Regulation,* 24**,** 193-201.

OTLEWSKI, J. & KROWARSCH, D. 1996. Squash inhibitor family of serine proteinases. *Acta Biochim Pol,* 43**,** 431-44.

PARKER, J. M. 2013. *Reptiles and amphibians of the Mojave Desert : a field guide,* Las Vegas, NV, Snell Press.

PIERRE, T. N., SEON, A. A., AMICHE, M. & NICOLAS, P. 2000. Phylloxin, a novel peptide antibiotic of the dermaseptin family of antimicrobial/opioid peptide precursors. *Eur J Biochem,* 267**,** 370-8.

PONZANO, S., NIGRELLI, G., FREGONESE, L., EICHLER, I., BERTOZZI, F., BANDIERA, T., GALIETTA, L. J. V. & PAPALUCA, M. 2018. A European regulatory perspective on cystic fibrosis: current treatments, trends in drug development and translational challenges for CFTR modulators. *Eur Respir Rev,* 27.

PRADO MONTES DE OCA, E. 2013. Antimicrobial peptide elicitors: new hope for the post-antibiotic era. *Innate Immun,* 19**,** 227-41.

QI, B., WANG, S., WANG, Q., ZHANG, H., BAI, X. Y., HE, H. N., SUN, W. J., LIU, L. & ZHAO, D. Q. 2016. Characterization and immunostimulating effects on murine peritoneal macrophages of a novel protein isolated from Panax quinquefolius L. *J Ethnopharmacol,* 193**,** 700-705.

QI, G., LI, J. Q., YANG, J. & SU, Z. X. 2010. An optimised, small-scale preparation of high-quality RNA from dry seeds of Davidia involucrata. *Phytochemical Analysis,* 20**,** 139-142.

QIAN, Y., TAN, F., QI, Z. & CHI, C. 1990. Studies on natural and modified peptide Trichosanthes trypsin inhibitors. *Science in China. Series B, Chemistry, life sciences & earth sciences,* 33**,** 599-605.

RADEK, K. & GALLO, R. 2007. Antimicrobial peptides: natural effectors of the innate immune system. *Semin Immunopathol,* 29**,** 27-43.

RAFEEQ, M. M. & MURAD, H. A. S. 2017. Cystic fibrosis: current therapeutic targets and future approaches. *J Transl Med,* 15**,** 84.

RAO, T., RUIZ-GOMEZ, G., HILL, T. A., HOANG, H. N., FAIRLIE, D. P. & MASON, J. M. 2013. Truncated and helix-constrained peptides with high affinity and specificity for the cFos coiled-coil of AP-1. *PLoS One,* 8**,** e59415.

REIHILL, J. A., WALKER, B., HAMILTON, R. A., FERGUSON, T. E., ELBORN, J. S., STUTTS, M. J., HARVEY, B. J., SAINT-CRIQ, V., HENDRICK, S. M. & MARTIN, S. L. 2016. Inhibition of Protease-Epithelial Sodium Channel Signaling Improves Mucociliary Function in Cystic Fibrosis Airways. *Am J Respir Crit Care Med,* 194**,** 701-10.

RODEL, M. O., BREDE, C., HIRSCHFELD, M., SCHMITT, T., FAVREAU, P., STOCKLIN, R., WUNDER, C. & MEBS, D. 2013. Chemical camouflage--a frog's strategy to co-exist with aggressive ants. *PLoS One,* 8**,** e81950.

RODRIGUEZ, M. C. S., DANIEL, E. R., HUSSAIN, S. S., DAVID, A., MORTEN, R., THOMAS, G., NIELSEN, B. R. H., DOROTHEA, B. & JOHN, M. 2010. Transcriptomes of the desiccation-tolerant resurrection plant Craterostigma plantagineum. *Plant Journal,* 63**,** 212.

ROLLINS-SMITH, L. A. 2009. The role of amphibian antimicrobial peptides in protection of amphibians from pathogens linked to global amphibian declines. *Biochim Biophys Acta,* 1788**,** 1593-9.

SANTHEKADUR, P. K., KUMAR, D. P., SENESHAW, M., MIRSHAHI, F. & SANYAL, A. J. 2017. The multifaceted role of natriuretic peptides in metabolic syndrome. *Biomed Pharmacother,* 92**,** 826-835.

SCHNARR, N. A. & KENNAN, A. J. 2001. Coiled-coil formation governed by unnatural hydrophobic core side chains. *J Am Chem Soc,* 123**,** 11081-2.

SCORCIAPINO, M. A., SERRA, I., MANZO, G. & RINALDI, A. C. 2017. Antimicrobial Dendrimeric Peptides: Structure, Activity and New Therapeutic Applications. *Int J Mol Sci,* 18.

SHAI, Y. 1999. Mechanism of the binding, insertion and destabilization of phospholipid bilayer membranes by alpha-helical antimicrobial and cell non-selective membrane-lytic peptides. *Biochim Biophys Acta,* 1462**,** 55-70.

SHANG, D., MENG, X., ZHANG, D. & KOU, Z. 2017. Antibacterial activity of chensinin-1b, a peptide with a random coil conformation, against multiple-drug-resistant Pseudomonas aeruginosa. *Biochem Pharmacol,* 143**,** 65-78.

SHAW, P. C., MEI-HING, Y., ZHU, R. H., WALTER, K. K. H., TZI-BUN, N. & HIN-WING, Y. 1991. Cloning of trichosanthin cDNA and its expression in Escherichia coli. *Gene,* 97**,** 267-272.

SHIN, J. M., GWAK, J. W., KAMARAJAN, P., FENNO, J. C., RICKARD, A. H. & KAPILA, Y. L. 2016. Biomedical applications of nisin. *J Appl Microbiol,* 120**,** 1449-65.

SIMMACO, M., KREIL, G. & BARRA, D. 2009. Bombinins, antimicrobial peptides from Bombina species. *Biochim Biophys Acta,* 1788**,** 1551-5.

STANTON, T. B. 2013. A call for antibiotic alternatives research. *Trends Microbiol,* 21**,** 111-3.

SULTAN, S., HUMA, N., BUTT, M. S., ALEEM, M. & ABBAS, M. 2018. Therapeutic potential of dairy bioactive peptides: A contemporary perspective. *Crit Rev Food Sci Nutr,* 58**,** 105-115.

SZCZECINSKA, M., SRAMKO, G., WOLOSZ, K. & SAWICKI, J. 2016. Genetic Diversity and Population Structure of the Rare and Endangered Plant Species Pulsatilla patens (L.) Mill in East Central Europe. *PLoS One,* 11**,** e0151730.

TANG, W. & EISENBRAND, G. 1992. Trichosanthes kirilowii Maxim. *Chinese Drugs of Plant Origin.* Springer.

THOMAS, P., KUMAR, T. V., RESHMY, V., KUMAR, K. S. & GEORGE, S. 2012. A mini review on the antimicrobial peptides isolated from the genus Hylarana (Amphibia: Anura) with a proposed nomenclature for amphibian skin peptides. *Mol Biol Rep,* 39**,** 6943-7.

TSAO, S., YAN, K. & YEUNG, H. 1986. Selective killing of choriocarcinoma cells in vitro by trichosanthin, a plant protein purified from root tubers of the Chinese medicinal herb Trichosanthes kirilowii. *Toxicon,* 24**,** 831-840.

VAN DER DOES, A. M., AMATNGALIM, G. D., KEIJSER, B., HIEMSTRA, P. S. & VILLENAVE, R. 2018. Contribution of Host Defence Proteins and Peptides to Host-Microbiota Interactions in Chronic Inflammatory Lung Diseases. *Vaccines (Basel),* 6.

VAN ZOGGEL, H., CARPENTIER, G., DOS SANTOS, C., HAMMA-KOURBALI, Y., COURTY, J., AMICHE, M. & DELBE, J. 2012. Antitumor and angiostatic activities of the antimicrobial peptide dermaseptin B2. *PLoS One,* 7**,** e44351.

VIEHMAN, J. A., NGUYEN, M. H. & DOI, Y. 2014. Treatment options for carbapenem-resistant and extensively drug-resistant Acinetobacter baumannii infections. *Drugs,* 74**,** 1315-33.

VINEETH KUMAR, T. V. & SANIL, G. 2017. A Review of the Mechanism of Action of Amphibian Antimicrobial Peptides Focusing on Peptide-Membrane Interaction and Membrane Curvature. *Curr Protein Pept Sci,* 18**,** 1263-1272.

WANG, C., ZOLOTARSKAYA, O. Y., NAIR, S. S., EHRHARDT, C. J., OHMAN, D. E., WYNNE, K. J. & YADAVALLI, V. K. 2016. Real-Time Observation of Antimicrobial Polycation Effects on Escherichia coli: Adapting the Carpet Model for Membrane Disruption to Quaternary Copolyoxetanes. *Langmuir,* 32**,** 2975-84.

WANG, G. 2015. Improved methods for classification, prediction, and design of antimicrobial peptides. *Methods Mol Biol,* 1268**,** 43-66.

WANG, G., MISHRA, B., LAU, K., LUSHNIKOVA, T., GOLLA, R. & WANG, X. 2015. Antimicrobial peptides in 2014. *Pharmaceuticals (Basel),* 8**,** 123-50.

WANG, G. F., WANG, G., ZHANG, X. W., WANG, F. & SONG, R. T. 2012. Isolation of high quality RNA from cereal seeds containing high levels of starch. *Phytochemical Analysis,* 23**,** 159-163.

WANG, J., WONG, Y. K. & LIAO, F. 2018. What has traditional Chinese medicine delivered for modern medicine? *Expert Reviews in Molecular Medicine,* 20.

WARBURG, M. R. 1997. *Ecophysiology of amphibians inhabiting xeric environments*, Berlin ;New York, Springer.

WELLS, K. D. 2007. *The ecology & behavior of amphibians*, Chicago, The University of Chicago Press.

WILCZYNSKI, W., LYNCH, K. S. & O'BRYANT, E. L. 2005. Current research in amphibians: studies integrating endocrinology, behavior, and neurobiology. *Horm Behav*, 48**,** 440-50.

WINSTANLEY, C., O'BRIEN, S. & BROCKHURST, M. A. 2016. Pseudomonas aeruginosa Evolutionary Adaptation and Diversification in Cystic Fibrosis Chronic Lung Infections. *Trends Microbiol*, 24**,** 327-337.

WONG, K. L., WONG, R. N. S., ZHANG, L., LIU, W. K., TZI BUN, N. G., PANG, C. S., KWOK, P. C. L., LAI, Y. M., ZHANG, Z. J. & ZHANG, Y. 2014. Bioactive proteins and peptides isolated from Chinese medicines with pharmaceutical potential. *Chinese Medicine,9,1(2014-07-19)*, 9**,** 19.

WU, R., WU, C., LIU, D., YANG, X., HUANG, J., ZHANG, J., LIAO, B., HE, H. & LI, H. 2015. Overview of Antioxidant Peptides Derived from Marine Resources: The Sources, Characteristic, Purification, and Evaluation Methods. *Appl Biochem Biotechnol*, 176**,** 1815-33.

XU, H., TIE, K., ZHANG, Y., FENG, X., CAO, Y. & HAN, W. 2018. Design, expression, and characterization of the hybrid antimicrobial peptide T-catesbeianin-1 based on FyuA. *J Pept Sci*, 24.

YANG, L., WEISS, T. M., LEHRER, R. I. & HUANG, H. W. 2000. Crystallization of antimicrobial pores in membranes: magainin and protegrin. *Biophys J*, 79**,** 2002-9.

YEAMAN, M. R. & YOUNT, N. Y. 2003. Mechanisms of antimicrobial peptide action and resistance. *Pharmacol Rev*, 55**,** 27-55.

YOUNT, N. Y. & YEAMAN, M. R. 2013. Peptide antimicrobials: cell wall as a bacterial target. *Ann N Y Acad Sci*, 1277**,** 127-38.

YU, J. H., LI, Y. Y., XIANG, M., ZHU, J. Q., HUANG, X. H., WANG, W. J., TAN, R., ZHOU, J. Y. & LIAO, H. 2016. Molecular cloning and characterization of α -amylase/subtilisin inhibitor from rhizome of Ligusticum chuanxiong. *Biotechnology Letters*, 39**,** 141-148.

YUAN, Y., ZAI, Y., XI, X., MA, C., WANG, L., ZHOU, M., SHAW, C. & CHEN, T. 2019. A novel membrane-disruptive antimicrobial peptide from frog skin secretion against cystic fibrosis isolates and evaluation of anti-MRSA effect using Galleria mellonella model. *Biochim Biophys Acta Gen Subj*, 1863**,** 849-856.

ZAIRI, A., TANGY, F., BOUASSIDA, K. & HANI, K. 2009. Dermaseptins and magainins: antimicrobial peptides from frogs' skin-new sources for a promising spermicides microbicides-a mini review. *J Biomed Biotechnol*, 2009**,** 452567.

ZANJANI, N. T., MIRANDA-SAKSENA, M., CUNNINGHAM, A. L. & DEHGHANI, F. 2018. Antimicrobial Peptides of Marine Crustaceans: The Potential and Challenges of Developing Therapeutic Agents. *Curr Med Chem*, 25**,** 2245-2259.

ZASLOFF, M. 1987. Magainins, a class of antimicrobial peptides from Xenopus skin: isolation, characterization of two active forms, and partial cDNA sequence of a precursor. *Proc Natl Acad Sci U S A*, 84**,** 5449-53.

ZASLOFF, M. 2002. Antimicrobial peptides of multicellular organisms. *Nature*, 415**,** 389-95.

ZHAO, H., MATTILA, J. P., HOLOPAINEN, J. M. & KINNUNEN, P. K. 2001. Comparison of the membrane association of two antimicrobial peptides, magainin 2 and indolicidin. *Biophys J,* 81**,** 2979-91.

ZHU, X., ZHANG, L., WANG, J., MA, Z., XU, W., LI, J. & SHAN, A. 2015. Characterization of antimicrobial activity and mechanisms of low amphipathic peptides with different alpha-helical propensity. *Acta Biomater,* 18**,** 155-67.

ZOU, T. B., HE, T. P., LI, H. B., TANG, H. W. & XIA, E. Q. 2016. The Structure-Activity Relationship of the Antioxidant Peptides from Natural Proteins. *Molecules,* 21**,** 72.